LBL-37477
UC-402

Lawrence Berkeley Laboratory
UNIVERSITY OF CALIFORNIA

ENERGY & ENVIRONMENT
DIVISION

Transport and Sorption of Volatile Organic Compounds and Water Vapor in Porous Media

T.-F. Lin
(Ph.D. Thesis)

July 1995

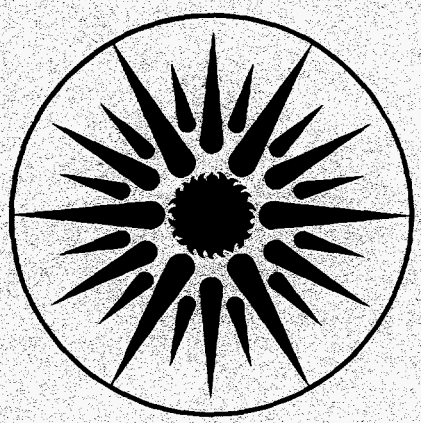

ENERGY
AND ENVIRONMENT
DIVISION

Prepared for the U.S. Department of Energy under Contract Number DE-AC03-76SF00098

LBL-37477
UC-402

Transport and Sorption of Volatile Organic Compounds and Water Vapor in Porous Media

Tsair-Fuh Lin
Ph.D. Thesis

Department of Civil Engineering
University of California, Berkeley

and

Energy and Environment Division
Lawrence Berkeley Laboratory
University of California
Berkeley, CA 94720

July 1995

This work was supported by the Director, Office of Energy Research, Office of Health and Environmental Research, Environmental Sciences Division of the U.S. Department of Energy (DOE), under Contract DE-AC03-76SF00098.

Transport and Sorption of Volatile Organic Compounds and Water Vapor in Porous Media

by

Tsair-Fuh Lin

B.S. (National Cheng-Kung University) 1985
M.S. (National Taiwan University) 1987

A dissertation submitted in partial satisfaction of the
requirements for the degree of
Doctor of Philosophy

in

Engineering-Civil Engineering

in the

GRADUATE DIVISION

of the

UNIVERSITY OF CALIFORNIA AT BERKELEY

Committee in charge:

Professor William W Nazaroff, Chair
Professor James R. Hunt
Professor Catherine P. Koshland

1995

Abstract

Transport and Sorption of Volatile Organic Compounds and Water Vapor in Porous Media

by

Tsair-Fuh Lin

Doctor of Philosophy in Engineering-Civil Engineering

University of California at Berkeley

Professor William W Nazaroff, Chair

Mechanisms governing the transport of organic contaminants in porous media must be understood for many environmental applications, such as modeling the transport and fate of volatile organic compounds (VOCs) in subsurface systems and removing VOCs from air streams by activated carbon adsorption. To gain insight into the controlling mechanisms for VOC transport in porous media, the relationships among sorbent properties, sorption equilibrium and intraparticle diffusion processes were studied at the level of individual sorbent particles and laboratory columns for soil and activated carbon systems. This research focuses on simple systems to represent those in natural and engineered environments. However, the results developed from this study provide useful information and insights for future experimental and theoretical designs applied to more complex (e.g. multicomponent) systems.

In this dissertation, the transport and sorption of VOCs and water vapor were first elucidated within individual dry soil mineral grains (Chapter II). Experimental measurements of soil properties, sorption capacity and sorption rates were conducted for three test soils. Analysis of the experimental results suggested that the soil grains are

porous, while the sorption isotherms are nonlinear and adsorption-desorption rates are slow and asymmetric. An intragranular pore diffusion model coupled with the nonlinear Freundlich isotherm was developed to describe the experimental sorption kinetic curves. The model fits the experimental data very well and the slow, asymmetric sorption and desorption rates were well resolved. In exercising the model, the degree of asymmetry between sorption and desorption was also found to depend on the nonlinearity of the isotherm, i.e. the exponent in the Freundlich equation.

Attempts to advance our understanding of the transport of benzene and water vapor within soil organic matter (peat) are discussed in Chapter III. Both partitioning equilibrium and sorption kinetics were determined using an electrobalance. The experimental sorption isotherm for water vapor was found to be similar to that reported in the literature; however, measured sorption capacity for benzene was not reproducible. A dual diffusion model, including gas-phase pore diffusion within peat grains and solid-phase diffusion within micro-spheres of soil organic matter (SOM), was developed to describe the asymmetric sorption rate data for both water vapor and benzene. Assuming that pore diffusion is the rate-limiting process, the model fits the sorption kinetic curves of water vapor very well; however, the benzene sorption data does not follow the predicted trend. Instead, a model accounting for solid-phase intra-SOM diffusion produces a better fit to the benzene kinetic data.

In Chapter IV, the transport of benzene in both dry and moist soil (mineral grain) columns was studied under various flow conditions. It is shown that, based on a single kinetic experiment conducted using a differential adsorption bed, the theoretical relationship between isotherm nonlinearity and adsorption-desorption rate asymmetry can be employed to predict the adsorption isotherms. The parameters extracted from the kinetic experiment were then used to predict column breakthrough curves (BTCs) by coupling column mass transfer equations (the advection-dispersion-sorption (ADS) equation) to the pore diffusion model for dry soil. The predictions conform to the

experimental data very well. For a moist soil column, the ADS model coupled with the intraparticle pore diffusion model, plus several simplified models, were used to generate BTC predictions. The results showed that the model predictions accounting for intragranular pore diffusion are in good agreement with the experimental data for both dry and moist soil columns for all cases, while models based on the assumption of local equilibrium can only describe the experimental data for low velocity regimes.

The porous diffusion model was also used to describe VOC transport in activated carbon systems: granular activated carbon (GAC) and activated carbon fibers (ACF). The model follows the experimental kinetic data, determined by an electrobalance, very well for all cases studied. Following the scheme developed in Chapter IV, the adsorption isotherms and column breakthrough curves were predicted using results from a single kinetic experiment. The errors in predicting breakthrough curves using this approach were found to be less than 5% on average, even though a very different method was used for BTC measurement than for sorbent characterization. The good agreement between the model predictions and the experimental results suggests that the model description captures the essential physical and chemical behavior of the system.

Finally, the intragranular diffusion model for individual grains was further refined to describe the sorption and desorption kinetics of water vapor to granular activated carbon (Chapter VI). A piecewise-linear isotherm was used to approximate the experimental isotherm data for water vapor. Despite the complicated shape and hysteresis of the isotherms, a model that considered gas-phase pore diffusion only (i.e., neglecting surface diffusion) was able to describe the experimental sorption kinetic curves for water vapor on the GAC up to about 60% relative humidity (RH). Surface diffusion was found to be important at higher water vapor concentrations.

In summary, the results of this research indicate that intraparticle diffusion processes along with a nonlinear sorption isotherm are responsible for the slow and asymmetric sorption-desorption rates observed in the systems studied. Diffusion models

accounting for the sorbent and sorbate properties are able to describe the experimental data for soil and activated carbon systems. When combined with appropriate mass transfer equations, the diffusion models accurately predict the experimental column breakthrough curves for several systems. Although the conditions tested are simplified, the mechanisms elucidated in this study should be informative enough to give a useful perspective when attempting to understand more complex systems involving transport and sorption of vapors in porous media.

To my family

Table of Contents

List of Figures

Chapter IV

Chapter V

Chapter VI

List of Tables

Acknowledgments

I cannot thank my advisor, Bill Nazaroff, enough. His extraordinary support and guidance helped me successfully complete my dissertation at Berkeley. Experiencing his serious manner of teaching and conducting high quality research has been most valuable. I am also very grateful to the two other members of my dissertation committee, Professors James Hunt and Catherine Koshland, for their valuable advice regarding my dissertation research.

I greatly appreciate having had the opportunity to work with Dr. Joan Daisey and other staff members of the soil gas transport project in the Indoor Environment Program (IEP) at Lawrence Berkeley Laboratory (LBL). For the past four and half years, Joan has always been very supportive and has given me great freedom in choosing the direction of my research. She also taught me, an engineer, about how to see things from a chemist's point of view. Al Hodgson (another chemist!) not only provided generous help with experimental apparatus, but also set a high standard in experimental work (±5% error!) for me. Dr. John Little (a post-doc and "big brother" to me in the project), now at Virginia Tech., guided me socially and professionally during my first two and half years at Berkeley. Without his help, I would not have been able to withstand the high-pressure academic life while trying to adjust to a new culture. Dr. Rich Sextro generously helped me obtain laboratory space in which to work; he also provided some experimental equipment and many useful suggestions. Working together with Mike Van Loy in the laboratory was enjoyable. I thank him for helping me conduct soil characterization measurements and some of the sorption experiments. I appreciate Dr. Marc Fischer's handling of the administrative work.

I value the technical and administrative support I received from the staff in the Indoor Environment Program: David Faulkner, Karina Garbesi, R. K. K. Mahanama, John Wooley, and Mindi Xu (technical support); and Elizabeth Chong, Joyce Cordell, Nori

Hudson, Pat Johnson and Gina Leong (administrative support). Special thanks go to Ted Chang in the Environmental Research Program, and Tim Nuzum and Doug Sullivan in IEP for their helpful loans of equipment, tools and fittings.

Several other people contributed to this work, and I would like to thank them. Regina Torgalkar produced high quality scanning electron microscope photos of soil and peat surfaces. Jeff Bullard kindly allowed me to perform specific surface area and pore size distribution analyses of soil samples in his laboratory. Joseph Hayes of American Kynol and Alan Roy of Calgon provided samples and information on activated carbon fibers and grains. I would also like to express my gratitude to Dr. Cary Chiou at U. S. Geological Survey for providing me with peat samples. I also gained knowledge of soil organic matter from him.

I am grateful for the financial support I received during my graduate study at Berkeley: a graduate student research assistantship from the Indoor Environment Program, and nonresident tuition scholarships as well as a teaching assistantship granted by the Civil Engineering Department at University of California, Berkeley.

I would like to thank all my friends in Civil and Environmental Engineering. My classmates, Hsiao-Lung Chang, Anushka Drescher, Humphrey Ho, Rong Liu, Yu-Sheng Liu and Tracy Thatcher all helped me in some way, including discussing course work, writing joint term papers, practicing for oral examinations, and conducting research. Bill's other research students, Shelly Miller-Leiden and Bill Riley, and his former post-doc Tonny Sasse are also acknowledged for their help with my research.

Most of all, I would like to express my gratitude to my family members. Although my parents, two sisters, and two brothers are far away in Taiwan, I can always feel their unlimited support of my study at Berkeley. I thank my wife, Athena, for being there with me through so many happy and difficult times. Without her constant support, I would not have been able to complete my doctoral study. I would also like to say thanks to our two

sons, Edward and Arthur. Although they know how to delay a Ph.D. dissertation, without them, life wouldn't be as much fun!

Chapter I

Introduction

BACKGROUND

The transport of contaminant-laden fluids through porous media is a process commonly found in many environmental applications, including systems for gas separation and water purification, and in subsurface environments. With its porous structure, the media often provides a relatively large number of easily accessible sites on which the contaminant may accumulate. In referring to this phenomenon, the solid medium may be called a *sorbent*, the adhering species are called *sorbates*, and the accumulation process is known as *sorption*. Sorption phenomena can be broadly categorized into two groups: *adsorption*, if the accumulation occurs only at the interface of solid and the fluid phases, and *absorption*, if the contaminants interpenetrate the sorbent phase by at least several nanometers (Weber et al., 1991). Adsorption can be further subdivided into physical adsorption, in which only dispersion forces are involved in binding the sorbate molecules, and chemical adsorption, in which chemical reactions bind the sorbates to the sorbent (Levine, 1988). Note that the term adsorption mentioned in this thesis refers to physical adsorption only, since chemical adsorption is not likely to occur in the systems of interest in this research. Sorption processes are key to many pollutant removal systems and contribute to the complexity of contaminant transport problems in the environment.

In a flow-through porous sorbent system, as is typically found in environmental applications, the movement of the concentration front of the sorbate (or contaminant) is generally described by the concentration-time profile at certain locations. This concentration-time profile is called a *breakthrough curve* (BTC). For an ideal plug flow reactor without sorption, considering a nonreactive sorbate, the elution time of the BTC for the effluent is expected be the same as the hydraulic detention time, and the shape of BTC

should be identical to the input function. In many real systems, because of sorption, the BTC is normally delayed relative to the hydraulic detention time, and the shape of the BTC is altered by the combined effects of axial dispersion and mass transfer resistance associated with sorption (Ruthven, 1984).

From an engineering perspective, one frequently seeks to predict the behavior of a system from limited measurements of its characteristics. For example, a better description of the breakthrough behavior for porous sorbents could lead to a more effective design for treatment devices as well as a more accurate prediction of contaminant transport. To accurately simulate the movement of contaminants in a porous sorbent system, the processes controlling transport retardation and the extent of spread for the BTC need to be understood. The mass transfer processes governing the elution time and shape of the BTC can be grouped into two categories: transport behavior in the bulk fluid phase external to the sorbent grain, and sorption kinetics at the grain scale. The following subsections summarize the current state of knowledge with respect to sorption equilibrium, sorption kinetics at the grain scale, and transport through porous sorbent columns, with emphasis on vapor transport through porous media.

Sorption Equilibrium. Sorption isotherms are generally used to describe the distribution of sorbate molecules among phases under equilibrium conditions at a fixed temperature. The simplest model to express the sorption isotherm is the linear model, which suggests that the sorbate concentration in the sorbed-phase (q) is proportional to the fluid phase concentration (C):

$$q=k_dC \tag{1}$$

where k_d is a partitioning coefficient. The linear isotherm results for a system in which the energetics of sorption are uniform and the loading of the sorbate is low (Weber et al., 1991).

This type of isotherm is commonly used to describe the adsorption equilibrium in the Henry's law region (very low concentration) (Ruthven, 1984), and to represent absorption partitioning (Chiou and Shoup, 1985). For example, a linear relationship has been found to describe the equilibrium sorption of organic contaminants to several soils from the aqueous phase (Karickhoff et al., 1979; Rutherford et al., 1992) and to soil organic matter (SOM) from the vapor phase (Rutherford and Chiou, 1992; Chiou and Kile, 1994). The linear isotherm provides the simplest representation of sorption equilibrium and therefore minimizes the complexity of incorporating sorption behavior into transport models.

However, nonlinear partition behavior for organic sorbates is often found in commercial sorbent systems, such as activated carbon and zeolite, and has also been found for soil and aquifer materials with low organic carbon content (Weber and Miller, 1988; Weber et al., 1992; Shonnard et al., 1993; Young and Ball, 1994). Therefore, a general description of transport through porous sorbents must account for nonlinear sorption.

The simplest nonlinear equilibrium model that possesses a sound theoretical basis is the Langmuir isotherm,

$$q = \frac{q_{mo} bC}{1 + bC} \tag{2}$$

where q_{mo} is the monolayer sorption capacity and b is a coefficient related to the enthalpy of adsorption. The isotherm results from a monolayer model of adsorption which assumes that the surface of the adsorbent comprises a fixed number of identical sites, that each site can only hold one sorbate molecule, and that no interaction occurs among sorbed molecules (Ruthven, 1984). The Langmuir isotherm has been applied extensively to represent sorption of organic molecules to commercial adsorbents with relatively homogeneous surface properties, such as zeolite (Ruthven and Derrah, 1972; Garg and Ruthven, 1972 and 1973) and activated carbon (Kapoor and Yang, 1991). Although the isotherm has also been used to model the sorption data for aquifer materials (Weber and Miller, 1988), the

assumption of homogeneous surface properties on which this model is based is not likely to be valid for many sorbents in the natural environment.

Unlike the Langmuir model, the Freundlich isotherm represents sorption on hetereogeneous surfaces and is not restricted to describe monolayer sorption (Weber et al., 1992). The formulation of the Freundlich isotherm can be expressed as

$$q = kC^n \tag{3}$$

where k and n are empirical parameters. Although the Freundlich isotherm originated as an empirical fit to experimental data, the equation has been derived mathematically based on the assumption that a distribution of Langmuir type adsorption processes simutaneously takes place on adsorbent surface (Sip, 1948; Sposito, 1980). The Freundlich isotherm is perhaps the most widely used nonlinear sorption model (Weber et al., 1991), and has been used to describe many environmental systems, including activated carbon (Hand et al., 1984; Gray and Do, 1989a, 1989b, and 1990), and soil and aquifer materials (Hutzler et al., 1986; Weber and Miller, 1988; Weber et al., 1992; Young and Ball, 1994).

Other sorption equilibrium models have also been used to describe more complex sorption phenomena, including condensation, multicomponent and temperature effects. Since they are beyond the scope of this thesis and excellent reviews can be readily found in the literature (Ruthven, 1984; Yang, 1987; Weber et al., 1991), no further discussion will be made here.

Sorption Kinetics at the Individual Grain Scale. Experimental studies of sorption kinetics have revealed slow and asymmetric sorption-desorption rates for some porous sorbent systems, including zeolite (Ruthven and Derrah, 1972; Garg and Ruthven, 1972) and activated carbon (Gray and Do, 1989a, 1989b, 1990, and 1991). Two classes of mechanisms could control the slow and asymmetric sorption kinetics: reaction rates and mass transfer processes (Weber et al., 1991). Typical models developed to simulate chemical reaction rate control are the so-called one-box and two-box models; diffusion

models are based on the assumption that mass transfer processes are rate-limiting. Although the box models may fit the experimental kinetic data to some extent, they are not truly predictive since their parameters are not known *a priori* (Yiacoumi and Tien, 1994). In addition, this class of models may require extra parameters to fit the observed asymmetric sorption-desorption rate data for porous sorbent systems. In fact, the reaction time needed to reach equilibrium for a physical adsorption process, such as those often found in activated carbon and soil systems, is generally of the order of milliseconds (Weber et al., 1991). Since the observed time to achieve equilibrium may be minutes to hours, the reaction rate is not likely to be the controlling mechanism for sorption kinetics.

Unlike chemical reaction models, mass transfer (diffusion) models have a stronger physical basis and do not need extra parameters to capture the asymmetry of sorption-desorption kinetics. Instead, the diffusion models incorporate isotherm nonlinearity to account for sorption rate asymmetry. Model results indicate that convex nonlinear isotherms (i.e., diminishing rate of increase in sorption capacity with increasing fluid-phase concentration) would accelerate the rate of uptake by sorption slightly, but would decelerate the rate of desorption more strongly (Ruthven and Derrah, 1972; Garg and Ruthven, 1972; Gray and Do, 1989a, 1989b, 1990, and 1991). Asymmetric sorption rates, although observed in many environmental applications, have only been studied systematically in a few cases, such as for hydrocarbons in zeolite and sulfur dioxide in activated carbon. The relationships between isotherm shape and sorption kinetics need to be explored for other environmental systems as well.

Two types of intraparticle diffusion—fluid-phase pore diffusion and sorbent surface diffusion—are normally incorporated in the diffusion models to describe intraparticle transport in porous sorbent systems. The formulations of an accurate diffusion model should take account of the sorbent properties (i.e., pore structure), the nature of sorbent-sorbate interaction, and the sorbate concentration. For example, whereas pore diffusion is expected to be significant for all environmental conditions, surface diffusion

should be important only in small diameter pores in which the pore diffusion flux is small, and only if the sorbed-phase concentration is high (Ruthven, 1984).

The intraparticle diffusion models have been applied to many commercial sorbent systems, including zeolite (Ruthven and Derrah, 1972; Garg and Ruthven, 1972), activated carbon (Gray and Do, 1989a, 1989b, 1990, and 1991) and activated alumina (Desai et al., 1992). Based on the unique pore structure of zeolite, Ruthven and co-workers (Ruthven and Derrah, 1972; Garg and Ruthven, 1972) developed a model to describe the sorption and diffusion of light-weight hydrocarbons in the macropores of the zeolite pellets and in the micropores of crystals within the pellet. Depending on the properties of zeolite, either macropore or micropore diffusion or both could be the rate-controlling mechanism. Using a similar idea, Gray and Do (1989a, 1989b, 1990, and 1991) developed models to describe sorption of sulfur dioxide and carbon dioxide onto activated carbon, accounting for gas-phase diffusion through macropores and micropores simultaneously, or else treating gas-phase macropore diffusion and surface diffusion together. However, often a model of macropore diffusion alone can produce a similar quality of predictions to the macropore and micropore diffusion model for activated carbon systems. In addition, equally good predictions to those of Gray and Do can be generated to describe their experimental data for sulfur dioxide while neglecting surface diffusion. In fact, since sorbate concentrations in environmental applications are generally much smaller than those in encountered the chemical engineering applications, a smaller effect of surface diffusion in environmental systems might be expected.

In addition to studies of commercial sorbents, diffusion models have been applied to resolve sorption kinetics of organic contaminants to natural sorbents, although mostly from the aqueous phase. Wu and Gschwend (1986) and Ball and Roberts (1991) successfully used simple pore diffusion models to fit the sorption rate data for chlorinated

hydrocarbons to soils, sediments and sandy aquifers. However, the tortuosity factors* they obtained were orders of magnitude higher than those that would be expected. Weber and Miller (1988) and Miller and Pedit (1992) employed surface diffusion models to simulate the transport of hydrophobic solutes within aquifer materials. They neglected the fact that the pore diffusion flux is probably more important than the surface diffusion flux at low sorbate concentrations. In fact, the models describing surface diffusion and pore diffusion become indistinguishable once the isotherm becomes linear. Yiacoumi and Tien (1994) recently proposed a dual diffusion model, including pore diffusion within soil grains, and partition and diffusion within soil organic matter, to describe existing experimental kinetic data. In their model, only SOM was considered as an active component and a linear isotherm was assumed. Although the model has a sound theoretical basis and yields reasonably good fits to the data, no experimental investigation of diffusion coefficients within SOM has yet been conducted.

Transport through Sorbent Columns. Transport of a single sorbate in the mobile phase (external to the sorbent grains) of a porous medium is often described by a one-dimensional advection-dispersion-sorption (ADS) (also called dispersed plug flow) equation (Ruthven, 1984; Weber et al., 1991). The equation is derived from a differential material balance assuming constant temperature and flow velocity:

$$\frac{\partial C_b}{\partial t} = D_L \frac{\partial^2 C_b}{\partial z^2} - u\frac{\partial C_b}{\partial z} - \left(\frac{1-\varepsilon}{\varepsilon}\right)\rho_b\left(\frac{\partial M}{\partial t}\right) \qquad (4)$$

where C_b is the fluid-phase sorbate concentration in the column pores (external to the sorbent grains), z is the axial coordinate for the column, u is the interstitial fluid velocity (i.e., the volumetric flow rate divided by the cross-sectional pore area), D_L is the

---

* Tortuosity factor, τ, is defined as $\tau = D/D_p$ in this case, where D_p is the observed pore diffusivity of molecules, and D is the molecular diffusivity for the aqueous phase or the combined diffusivity (including both molecular diffusion and Knudsen diffusion) for the gas phase.

dispersion coefficient generally related to both molecular diffusion and mechanical dispersion processes, ε is the porosity, ρ_b is the grain density of the sorbent and M is the sorbed mass of sorbate per mass of sorbent.

In the ADS model, the effects of all mechanisms which contribute to axial dispersion are lumped into one parameter (Ruthven, 1984). In general, larger axial dispersion will produce a broader BTC. Detailed reviews of the effects of dispersion on transport through packed beds have been presented by Langer et al. (1978) and Wakao and Kaguei (1982). In general, the value of the dispersion coefficient, D_L, can be determined either using a tracer method or by means of empirical correlations.

Whereas the effects of advection and dispersion on transport through porous media have been studied extensively, the effects of sorption are highly sorbent-specific and need further elucidation. It is the sorption term that links the ADS equation to the sorption equilibrium and kinetic models summarized in previous sections, thereby complicating the analysis of transport problems. Depending on the time scale associated with attainment of equilibrium at the single particle scale, compared with that for concentration changes due to advection and dispersion processes, the ADS may or may not need to incorporate sorption kinetic models to describe column breakthrough.

If sorption rates at the single particle scale are fast enough to allow attainment of equilibrium, the ADS equation can be used to describe the movement of contaminants in the system by simply applying the assumption of local equilibrium. Under this assumption, the sorbed-phase concentration at any position within the sorbent column is considered to be in equilibrium with the adjacent fluid-phase concentration. The local equilibrium approximation provides simple (often analytical) solutions, which are convenient for engineering purposes and which may give useful insight into the behavior of more complex systems. In fact, this approach has been successfully used in several cases, including VOC transport in low moisture soils under specific flow conditions (Shonnard et al., 1993; Batterman et al., 1995). However, real systems are not always so simple. Recent studies

(Miller and Weber, 1988; Pignatello, 1991; Harmon et al., 1992) suggest that the local equilibrium approximation does not adequately account for the observed transport behavior of organic contaminants in many instances. Therefore, kinetic sorption models, as described in the previous section, may need to be considered in describing contaminant movement through porous media.

Finally, to predict the breakthrough behavior from model simulations, parameters that characterize sorbent-sorbate interaction must be determined. Although models involving the ADS equation and sorption kinetics have been successfully applied to predict the experimental behavior in laboratory columns (Garg and Ruthven, 1973 and 1974; Young and Ball, 1994) and in controlled field studies (Harmon et al., 1992), the procedures needed to obtain input parameters are rather tedious. Conventionally, several separate experiments must be conducted to extract the required sorption equilibrium and kinetic parameters for each specific sorbent-sorbate system. A simpler technique by which to obtain all the input parameters would be greatly beneficial in modeling transport through real porous media.

Summary. Transport of sorbates through sorbent columns has been shown to be governed by three elements: sorption equilibrium, sorption kinetics at the individual grain scale, and mass transport through the column. To model the breakthrough behavior of sorbates, all three processes must be considered. In sorption equilibrium models, the linear isotherm typically represents either adsorption at low adsorbate concentration or partitioning absorption. For the two most commonly employed nonlinear isotherm models, the Langmuir isotherm is appropriate for monolayer adsorption onto homogeneous surface adsorption sites, whereas the Freundlich isotherm may be appropriate for the sorption onto a heterogeneous surface.

Intraparticle diffusion is considered to be the most likely mechanism responsible for slow sorption kinetics. When coupled with a nonlinear isotherm, the model requires no extra parameters to capture the asymmetry of sorption-desorption kinetics. Although

asymmetric sorption rates are commonly found in environmental applications, few systems have been studied systematically. The relationships between isotherm shape and sorption kinetics should be explored for a broader range of sorbent-sorbate systems, particularly those of environmental significance.

Since the model formulations are very sorbent and sorbate dependent, diffusional processes at the grain scale must be carefully considered. Models based on intraparticle diffusion have been successfully employed to describe the sorption kinetics for zeolite and activated carbon systems. However, similar modeling efforts applied to the sorption of organic contaminants in soil systems, although generating good fits to the data, did not yield physically meaningful diffusion coefficients. Furthermore, additional experiments need to be conducted for determining diffusional properties in sorbents, such as the diffusion coefficient within soil organic matter, so that more accurate model predictions can be made.

When coupled with appropriate sorption equilibrium and kinetic models, the ADS equation can be used to predict BTCs for laboratory columns and controlled field studies. However, the procedures for determining the required input parameters are tedious. A technique that requires less experimental effort is therefore desired.

APPLICATIONS

Of the many environmental systems involving transport of contaminants through porous sorbents, this dissertation focuses on gas-phase transport of volatile organic compounds (VOCs) and water vapor in soil and activated carbon systems. VOCs are chosen as a representative contaminant group as many of them are highly toxic and they are commonly encountered in environmental applications. In contrast, water vapor is selected because it is present in most environmental systems and may have strong influence on sorption processes for both soil and activated carbon systems.

A better understanding of the transport mechanisms for VOCs in water-unsaturated soil systems may improve our ability to evaluate (a) the health risk associated with indoor

VOCs transported from contaminated subsurfaces (Little et al., 1992), (b) the performance of clean-up techniques for contaminated sites (e.g., soil vapor extraction) (Johnson et al., 1988), and (c) the design procedures for appropriate soil cover depth for landfill sites (Karimi et al., 1987). Part of this study is aimed at improving our knowledge of the mechanisms governing the transport of VOCs and water vapor in soils. Since soil is acknowledged to be a dual sorbent, in which soil organic matter (SOM) acts as a partition medium and mineral surface as a conventional adsorbent (Chiou and Shoup, 1985, Rutherford et al., 1992; Rutherford and Chiou, 1992), the transport and sorption of VOCs and water vapor in the two soil components are studied separately as a foundation for future investigations of more complex systems, such as those involving multiple sorbents and multiple sorbates.

For activated carbon, a thorough knowledge of the mechanisms controlling intragranular VOC transport may improve the design of more efficient and reliable sorbent-based devices, such as those used to remove VOCs in air stripper off-gas (Crittenden et al., 1988) and to reduce VOC concentrations in indoor air (Liu, 1993). No prior studies of activated carbon have specifically addressed the relationships between adsorption/desorption kinetics and equilibrium for VOCs and water vapor and their impact on transport through sorbent columns, even though these sorbent-sorbate combinations are commonly found in environmental applications. Part of this research is designed to improve our understanding of these issues.

SCOPE AND OBJECTIVES

The aim of this thesis is to improve our understanding of the relationships among sorbent properties, equilibrium isotherms and intraparticle diffusion processes for the transport and sorption of VOCs and water vapor in soil and activated carbon systems. In engineering analysis, it is desirable to be able to extrapolate from experimental observations in one setting to a different environment. One goal of the present study is to be able to

predict sorbent column behavior from batch experiments on the characteristics of individual sorbent grains.

Both theoretical analysis and laboratory experiments are conducted to characterize the transport behavior at sorbent grain/fiber scale and at the laboratory column scale. The relationships among sorbent properties, equilibrium isotherms and sorption kinetics at the individual sorbent particle scale are first studied using appropriate intraparticle diffusion models. The results at this scale are then used as a basis to predict the breakthrough behavior for transport through laboratory columns. The experimental and theoretical findings from this research are aimed at serving as a basis for investigations aimed at understanding more complex environmental systems.

These are the specific objectives of this research:

1. to explain the commonly observed slow, asymmetric sorption-desorption rates for VOC and water vapor in mineral soil systems;
2. to study the relationships between sorption equilibrium and sorption kinetics for water vapor and VOC sorption on soil organic matter;
3. to develop a scheme to predict sorption isotherms and column breakthrough curves for VOCs to soil and activated carbon systems based on minimum experimental effort; and
4. to characterize the intraparticle diffusional processes as well as the relationships between the complicated adsorption-desorption isotherms and sorption kinetics for water vapor sorption on activated carbon.

DISSERTATION OVERVIEW

In Chapter II, the transport and sorption of VOCs and water vapor are studied at the level of individual grains for three different dry soils. Experimental measurements are made of soil properties, sorption capacity, and sorption and desorption rates. A porous sphere model, which accounts for internal diffusion, is coupled with the nonlinear Freundlich isotherm to interpret the sorption rate data. The model shows that the degree of

asymmetry between sorption and desorption rates depends on the nonlinearity of the isotherm, i.e. the exponent in the Freundlich equation. The model follows both sorption and desorption trends reasonably well using a single fitted parameter, the effective diffusivity. The model also provides good resolution of the substantial asymmetry in the rates of sorption and desorption.

Equilibrium partitioning and the kinetics for sorption of water vapor and benzene to a model soil organic matter, peat, is studied in Chapter III. Sorption characteristics are determined using an electrobalance. Experimental results reveal that the water vapor sorption isotherm is similar to that reported in the literature. However, no reproducible values for sorption capacity could be obtained for the benzene/peat system. For both water vapor and benzene, the sorption rates of peat are substantially faster than desorption rates. The pore diffusion model is found to describe the sorption rates of water vapor very well assuming that pore diffusion is the rate limiting intragranular transport process. The possible reasons causing sorption rate asymmetry of benzene to peat are also discussed.

In Chapter IV, the breakthrough behavior of benzene through both dry and moist soil columns under various flow conditions is explored. Sorption kinetic experimental data are determined using a differential adsorption bed (DAB) technique, and breakthrough curves are measured for a packed column for both dry and moist soil. For the case of dry soil, the sorption isotherm is nonlinear. The experimental findings in this study show that the asymmetry between adsorption and desorption rates can be used to predict the sorption isotherm from a single kinetic experiment. Predictions based on the parameters extracted from the kinetic experiment, combined with transport equations for a dry soil column, are found to be in good agreement with the experimental BTCs. Because the isotherm is linear for the moist soil, several simplified models appropriate for linear isotherms are compared with the experimental results under three different flow regimes. The model predictions conform to the experimental data very well for all cases despite the wide range of flow conditions.

The relationship between sorption equilibria and kinetics for benzene and vinyl chloride on activated carbon grains and fibers is investigated in Chapter V. Sorption kinetics are determined with a an electrobalance, while sorption equilibria are determined both with the electrobalance and through column experiments. The porous sphere model (developed in Chapter II) and a similar porous cylinder model are used to interpret the experimental data. The models provide good fits to the experimental data for both adsorption and desorption. Using the same technique developed in Chapter IV, it is shown that the sorption isotherm and column breakthrough curves can be accurately predicted from a single kinetic experiment.

Chapter VI describes the transport and sorption of water vapor within individual activated carbon grains. Sorption kinetics and equilibrium partitioning of water vapor were determined using an electrobalance for relative humidities (RH) in the range 0 to 86% at 20 °C. A model accounting for both pore and surface diffusion along with the experimentally determined piecewise-linear isotherm is used to interpret the sorption rate data. The model fits all of the experimental data very well and the asymmetry between adsorption and desorption rates is well resolved, despite the complicated shape and hysteresis of the isotherm. The model assuming intragranular transport by pore diffusion only is found to yield reasonable agreement with experimental data up to RH=60% in our system; surface diffusion is found to be important at higher RH values.

Chapter VII summarizes the experimental and theoretical findings for transport and sorption of VOCs and water vapor in the porous media studied in this dissertation. Implications of these findings and future research directions related to this topic are also discussed.

APPENDIX I. REFERENCES:

Ball, W.P., and Roberts, P.V. (1991). "Long-term sorption of halogenated organic chemicals by aquifer material: 2. Intraparticle diffusion." *Environ. Sci. Technol., 25,* 1237-1249.

Batterman, S., Kulshrestha A., and Cheng, H.-Y. (1995). "Hydrocarbon vapor transport in low moisture soils." *Environ. Sci. Technol., 29,* 171-180.

Chiou, C.T., and Kile, D.E. (1994) "Effects of polar and nonpolar groups on the solubility of organic compounds in soil organic matter." *Environ. Sci. Technol., 28,* 1139-1144.

Chiou, C.T., and Shoup, T. D. (1985). "Soil sorption of organic vapors and effects of humidity on sorptive mechanism and capacity." *Environ. Sci. Technol., 19,* 1196-1200.

Crittenden, J.C., Cortright, R.D., Rick, B., Tang, S.-R., and Perram, D. (1988). "Using GAC to remove VOCs from air stripper off-gas." *J. AWWA, 80,* 73-84.

Desai, R., Hussain, M., and Ruthven, D.M. (1992). "Adsorption on activated alumina. II. Kinetic behaviour." *Can. J. Chem. Eng., 70,* 707-715.

Garg, D.R., and Ruthven, D.M. (1972). "The effect of the concentration dependence of diffusivity on zeolite sorption curves." *Chem. Eng. Sci., 27,* 417-423.

Garg, D.R., and Ruthven, D.M. (1973). "Theoretical prediction of breakthrough curves for molecular sieve adsorption columns: I. Asymptotic solutions." *Chem. Eng. Sci., 28,* 791-798.

Garg, D.R., and Ruthven, D.M. (1974). "The performance of molecular sieve adsorption columns: Systems with macropore diffusion control." *Chem. Eng. Sci., 29,* 1961-1967.

Gray, P.G., and Do, D.D. (1989a). "Adsorption and desorption of gaseous sorbates on a bidispersed particle with Freundlich isotherm: I. Theoretical analysis." *Gas Sep. Purif., 3,* 193-200.

Gray, P.G., and Do, D.D. (1989b). "Adsorption and desorption of gaseous sorbates on a bidispersed particle with Freundlich isotherm: II. Experimental study of sulphur dioxide sorption on activated carbon particles." *Gas Sep. Purif.*, *3*, 201-208.

Gray, P.G., and Do, D.D. (1990). "Adsorption and desorption dynamics of sulphur dioxide on a single large activated carbon particle." *Chem. Eng. Comm.*, *96*, 141-154.

Gray, P.G., and Do, D.D. (1991). "Dynamics of carbon dioxide sorption on activated-carbon particles" *AIChE J.*, *37*, 1027-1034.

Hand, D.W., Crittenden, J.C., and Thacker, W.E. (1984). "Simplified models for design of fixed-bed adsorption systems." *J. Env. Eng., ASCE, 110*, 440-456.

Harmon, T.C., Semprini, L., and Roberts, P.V. (1992). "Simulating solute transport using laboratory-based sorption parameters." *J. Env. Eng., ASCE, 118*, 666-689.

Hutzler, N.J., Crittenden, J.C., Gierke, J.S., and Johnson, A.S. (1986). "Transport of organic compounds with saturated groundwater flow: Experimental results." *Water Resources Res.*, *22*, 285-295.

Johnson, P.C., Kemblowski, M.W., and Colthart, J.D. (1988). "Practical screening models for soil venting applications." *Proceedings of NWWA/API Conference on Petroleum Hydrocarbons and Organic Chemicals in Ground Water*, Houston, TX, pp. 521-546.

Kapoor, A., and Yang, R.T. (1991). "Contribution of concentration-dependent surface diffusion to rate of adsorption." *Chem. Eng. Sci.*, *46*, 1995-2002.

Karickhoff, S.W., Brown, D.S., and Scott, T.A. (1979). "Sorption of hydrophobic pollutants on natural sediments." *Water Research* , *13*, 241-248.

Karimi, A.A., Farmer, W.J., and Cliath, M.M. (1987). "Vapor-phase diffusion of benzene in soil." *J. Environ. Qual.*, *16*, 38-43.

Langer, G., Roethe, A., Roethe, K.-P., and Gelbin, D. (1978). "Heat and mass transfer in packed beds: III. Axial mass dispersion." *Int. J. Heat Mass Transfer*, *21*, 751-759.

Levine, I.N. (1988). *Physical Chemistry.* 3rd ed., McGraw-Hill, New York, N.Y.

Little, J.C., Daisey, J.M., and Nazaroff, W.W. (1992). "Transport of subsurface contaminants into buildings: An exposure pathway for volatile organics." *Environ. Sci. Technol., 26,* 2058-2066.

Liu, R.-T. (1993). "Model simulation of the performance of activated carbon adsorbers for the control of indoor VOCs." *Proceedings of the 6th International Conference on Indoor Air Quality and Climate*, Vol. 6, Indoor Air '93, Helsinki, Finland, pp. 421-428.

Miller, C.T., and Pedit, J.A. (1992). "Use of a reactive surface-diffusion model to describe apparent sorption-desorption hysteresis and abiotic degradation of lindane in a subsurface material." *Environ. Sci. Technol., 26,* 1417-1427.

Miller, C.T., and Weber, W.J. (1988). "Modeling the sorption of hydrophobic contaminants by aquifer materials: II. Column reactor systems." *Water Research, 22,* 465-474.

Pignatello, J.J. (1991). "Desorption of tetrachloroethene and 1,2-dibromo-3-chloropropane from aquifer sediments." *Environ. Toxi. Chem., 10,* 1399-1404.

Rutherford, D.W., and Chiou, C.T. (1992). "Effect of water saturation in soil organic matter on the partition of organic compounds." *Environ. Sci. Technol., 26,* 965-970.

Rutherford, D.W., Chiou, C.T., and Kile, D.E. (1992). "Influence of soil organic matter composition on the partition of organic compounds." *Environ. Sci. Technol., 26,* 336-340.

Ruthven, D.M. (1984). *Principles of Adsorption and Adsorption Processes*. John Wiley and Sons, New York, N.Y.

Ruthven, D.M., and Derrah, R.I. (1972). "Sorption in Davison 5A molecular sieves." *Can. J. Chem. Eng., 50,* 743-747.

Shonnard, D.R., Bell, R.L., and Jackman A.P. (1993). "Effects of nonlinear sorption on the diffusion of benzene and dichloromethane from two air-dry soils." *Environ. Sci. Technol., 27,* 457-466.

Sip, R. (1948). "On the structure of a catalyst surface." *Journal of Chemical Physics, 16,* 490-495.

Sposito, G. (1980). "Derivation of the Freundlich equation for ion exchange reactions in soils." *Soil Sci. Soc. Am. J., 44,* 652-654.

Wakao, N. and Kaguei, S. (1982). *Heat and Mass Transfer in Packed Bed,* Gordon and Breach Science Publishers, New York, N.Y.

Weber, W.J., and Miller, C.T. (1988). "Modeling the sorption of hydrophobic contaminants by aquifer materials: I. Rates and equilibria." *Water Research, 22,* 457-464.

Weber, W.J., McGinley, P.M., and Katz, L.E. (1991). "Sorption phenomena in subsurface systems: Concepts, models and effects on contaminant fate and transport." *Water Research, 25,* 499-528.

Weber, W.J., McGinley, P.M., and Katz, L.E. (1992). "A distributed reactivity model for sorption by soils and sediments. 1. Conceptual basis and equilibrium assessments." *Environ. Sci. Technol., 26,* 1955-1962.

Wu, S.-C., and Gschwend, P.M. (1986). "Sorption kinetics of hydrophobic organic compounds to natural sediments and soils." *Environ. Sci. Technol., 20,* 717-725.

Yang, R.T. (1987). *Gas Separation by Adsorption Processes.* Butterworths, Stoneham, MA.

Yiacoumi, S., and Tien, C. (1994). "A model of organic solute uptake from aqueous solutions by soils." *Water Resources Res., 30,* 571-580.

Young, D.F., and Ball, W.P. (1994). "*A priori* simulation of tetrachloroethene transport through aquifer material using an intraparticle diffusion model." *Environmental Progress, 13,* 9-20.

Chapter II

Transport and Sorption of Volatile Organic Compounds and Water Vapor within Dry Soil Grains*

ABSTRACT

Mechanisms governing the rates of adsorption and desorption of benzene, trichloroethylene, and water vapor by dry soil grains are investigated. For three different test soils, determinations are made of organic carbon content, specific surface area, grain density, grain porosity, and pore size distribution. Experimental measurements of the rates of adsorption and desorption show that periods of hours are required to achieve equilibrium. In addition, adsorption is observed to be much faster than desorption. A porous sphere model accounting for internal diffusion in spherical grains coupled with a nonlinear Freundlich isotherm is used to interpret the sorption rate data. The model follows both adsorption and desorption trends reasonably well using a single fitted parameter, the effective diffusivity. The model also provides good resolution of the substantial asymmetry in the rates of uptake and release. In a refinement, a parallel pore model is used to account more fully for effects of the experimentally measured pore size distribution.

---

* This chapter is taken from a published paper: Lin, T.-F., Little, J.C., and Nazaroff, W.W. (1994). "Transport and sorption of volatile organic compounds and water vapor within dry soil grains." *Environ. Sci. Technol.*, *28*, 322-330. Minor changes have been made to fit the format of this dissertation.

INTRODUCTION

For those living near contaminated subsurface sites, transport of volatile organic compounds (VOCs) through the unsaturated zone and into buildings may represent a significant exposure pathway (Little et al., 1992). To gain a clearer understanding of this transport route, research was initiated to investigate the sorption of VOCs on relatively dry soils such as might be expected beneath buildings. Since the presence of moisture strongly influences the sorption capacity, our first experiments were conducted using completely dry soil grains exposed to air containing either benzene, trichloroethylene or water vapor. These relatively simple experiments revealed some surprising results. First, it took several hours to reach equilibrium suggesting that a kinetic limitation was governing the uptake and release. In addition, adsorption was significantly faster than desorption, and the asymmetry in response was more marked for the VOCs than for water vapor. Although dry soil grains represent an improbable extreme for natural soils, we felt that a sound understanding of the processes involved was needed as a foundation to fully understand sorption of VOCs in the more complex case of moist soils.

Sorption processes are widely acknowledged to play an important role in the transport and fate of organic contaminants in subsurface systems (Weber et al., 1992). However, most sorption research has focused on equilibrium conditions and relatively few studies have considered kinetics. In fact, a lumped retardation coefficient, which assumes local equilibrium, does not adequately account for the observed subsurface transport of VOCs in many instances (Pignatello, 1991). Recent studies have suggested that intragrain diffusion is the major reason for a slow approach to equilibrium (Wu and Gschwend, 1986; Steinberg et al., 1987; Pignatello, 1991; Ball and Roberts, 1991b). For example, Wu and Gschwend (1986) have noted that the kinetic data for sorption of hydrophobic organic compounds onto sediments from water can be explained by a simple diffusion model. Thus far, the few kinetic studies have been limited to sorption in water saturated

systems. However, it is also important to understand sorption kinetics in unsaturated soil media.

In this chapter, mechanisms for the adsorption and desorption of benzene, trichloroethylene and water vapor by dry soil grains are elucidated. Three soil samples having different properties are well characterized. The samples are then exposed to stepwise increase and decrease in the concentration of the sorbate in air. During exposure, the adsorption/desorption process is continuously monitored by measuring the mass of the soil grains in a microbalance. Intragrain diffusion models coupled with a nonlinear sorption isotherm are used to account for the observed asymmetry in kinetics. The relationship between sorption mechanisms and the soil grain structure is developed.

MATERIALS AND METHODS

Adsorbates and Adsorbents. Benzene and trichloroethylene (TCE) were chosen as representative VOCs as each is commonly found at contaminated subsurface sites. For this study, the concentration ranges were set between 100 and 1000 ppm_v, or 2 to 3 orders of magnitude lower than the saturated vapor concentrations. In addition to these two VOCs, water vapor was studied because the presence of moisture can strongly suppress the uptake of VOCs (Chiou and Shoup, 1985). The water vapor concentrations were varied between 12 and 88% relative humidity at 20 °C. The gas phase concentrations of the two VOCs and water vapor used in this study were chosen to reflect conditions of soil gas near houses.

Three soils were used: sand, representing a simple and low organic carbon content soil; a synthetic soil matrix (SSM) (USEPA, 1988) prepared by the Environmental Protection Agency; and a field soil (McAFB) from a Superfund site at McClellan Air Force Base near Sacramento in California. To simplify interpretation of the data, only a narrow particle size range from each soil was used. For SSM and McAFB a size range of between 20 and 30 US standard mesh (0.60-0.85 mm) was chosen, while for sand a size range of between 30 and 60 mesh (0.25-0.60 mm) was used.

Soil Characterization. Various measures were used to characterize the three soils. A photomicrograph of the exterior soil grain surface was obtained with a scanning electron microscope (SEM). Specific surface area[1] and organic carbon content[2] (OC) were measured, as these can strongly influence VOC sorption behavior (Karickhoff et al., 1979; Chiou and Shoup, 1985). Mineral surface area is especially important in sorption by dry soils (Ong and Lion, 1991a). Grain density, grain porosity, and pore size distribution were also determined as these were required to interpret the kinetic data.

Surface area was measured by low-temperature nitrogen adsorption as well as by mercury intrusion. The nitrogen adsorption data were interpreted using the BET[3] equation (Brunauer et al., 1938) and the mercury intrusion data were analyzed with the Washburn equation[4] (Lowell and Shields, 1984). The nitrogen adsorption method measures the

---

[1] Specific surface area is defined as the surface area (m^2) per unit mass (g) of a solid.

[2] Organic carbon (OC) content is defined as the mass fraction of dry soil that is carbon in an organic form. It is often measured by a combustion procedure, whereby the C is converted to CO_2, or, alternatively, by chemical reduction of potassium dichromate by organic matter, in which potassium dichromate is measured by titration (Allison, 1965).

[3] BET (Brunauer-Emmett-Teller) equation is expressed as

$$\frac{1}{q(\frac{P}{P_o}-1)} = \frac{1}{C_B q_{mo}} + \frac{(C_B-1)\ (\frac{P}{P_o})}{C_B q_{mo}}$$

where q_{mo} is the monolayer adsorption capacity, which is proportional to the total surface area, and C_B is a parameter that depends on the shape of the isotherm. By fitting this equation to measurements of q and (P/P_o) at several conditions in the range $0.05 < P/P_o < 0.35$, the surface area of the sample can be inferred.

[4] The general form of Washburn equation is

$$P_{ap}\, dV = -\gamma_m \cos\theta_c\, dA$$

surface area of pores with radii larger than about 0.35 nm (the diameter of a nitrogen molecule), while mercury intrusion measures the surface area of pores with radii between about 1.8 nm and 1000 nm. If the surface area associated with pores larger than 1000 nm may be ignored, then the difference between these two measurements provides an indication of the degree of porosity in the size range 0.35 to 1.8 nm (Lowell and Shields, 1984). Before performing the nitrogen adsorption and mercury intrusion tests, the soil samples were held under vacuum of less than 1.3 Pa at 130°C for more than 24 hours. Ball et al. (1990) have shown that this treatment effectively removes water and other adsorbed gases. Samples with a total surface area larger than 1 m^2 were used for each of the runs. The nitrogen adsorption and mercury intrusion tests were carried out in a Quantasorb Surface Area Analyzer at 77 K and a Quantachrome Mercury Porosimeter (Quantachrome Corp., Syosset, N.Y.), respectively. In addition to obtaining the specific surface area, the mercury intrusion results were also interpreted to obtain grain porosity and pore size distribution (Lowells and Shields, 1984).

Organic carbon was measured by the Walley-Black method (Allison, 1965) in which potassium dichromate is used to oxidize 3 to 10 grams of pulverized soil sample with OC determined by ferrous sulfate back titration. The grain density of the soils was measured by the water displacement method of Blake (1965).

Sorption Experiments. Sorption experiments were performed with a Cahn-1000 electrobalance (Cahn Inc., Cerrito, CA) enabling the determination of both sorption

---

where P_{ap} is the applied pressure, dV is the incremental volume of pores in the solid filled by mercury at P_{ap}, γ_m is the surface tension of mercury, θ_c is the contact angle of mercury and solid interface, and dA is the incremental surface area of the pores associated with dV (Lowell and Shields, 1984). By conducting a mercury intrusion experiment, the cumulative pore-volume intruded by mercury can be obtained as a function of P_{ap}. Interpretation of the cumulative pore-volume curve yields dV as a function of P_{ap}. Using the Washburn equation, dA can be calculated from this information. The surface area can then be estimated by integrating dA over the pressure range of the intrusion experiment.

kinetics and isotherms. The electrobalance, which can weigh to a precision of ±1 μg provided that careful control is exercised, was maintained at 20.0±0.1°C inside a temperature-controlled cabinet as shown in Figure 1.

A pre-weighed sample of 0.05 to 0.2 g of oven-dried (24 hrs at 105 °C) soil was placed in a single layer of grains on the pan inside the electrobalance. High purity hydrocarbon-free (HC-free) air (Scott Specialty Gases, Fremont, CA) was then passed through the electrobalance to condition the soil sample. Generally the sample weight stabilized within 24 hours. The total hydrocarbon content (as methane) in the HC-free air is less than 0.1 ppm_v while water vapor is less than 5 ppm_v. The overall sample weight change during this conditioning period was less than 0.5%.

On reaching constant weight, the HC-free air was diverted through a VOC or water vapor generator and then back to the electrobalance. A diffusion vial filled with liquid benzene or TCE and placed inside a permeation tube holder (VICI, Santa Clara, CA) was used as a VOC generator, while a gas bubbler was used as a water vapor generator. The temperature of both generators was controlled within ±0.1°C of the preset temperature. The concentrations of VOCs in the air were determined by a gas chromatograph equipped with a flame ionization detector (Varian, Model 3700, Palo Alto, CA), while relative humidity was measured by a dew-point hygrometer (EG&G, Model 911, Waltham, MA). As the sample started to adsorb the VOCs or water vapor, the weight change on the sample pan was plotted on a chart recorder (Fisher, Model D-500, Austin, TX). After some time, the weight of the sample again became constant. The air supply was then replaced by clean HC-free air and a desorption curve was obtained. Typically, an adsorption time of 2 to 4 hours was required for the soil sample to reach equilibrium, while more than 6 hours was needed for complete desorption. Since gas retention time in the electrobalance chamber is short (~ 10 s in this case) relative to that for the kinetic experiment, the impact of mixing problem within the chamber is neglected.

RESULTS AND DISCUSSION

Soil Properties. Figure 2 shows the SEM photos for all three soils. Careful examination suggests that there are relatively few pores in the soil grains having radii much larger than about 1 μm.

The results of the soil property tests are summarized in Table 1. Evidence suggests that the OC in the dry soils used in this study did not play a large role in the gas-phase sorption process under dry conditions. The values of OC are all relatively low. As expected, sand is lowest at 0.014% while SSM and McAFB are 0.25 and 0.43%, respectively. Rutherford and Chiou (1992) found that soil organic matter (SOM) takes up about 400 mg/g of water vapor under saturated conditions. The equivalent values for benzene and TCE are about 40 mg/g and 80 mg/g, respectively. Broadbent (1965) has suggested that the ratio of SOM to OC in mineral soils is about 2. Accordingly, the saturation water sorption capacities attributable to the OC in SSM, McAFB and sand are roughly 2, 3 and 0.1 mg/g, respectively. The values for SSM and sand are one to two orders of magnitude lower than the measured water uptake at RH=85%, although the value for McAFB is closer to that observed. Similarly, the saturation sorption capacity of benzene and TCE in the OC of SSM is roughly 0.2 and 0.4 mg/g, respectively. These values are about one order of magnitude less than the observed sorption capacity at vapor concentrations that are well below saturation.

SSM has a relatively high specific surface area, 8 m^2/g. Corresponding values for McAFB and sand are significantly lower at 0.6 and 0.4 m^2/g, respectively. A nominal surface area may be calculated by assuming that all grains are smooth spheres with diameter equal to the geometric mean of the size range. The ratios of the measured surface area to the nominal surface area for SSM, McAFB and sand are about 3000, 300 and 60, respectively. Taken together with the relatively smooth exterior surfaces shown in the photomicrographs, these ratios suggest that most of the accessible surface area lies within the soil grains.

The grain porosity varies from a substantial 15% for SSM to 6.2% for McAFB and 1.4% for sand. These results are consistent with previous studies, in which the porosity of sand was found to vary from 0.3 to 5% (Ball and Roberts, 1991a) and soil from 5 to 19% (Wood et al., 1990). The pore volume and surface area distribution for SSM shown in Figure 3 is typical of the three soils. Most of the pore volume is associated with the pores larger than 50 nm while most of the pore surface is associated with pores smaller than 5 nm. Since sorption on dry soil grains is thought to be predominantly a surface phenomenon (Chiou and Shoup, 1985), the small pores may be expected to play a large role.

Sorption Isotherms. The sorption isotherms for benzene, TCE and water vapor on SSM, McAFB and sand were all found to be nonlinear. The Freundlich isotherm, expressed in a surface sorption form, was used to fit the experimental data:

$$q = kC^n \tag{1}$$

where q is the sorbed mass (mg adsorbate/cm^2 adsorbent surface area) in equilibrium with C, the gas-phase concentration (mg adsorbate/cm^3 air), and k and n are empirical parameters. The Freundlich isotherm yielded a good fit to the equilibrium data in this study. However, the method of interpreting the kinetic results does not depend on the form of the isotherm. Typical isotherms are shown in Figure 4, with complete results summarized in Table 2. Assuming that the cross-sectional area of water molecules is 10.8 $\times 10^{-20}$ m^2 (Ong and Lion, 1991b), the average surface coverage of water molecules on SSM, McAFB and sand is 6, 17 and 13 layers, respectively, at RH=68%. The relative consistency of these numbers is in accord with Ong and Lion (1991a) who found that the sorption capacity of oven-dry soil is proportional to the available surface area. The average surface coverage on SSM for benzene (relative saturation pressure, p/p_o=0.0065) and TCE (p/p_o=0.0091) is only 0.56 and 0.32 of a layer, respectively, under the assumption that the cross-sectional areas of benzene and TCE molecules are 40.0 and 30.7 $\times 10^{-20}$ m^2, respectively (Ong and Lion, 1991b). These surface coverages are much lower than those

of water for two reasons: (1) the lower strength of physical interaction between the mineral surface and the non-polar organic molecules, and (2) the fact that the gas-phase concentration employed in these studies is much higher in the case of water vapor.

Sorption Curve Asymmetry. Typical kinetic sorption data for water vapor and benzene are shown in Figures 5a and 5b, respectively. The sorption processes are relatively slow, if compared with the time for molecule diffusing in air, and desorption rates are always slower than adsorption rates. The difference between adsorption and desorption is much greater for benzene and TCE than for water vapor. Similar asymmetry in sorption rates for 1,2-dibromoethane and TCE on dry clay was reported by Sawhney and Gent (1990). Crank (1975) showed that concentration-dependent diffusion can result in different rates of adsorption and desorption. Ruthven and coworkers (Garg and Ruthven, 1972; Ruthven and Derrah, 1972), working on diffusion of hydrocarbons in zeolites, extended the idea and showed that a nonlinear Langmuir sorption isotherm can produce similar results. Recently, Miller and Pedit (1992) suggested that asymmetry of sorption rates (referred to in their paper as "sorption-desorption hysteresis") may be attributed to an n value in the Freundlich isotherm of less than one.

Porous Sphere Model. To interpret the kinetic results, a mathematical model is formulated that couples intragrain diffusion with the nonlinear Freundlich isotherm describing partitioning between the solid surface and the gas phase in the pores. The soil grains are assumed to be spheres of constant diameter with accessible pore surface area distributed uniformly throughout the grain. Considering transient diffusion and sorption, a mass balance on a small volume element within the grain is combined with Fick's first law of diffusion to give (Ruthven, 1984)

$$\varepsilon\frac{\partial C}{\partial t}+(1-\varepsilon)\rho_p S\frac{\partial q}{\partial t}=\frac{\varepsilon}{r^2}\frac{\partial}{\partial r}\left(r^2 D_p\frac{\partial C}{\partial r}\right) \qquad (2)$$

where ε is the grain porosity, ρ_p is the density of the solid part of the adsorbent, S is the BET specific surface area of the adsorbent, r is the radius, t is time and D_p is the gas

diffusivity of sorbate molecules through the intragranular pore space. In equation (2), transport is assumed to occur only by gas-phase diffusion; in particular, surface diffusion (Satterfield, 1970) is not included. Based on available evidence (Sladek et al., 1974), approximate calculations suggest that the adsorbed-phase diffusive flux may approach the gas-phase flux under certain circumstances in our experiments. However, the nature of our experiments does not readily permit distinction between surface diffusion and gas-phase diffusion within soil grains.

Since the sorbed state is strongly favored (the mass of adsorbate in the gas phase is always well below 1% of the sorbed mass) the first term in eq (2) can be safely neglected. Assuming that sorption within the pores follows the Freundlich equation, and is locally instantaneous, eqs (1) and (2) can be combined to give

$$\frac{\partial q}{\partial t} = \frac{D_e}{r^2}\frac{\partial}{\partial r}\left(r^2 (q/q_o)^{\frac{1-n}{n}} \frac{\partial q}{\partial r} \right) \tag{3}$$

where

$$D_e = \frac{\varepsilon D_p}{(1-\varepsilon) S \rho_p n} k^{\frac{-1}{n}} q_o^{\frac{1-n}{n}} \tag{4}$$

is an effective diffusivity. Note that q_o is the sorbed mass in equilibrium with the imposed external gas-phase concentration. Equation (3) can be rendered dimensionless:

$$\frac{\partial Q_m}{\partial \theta} = \frac{1}{x^2}\frac{\partial}{\partial x}\left(x^2 (Q_m^{n'}) \frac{\partial Q_m}{\partial x} \right) \tag{5}$$

where $Q_m = q/q_o$, $x = r/a$, $n' = (1-n)/n$, $\theta = tD_e/a^2$, and a is the grain radius. Mathematically, equation (5) corresponds to the diffusion equation in spherical coordinates with radial symmetry and with a concentration-dependent diffusion coefficient, $Q_m^{n'}$.

The appropriate initial and boundary conditions for a step increase in gas-phase concentration (adsorption) are:

$$Q_m(0<x<1,\ \theta=0) = 0$$
$$Q_m(x=1,\theta>0) = 1 \qquad (6)$$
$$\partial Q_m/\partial x(x=0,\theta) = 0$$

and for a step decrease in gas-phase concentration from steady state (desorption) are:

$$Q_m(0<x<1,\ \theta=0) = 1$$
$$Q_m(x=1,\theta>0) = 0 \qquad (7)$$
$$\partial Q_m/\partial x(x=0,\theta) = 0$$

Equations (5)-(7) were solved by the Crank-Nicholson finite-difference scheme coupled with the Newton-Raphson method for solving the nonlinear equation. Typically, increments of 0.02 for x and 0.0002 for θ were used. Having obtained Q_m as a function of θ and x, the relative mass uptake for adsorption, or for desorption, at a specific time can be found by integration as

$$\frac{M_\theta}{M_\infty} = 3\int_0^1 x^2 Q_m(\theta)dx \qquad (8)$$

where M_θ is the mass uptake at dimensionless time θ and M_∞ is the mass uptake at steady-state. This integration was carried out numerically using Simpson's rule.

Figure 6 shows the relative mass increase or decrease as a function of time for various Freundlich n values. Smaller n values are associated with slower kinetics, and as n decreases, the asymmetry between adsorption and desorption curves becomes more apparent, with the rate of desorption becoming increasingly slower than adsorption. For a linear isotherm, n=1 and the adsorption and desorption curves coincide. An analytical solution given by Crank (1975) for this specific condition was used to partially validate the numerical solution.

The porous sphere model can be used to interpret the experimental data using plots of relative mass gain (or loss), M_θ/M_∞ $(1-M_\theta/M_\infty)$, versus the square-root of dimensionless time, or $(tD_e/a^2)^{0.5}$. A scheme similar to the least-squares method was used to determine

the best fit of the experimental data to the model. In this scheme, D_e was varied, and the difference in M_θ/M_∞ between experimental data points and the corresponding model predictions were squared and summed. The value of D_e that yielded the minimum summation value was considered to be the best fit. Figures 7 and 8 show the experimental data and the best fit found for the model. Note that in fitting the model the long-term data for desorption of the VOCs are ascribed less weight due to the greater uncertainty associated with their measurement. It should be emphasized that the effective diffusivity, D_e, is the only adjustable parameter and that a single value for D_e is used for both adsorption and desorption curves for each sorbate-sorbent combination. The porous sphere model is seen to be in reasonably good agreement with the entire set of experimental data and the asymmetry between adsorption and desorption is especially well resolved.

A pore diffusivity, D_p, can be calculated from the estimated values for the effective diffusivity, D_e, using eq (4). The required parameters (ε, ρ_p, n, k, q_o, and S) were either directly measured or interpreted from experimental data with results listed in Tables 1 and 2. If the porous sphere model is a good approximation of the actual grain structure, the calculated D_p should be close to the diffusion coefficient of the same compound in air, D_a, provided that the pore size is sufficiently large to avoid surface hindered (Knudsen) diffusion. Since the mean free path of typical gas molecules is about 65 nm at one atmosphere (Flagan and Seinfeld, 1988), both Knudsen diffusion and molecular diffusion should be considered in pores with a radius of less than about 250 nm (Wheeler, 1955). In fact, a significant portion of the pores within the three soils lies in the Knudsen diffusion domain (Figure 3), and therefore, the influence of Knudsen diffusion must be included in the analysis.

Influence of Knudsen Diffusion. Knudsen diffusivity, D_k, can be obtained from the kinetic theory of gases (Satterfield, 1974) as

$$D_k = (2/3)\, r_p\, v = (2/3)\, r_p\, (8RT/\pi M)^{1/2} \qquad (9)$$

where r_p is pore radius, v is average molecular velocity, R is the gas constant, T is absolute temperature, and M is molecular weight. A combined diffusivity, D, can then be estimated (Sherwood et al., 1975) as

$$\frac{1}{D} = \frac{1}{D_a} + \frac{1}{D_k} \tag{10}$$

If there is a distribution of pore sizes, both D_k and D are functions of the pore radius. For such cases, Wang and Smith (1983) have suggested that a reasonable average value can be found by weighting according to the pore volume distribution, or

$$D = \int_0^\infty \left(\frac{1}{D_a} + \frac{1}{D_k(r_p)} \right)^{-1} f(r_p)\, dr_p \tag{11}$$

where $f(r_p)dr_p$ is the fractional pore volume associated with pores of size r_p to r_p+dr_p.

A tortuosity factor τ, which allows for the influence of Knudsen diffusion, is therefore defined as

$$\tau = D/D_p \tag{12}$$

and depends only on the pore structure of the grain. Many of these characteristics, such as a tortuous path and pore constrictions, reduce the diffusing flux, causing τ to be greater than unity, while others, for example, pore interconnections, can increase the flux (Wang and Smith, 1983). Generally, τ values of between 2 and 6 are found for zeolites (Ruthven, 1984) while values as high as 100 have been found for low porosity (ε=0.03) nickel oxide pellets (Kim and Smith, 1974). Kim and Smith (1974) found that tortuosity generally increases rapidly as the porosity decreases and ascribed this effect to the decreasing likelihood for interconnections between pores. The values of τ inferred for our soil samples lie between 10 and 33 (Table 3). These values appear reasonable since soil and sand have much lower grain porosity than zeolites or catalysts. Indeed the relationship between τ and ε found for SSM and McAFB follows very closely the trend in experimental data given by Kim and Smith (1974).

Theoretically, τ values for different compounds in the same adsorbent should be the same because they have identical diffusion pathways. The fact that the τ values for the three compounds in SSM are quite similar, considering the large differences in the sorption isotherms for water and the VOCs, provides some support for the assumed physical basis of the porous sphere model. However, in applying this model to a water-saturated or semi-saturated system, a careful modification should be made. Since the organic matter within the soil grains would dominate the sorption process under these systems, besides pore diffusion, a diffusional transport within SOM and the partitioning between SOM and water/air may need to be considered.

Parallel Pore Model. The porous sphere model captures the dominant features of adsorption and desorption kinetics with a reasonable and self-consistent physical description of soil grains. However, the agreement between the model and the experimental data is not perfect, especially at longer times. One limitation of the porous sphere model is that a single effective diffusivity is assumed to apply for all pores. In reality, due to their large surface to volume ratio, diffusion through small pores will occur at a lower effective rate. Therefore, in addition to the porous sphere model, a modified version of a parallel pore model (Johnson and Stewart, 1965) was applied to interpret the kinetic data. This model fully incorporates the experimental data on pore size distribution. The pore structure in the model is visualized as comprising an array of parallel cylindrical pores with a pore size distribution that conforms with experimental results and a length equal to the grain radius. The tortuosity factor was assumed to be independent of pore size. In developing the parallel pore model Johnson and Stewart (1965) simplified the analysis by assuming that at any cross section perpendicular to the direction of mass transport, the concentration was independent of pore size. The last assumption is physically plausible for a relatively porous catalyst that has substantial interconnections among pores. However, the porosities of the three soils studied here are much lower than those of catalysts and much less cross passage would be expected. Therefore, in this study

each pore is considered to act independently and the concentration in the pores is allowed to be pore-size dependent.

Assuming that the sorption isotherm holds for each pore, and following a similar approach to the porous sphere model, the transient diffusion and sorption equation for a given cylindrical pore size becomes

$$\frac{\partial q_i}{\partial t} = D_{ei}\frac{\partial}{\partial z}\left((q_i / q_o)^{n'}\frac{\partial q_i}{\partial z}\right) \tag{13}$$

where

$$D_{ei} = D_{pi}\frac{r_{pi}}{2n}k^{\frac{-1}{n}}q_o^{\,n'} \tag{14}$$

is an effective diffusivity, z is the axial coordinate of the pore, D_{pi} is the pore diffusivity, q_i is the sorbed mass in the pores of radius r_{pi}, and q_o is the sorbed mass in equilibrium with the imposed external gas-phase concentration.

Equation (13) is solved for various pore sizes using the same approach as for the previous model. The total mass uptake and loss for soil grains at any time can then be obtained by summing the fractional mass uptake for each pore size range:

$$\frac{M_{\theta o}}{M_\infty} = \frac{\sum A_i (M_{\theta o} / M_\infty)_i}{\sum A_i} \tag{15}$$

where $\theta_o = D_{eo}t/a^2$, D_{eo} is the effective diffusivity for a reference pore size, r_{po} (950 nm used in this study), and A_i is the surface area of pores with size r_{pi}.

The parallel pore model was applied to the sorption of benzene by SSM and water vapor by McAFB. In both cases, 29 size ranges of pores between 1.8 nm and 1 μm extracted from mercury intrusion data were used. The model indicated a similar degree of fit to the benzene/SSM data with the porous sphere model. However, for water vapor/McAFB case, this model (Figure 9) yields a somewhat better fit than the previous one (Figure 8b) in both sorption and desorption curves, especially at larger times. The parameter D_{eo}/a^2 was found to be 570 min^{-1} for RH=85% and r_{po} at 950 nm. Applying k

and q_o values based on the surface area measured by mercury instrusion, this result yields a tortuosity equal to 0.1 (this value will be even smaller if k and q_o are based on BET/N_2 surface area) assuming all pores have a length equal to the grain radius, a. The fact that the inferred tortuosity of 0.1 is significantly less than unity suggests that some key aspect of intragranular sorption is lacking in this model description. It is clear that the parallel pore model depends strongly on the assumptions made when inferring the pore size distribution from the mercury intrusion data. The model used to interpret the intrusion data may be a gross simplification of the actual internal pore structure. Also, it is assumed that the length of all the pores is equal to the grain radius, a fact that cannot be verified from the experimental measurements. If the average pore length is shorter than the grain radius, the calculated tortuosity will increase. More accurate methods for characterizing the physical structure of soil grains would be of considerable value in ongoing efforts to understand contaminant transport in soils.

APPENDIX I. REFERENCES

Allison, L.E. (1965). "Organic carbon." In *Methods of Soil Analysis*, Black, C.A., Evans, D.D., White, J.L., Ensminger, L.E., and Clark, F.E. eds., Am. Society of Agronomy: Madison, WI, Part 2, pp. 1367-1378.

Ball, W.P., Buchler, C.H., Harmon, T.C., McKay, D.M., and Roberts, P.V. (1990). "Characterization of a sandy aquifer material at the grain scale." *J. Contam. Hydrol .*, *5*, 253-295.

Ball, W.P., and Roberts, P.V. (1991a). "Long-term sorption of halogenated organic chemicals by aquifer material: 1. Equilibrium." *Environ. Sci. Technol.*, *25*, 1223-1236.

Ball, W.P., and Roberts, P.V. (1991b). "Long-term sorption of halogenated organic chemicals by aquifer material: 2. Intraparticle diffusion." *Environ. Sci. Technol.*, *25*, 1237-1249.

Blake, G.R. (1965). "Particle density." In *Methods of Soil Analysis*, Black, C.A., Evans, D.D., White, J.L., Ensminger, L.E., and Clark, F.E. eds., Am. Society of Agronomy: Madison, WI, Part 1, pp. 371-373.

Broadbent, F.E. (1965). "Organic matter." In *Methods of Soil Analysis*, Black, C.A., Evans, D.D., White, J.L., Ensminger, L.E., and Clark, F.E. eds., Am. Society of Agronomy: Madison, WI, Part 2, pp. 1397-1400.

Brunauer, S.P., Emmett, P.H., and Teller, E. (1938). "Adsorption of gases in multimolecular layers." *J . Am. Chem. Soc.*, *60*, 309-319.

Chiou, C.T., and Shoup, T.D. (1985). "Soil sorption of organic vapors and effects of humidity on sorptive mechanism and capacity." *Environ. Sci. Technol.*, *19*, 1196-1200.

Crank, J. (1975). *The Mathematics of Diffusion*. 2nd edn., Clarendon: Oxford, England.

Flagan, R.C., and Seinfeld, J.H. (1988) *Fundamentals of Air Pollution Engineering*, Prentice Hall: Englewood Cliffs, NJ, p. 294.

Garg, D.R., and Ruthven, D.M. (1972). "The effect of the concentration dependence of diffusivity on zeolite sorption curves." *Chem. Eng. Sci.*, *27*, 417-423.

Johnson, M.F.L., and Stewart, W.E. (1965). "Pore structure and gaseous diffusion in solid catalysts." *Journal of Catalysis*, *4*, 248-252.

Karickhoff, S.W., Brown, D.S., and Scott, T.A. (1979). "Sorption of hydrophobic pollutants on natural sediments." *Water Research*, *13*, 241-248.

Kim, K.K., and Smith, J.M. (1974). "Diffusion in nickel oxide pellets: effects of sintering and reduction." *AIChE Journal*, *20*, 670-678.

Little, J.C., Daisey, J.M., and Nazaroff, W.W. (1992). "Transport of subsurface contaminants into buildings: An exposure pathway for volatile organics." *Environ. Sci. Technol.*, *26*, 2058-2066.

Lowell, S., and Shields, T.E. (1984). *Powder Surface Area and Porosity*, John Wiley & Sons, Inc.: New York.

Miller, C.T., and Pedit, J.A. (1992). "Use of a reactive surface-diffusion model to describe apparent sorption-desorption hysteresis and abiotic degradation of lindane in a subsurface material." *Environ. Sci. Technol.*, *26*, 1417-1427.

Nafikov, E.M., and Usmanov, A.G. (1967). "Vapor diffusion coefficients for some saturated hydrocarbons." *Chemical Abstracts* , 67, 25934d.

Ong, S.K., and Lion, L.W. (1991a) "Effects of soil properties and moisture on the sorption of trichloroethylene vapor." *Water Research* , *25*, 29-36.

Ong, S.K., and Lion, L.W. (1991b) "Trichloroethylene vapor sorption onto soil minerals." *Soil Sci. Soc. Am. J.*, *55*, 1559-1568.

Pignatello, J.J. (1991). "Desorption of tetrachloroethene and 1,2-dibromo-3-chloropropane from aquifer sediments." *Environ. Toxi. Chem.*, *10*, 1399-1404.

Reid, R.C., Prausnitz, J.M., and Sherwood, T.K. (1976) *The Properties of Gases and Liquids*, 3rd edn., McGraw Hill: New York, p. 544.

Rutherford, D.W., and Chiou, C.T. (1992). "Effect of water saturation in soil organic matter on the partition of organic compounds." *Environ Sci. Technol., 26*, 965-970.

Ruthven, D. M. (1984) *Principles of Adsorption and Adsorption Processes*, John Wiley & Sons: New York.

Ruthven, D.M., and Derrah, R.I. (1972). "Sorption in Davison 5A molecular sieves." *Can. J. Chem. Eng., 50*, 743-747.

Satterfield, C.M. (1970) *Mass Transfer in Heterogeneous Catalysis*, MIT Press: Cambridge, MA.

Sawhney, B.L., and Gent, M.P.N. (1990). "Hydrophobicity of clay surfaces: Sorption of 1,2-dibromoethane and trichloroethene." *Clays and Clay Minerals, 38*, 14-20.

Selleck, R.E., Marinas, B.J., and Diyamandoglu, V. (1988). "Treatment of water contaminants with aeration in counterflow packed towers: theory, practice and economics." *Sanitary Engineering and Environmental Health Research Laboratory*, UCB/SEEHRL Report No. 88-3/1, University of California, Berkeley, CA.

Sherwood, T.K., Pigford, R.L., and Wilke, C.R. (1975). *Mass Transfer*, McGraw-Hill: New York, pp. 29-42.

Sladek, K.J., Gilliland, E.R., and Baddour, R.F. (1974). "Diffusion on surfaces. II. Correlation of diffusivities of physically and chemically adsorbed species." *Ind. Eng. Chem. Fundam., 13*, 100-105.

Steinberg, S.M., Pignatello, J.J., and Sawhney, B.L. (1987). "Persistence of 1,2-dibromoethane in soils: Entrapment in intraparticle micropores." *Environ. Sci. Technol., 21*, 1201-1208.

U.S. Environmental Protection Agency, Risk Reduction Engineering Laboratory, Release Control Branch (1988). *Synthetic Soil Matrix (SSM-SARM) User's Manual.* Edison, N.J.

Wang, C.-T., and Smith, J.M. (1983). "Tortuosity factors for diffusion in catalyst pellets." *AIChE Journal, 29*, 132-136.

Weber, W.J., McGinley, P.M., and Katz, L.E. (1992). "A distributed reactivity model for sorption by soils and sediments. 1. Conceptual basis and equilibrium assessments." *Environ. Sci. Technol., 26*, 1955-1962.

Wheeler, A. (1955). "Reaction rates and selectivity in catalyst pores." In *Catalysis Vol. II, Fundamental Principles (part 2)*, P.H. Emmet ed., Reinhold Publishing Corp.: New York.

Wood, W.W., Kraemer, T.F., and Hearn, P.P. (1990). "Intragranular diffusion: An important mechanism influencing solute transport in clastic aquifers?" *Science, 247*, 1569-1572.

Wu, S.-C., and Gschwend, P.M. (1986). "Sorption kinetics of hydrophobic organic compounds to natural sediments and soils." *Environ. Sci. Technol., 20*, 717-725.

APPENDIX II. NOMENCLATURE

a	radius of soil grain (m)
C	gas-phase species concentration (g m^{-3})
D	combined diffusivity accounting for both molecular diffusivity and Knudsen diffusivity (m^2 s^{-1})
D_a	diffusivity in air (m^2 s^{-1})
D_e	effective diffusivity (m^2 s^{-1})
D_{eo}	effective diffusivity in the pore with radius r_{po} (m^2 s^{-1})
D_k	Knudsen diffusivity (m^2 s^{-1})
D_p	pore diffusivity in soil grain (m^2 s^{-1})
k	Freundlich isotherm parameter ((g m^{-2}) × (g m^{-3})$^{-n}$)
MW	molecular weight (g $mole^{-1}$)
M_θ/M_∞	cumulative mass gain or loss relative to that at equilibrium (dimensionless)
n	Freundlich isotherm parameter (dimensionless)
n'	[= (1-n) n^{-1}] (dimensionless)
P	vapor pressure of adsorbate (kPa)
P_o	saturated vapor pressure of adsorbate (kPa)
q	sorption capacity (g m^{-2})
q_o	sorption capacity at equilibrium (g m^{-2})
Q_m	sorption capacity [= q q_o^{-1}] (dimensionless)
r	radial coordinate in soil grain (m)

r_p	pore radius in soil grain (m)
r_{po}	reference pore radius (m)
R	gas constant (8.314×10^3 g m s^{-2} $mole^{-1}$ K^{-1}))
S	specific surface area of soil grains (m^2 g^{-1})
t	adsorption or desorption time (s)
T	temperature (K)
v	average gas molecular velocity (m s^{-1})
x	radial coordinate in soil grain (dimensionless)
z	axial coordinate in the parallel pore model (m)
ϵ	grain porosity (dimensionless)
ρ_p	grain density (g m^{-3})
θ	adsorption or desorption time (dimensionless)
θ_o	adsorption or desorption time associated with D_{eo} (dimensionless)
τ	tortuosity factor (dimensionless)

Table 1. Characteristics of Three Test Soils (See text for details).

Soil	Grain Size, U.S. mesh	Specific Surface Area, S, m^2/g		Grain Porosity, ε	Grain Density, ρ_p g/m^3	Organic Carbon, % mass
		N_2 adsorption	Hg Intrusion			
SSM	20-30	8±2 (N‡=2)	8	0.15	2.61×10^6	0.25±0.02 (N=3)
McAFB	20-30	0.6	2	0.062	2.76×10^6	0.43±0.07 (N=3)
Sand	30-60	0.4±0.1 (N=4)	na†	0.014	2.61×10^6	0.014

‡ number of samples.

† not available.

Table 2. Gas-Phase Freundlich Isotherms for VOCs and Water Vapor on Dry Soil Grains at 20 °C.

Soil	Adsorbate	Isotherm ($q=kC^n$)†	Correlation Coefficient‡
SSM	benzene	$q=1.6\times10^{-4}\ C^{0.28}$	0.995
SSM	trichloroethylene	$q=1.7\times10^{-4}\ C^{0.28}$	0.992
SSM	water	$q=2.4\times10^{-4}\ C^{0.75}$	0.994
McAFB	water	$q=1.2\times10^{-3}\ C^{0.55}$	0.981
Sand	water	$q=6.0\times10^{-4}\ C^{0.70}$	0.997

†q is sorbed mass (g/m^2) and C is gas-phase concentration (g/m^3)

‡based on regression of log(q) vs. log(C)

Table 3. Estimated Diffusion Coefficients and Tortuosity (τ) for Three Test Soils Based on Porous Sphere Model (Symbols defined in nomenclature and text).

Soil	Adsorbate	Concentration	D_e, m^2/sec	D_p, m^2/sec	D_a, m^2/sec	D, m^2/sec	τ
SSM	benzene	650 ppm_v	1.6×10^{-10}	4.8×10^{-7}	8.8×10^{-6}†	4.8×10^{-6}	10
SSM	trichloroethylene	720 ppm_v	2.0×10^{-10}	4.2×10^{-7}	8.4×10^{-6}‡	4.3×10^{-6}	10
SSM	water	85% R.H.	7.4×10^{-11}	9.0×10^{-7}	2.4×10^{-5}*	1.2×10^{-5}	13
McAFB	water	85% R.H.	9.6×10^{-11}	4.9×10^{-7}	2.4×10^{-5}*	1.4×10^{-5}	29
Sand	water	68% R.H.	1.6×10^{-11}	3.1×10^{-7}	2.4×10^{-5}*	1.0×10^{-5}	33

*Reid et al., 1976; †Nafikov and Usmanov, 1967 ; ‡Selleck et al., 1988.

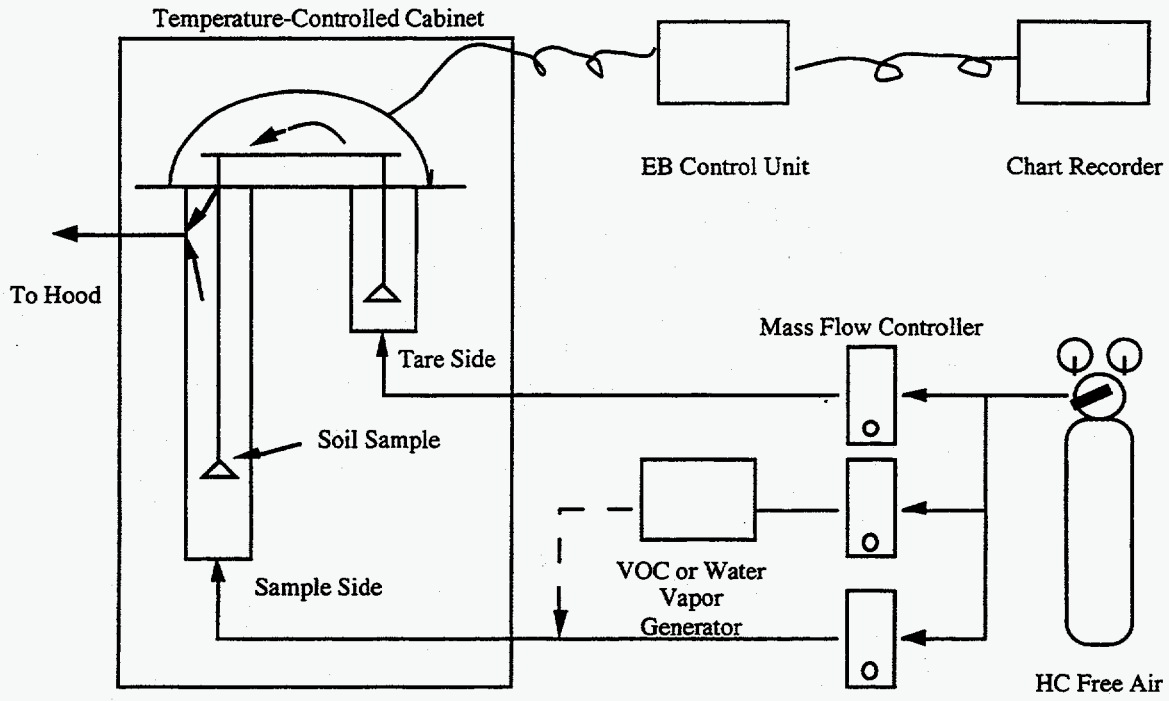

Figure 1. Schematic diagram of the electrobalance (EB) system.

(a)

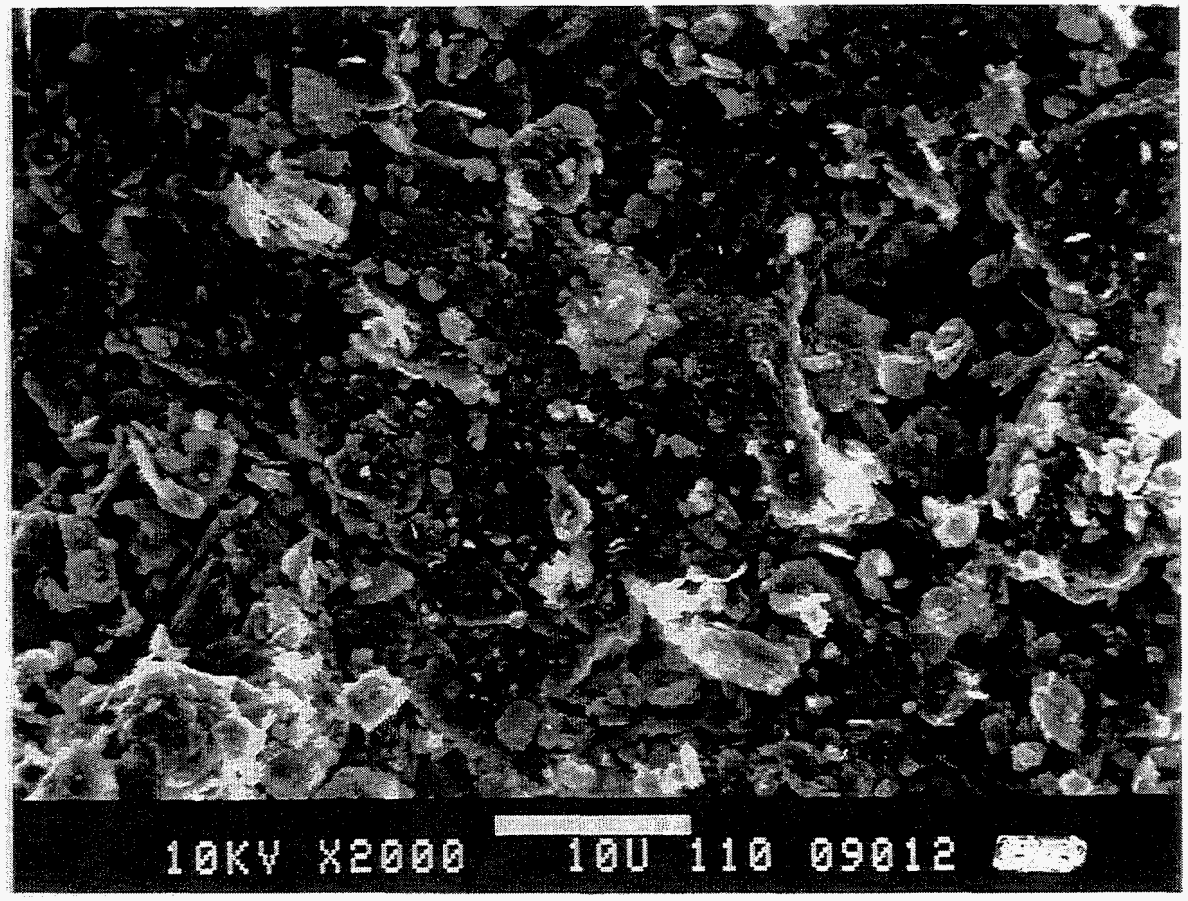

Figure 2. SEM photomicrographs of (a) SSM, (b) McAFB and (c) sand grain surface. The grain diameter is about 700 μm for SSM and McAFB and is about 250 μm for sand. The "10U" bar in each photograph represents a length of 10 μm.

(b)

Figure 2. SEM photomicrographs of (a) SSM, (b) McAFB and (c) sand grain surface. The grain diameter is about 700 μm for SSM and McAFB and is about 250 μm for sand. The "10U" bar in each photograph represents a length of 10 μm.

(c)

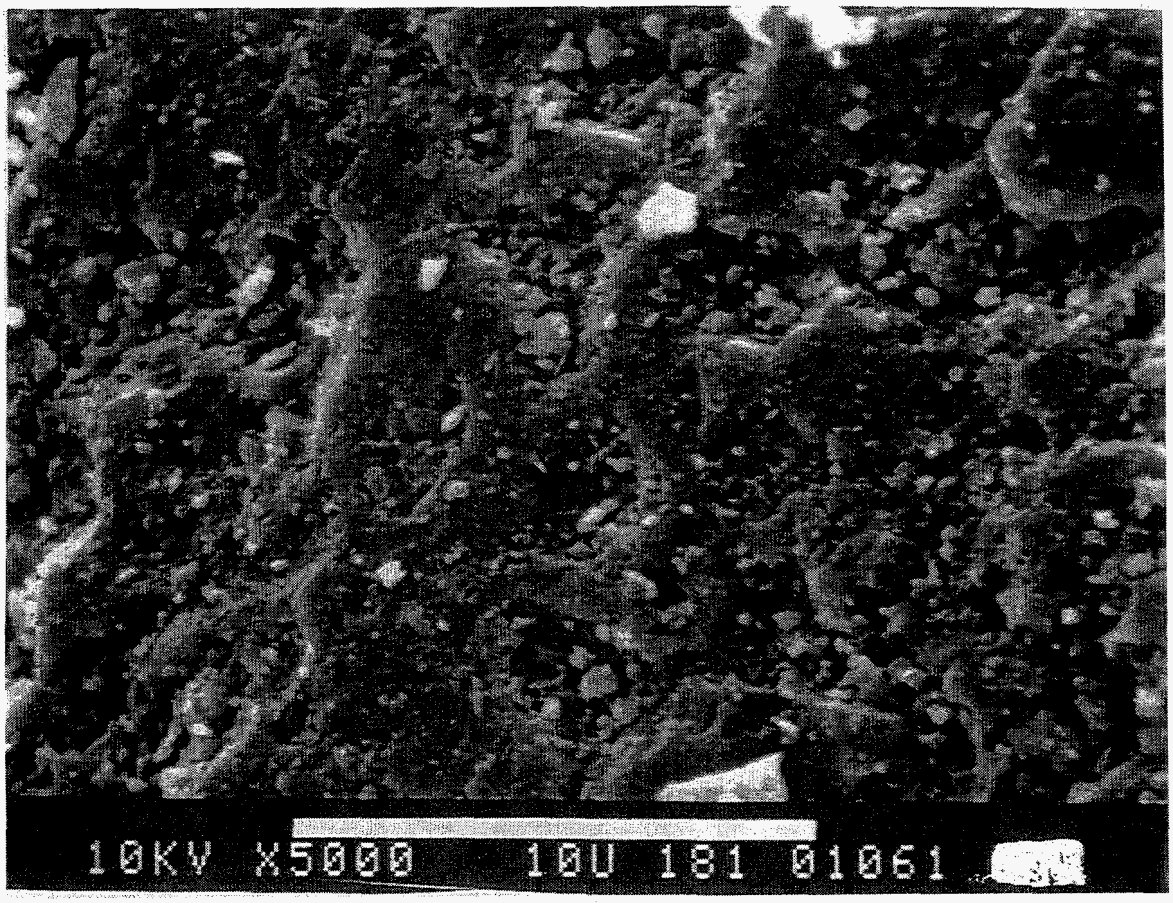

Figure 2. SEM photomicrographs of (a) SSM, (b) McAFB and (c) sand grain surface. The grain diameter is about 700 μm for SSM and McAFB and is about 250 μm for sand. The "10U" bar in each photograph represents a length of 10 μm.

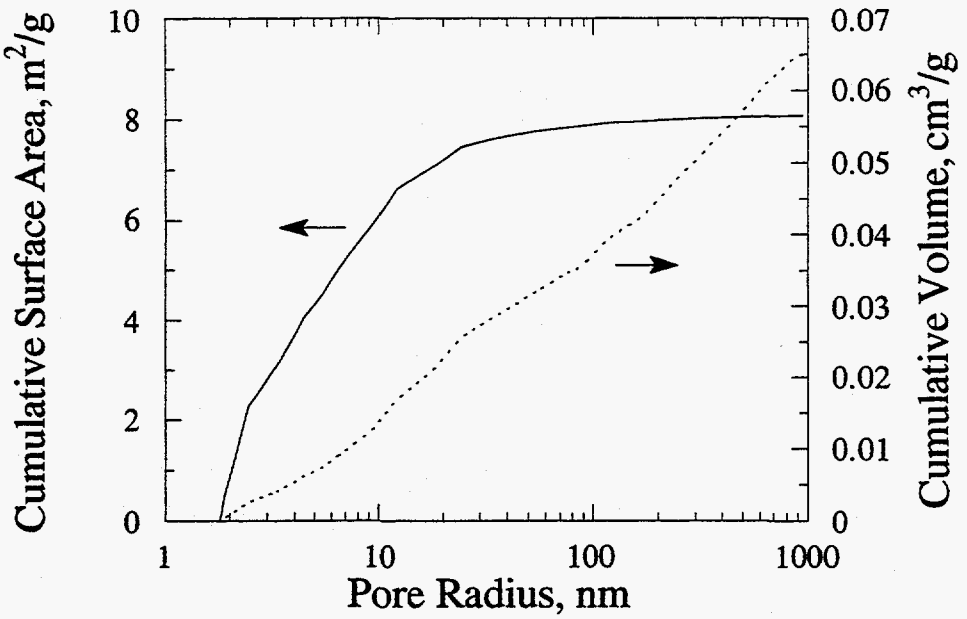

Figure 3. Cumulative pore surface and pore volume distribution as a function of pore radius for SSM grains.

(a)

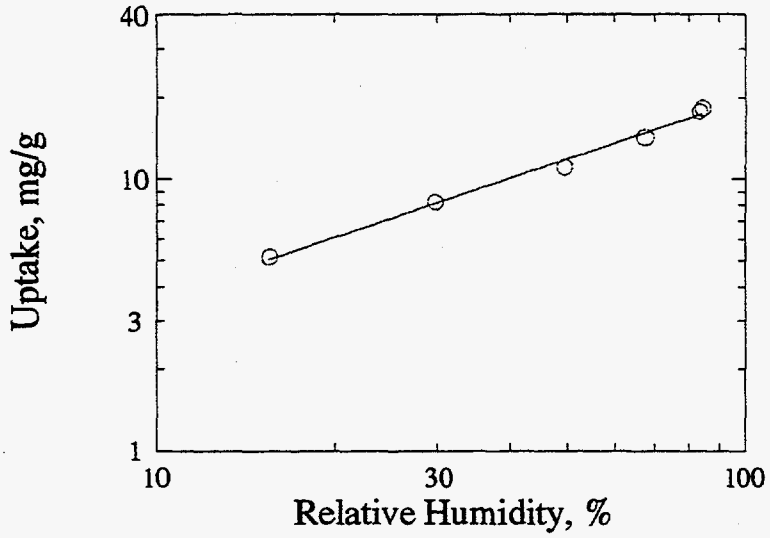

(b)

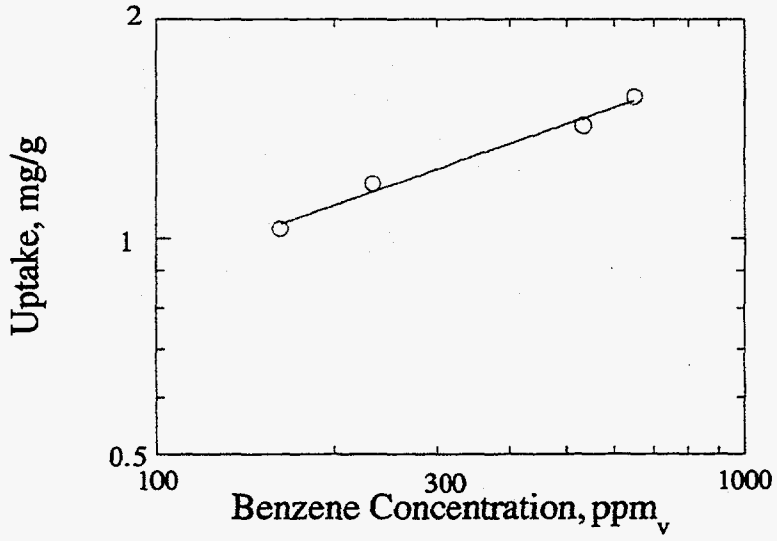

Figure 4. Typical experimental sorption isotherms of (a) water vapor, and (b) benzene onto SSM, where the points represent experimental data and lines represent fitted Freundlich isotherms.

(a)

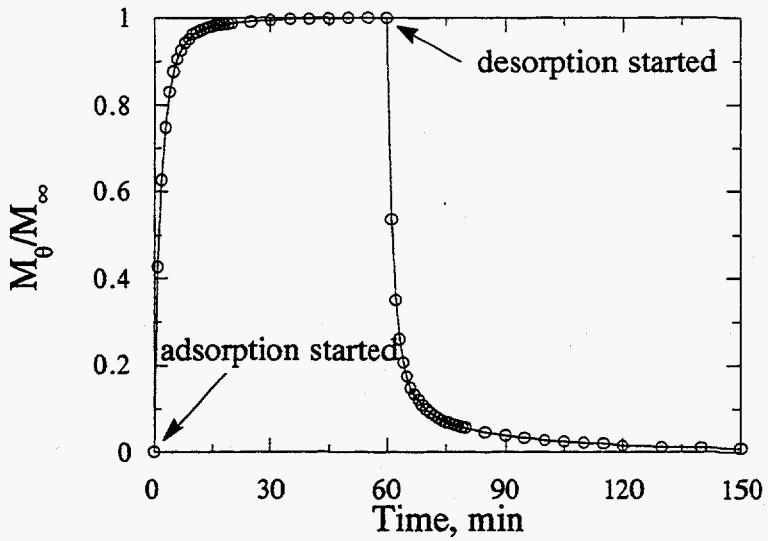

(b)

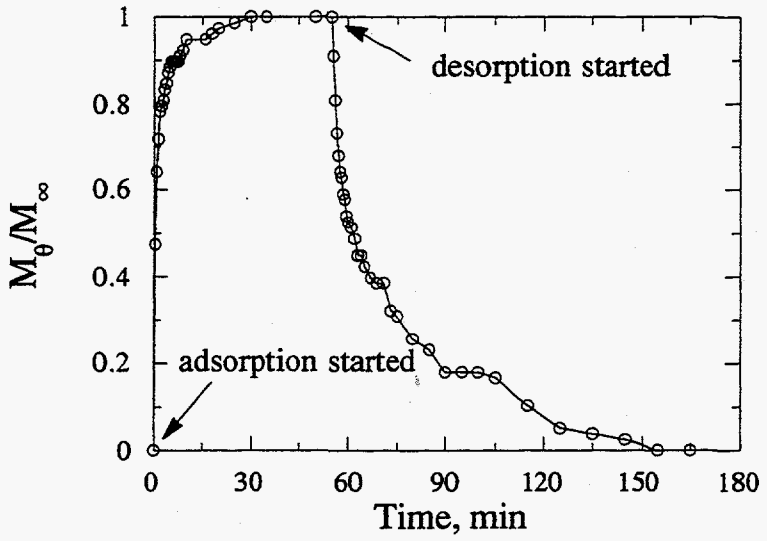

Figure 5. Typical experimental sorption kinetic curves for SSM where (a) represents water vapor at relative humidity 85%, and (b) represents benzene with concentration 650 ppm_V.

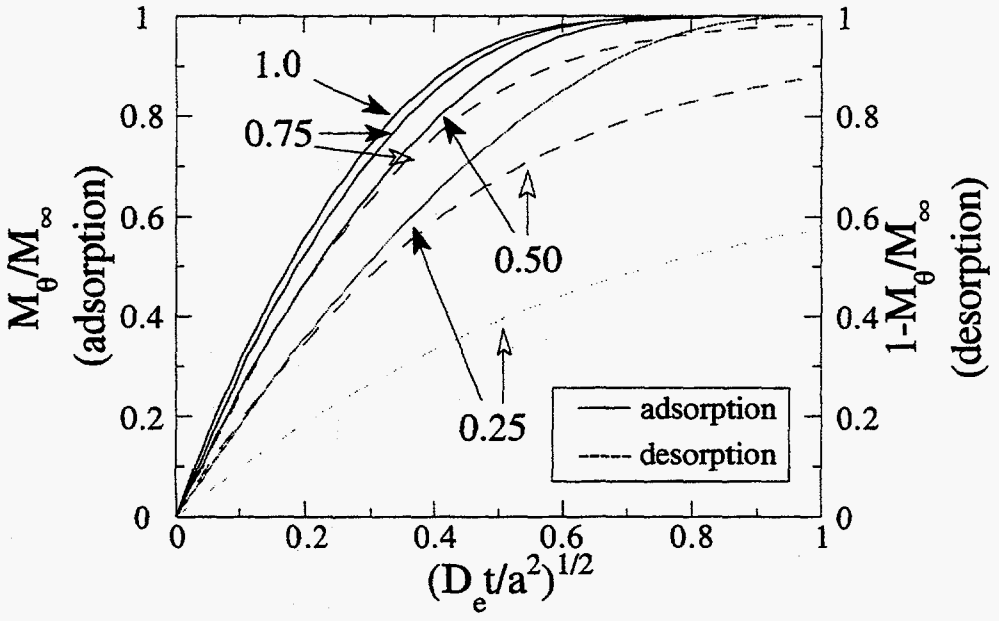

Figure 6. Numerical solution of sorption and desorption kinetic curves based on the porous sphere model with nonlinear Freundlich isotherm where M_θ/M_∞ is the cumulative mass gain relative to that at equilibrium, $(D_e t/a^2)^{1/2}$ is the square root of dimensionless time, D_e is the effective diffusivity (eq. 4), a is grain radius, and t is time. The numbers that label the curves represent the n value in the Freundlich isotherm.

(a)

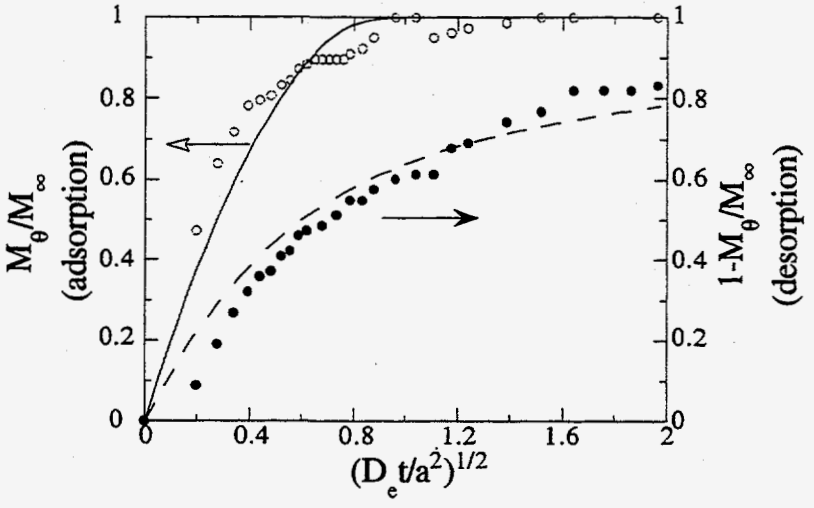

(b)

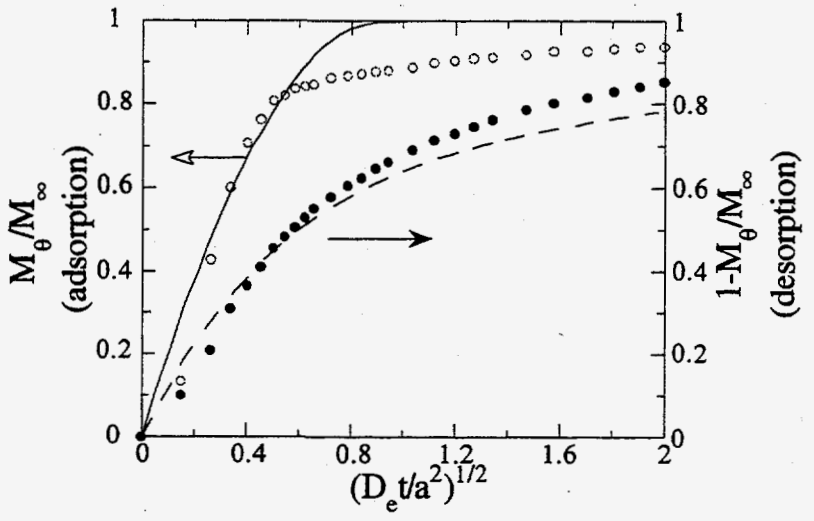

Figure 7. Sorption kinetics for SSM where (a) represents benzene at 650 ppm_v and (b) represents trichloroethylene at 720 ppm_v. M_θ/M_∞ is the cumulative mass gain relative to that at equilibrium, $(D_e t/a^2)^{1/2}$ is the square root of dimensionless time, D_e is the effective diffusivity (eq. 4), a is grain radius, and t is time. The open and filled symbols denote experimental adsorption and desorption data, respectively. The fitted porous sphere model is shown as a solid line for adsorption and as a dashed line for desorption.

(a)

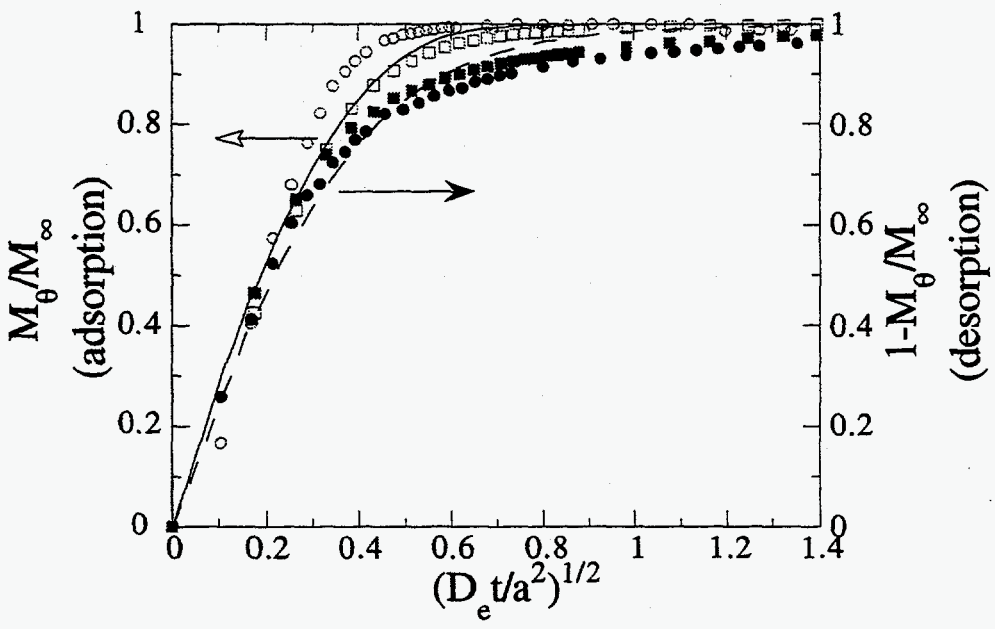
M_θ/M_∞ (adsorption)
$1-M_\theta/M_\infty$ (desorption)
$(D_e t/a^2)^{1/2}$
0
0.2
0.4
0.6
0.8
1
1.2
1.4

(b)

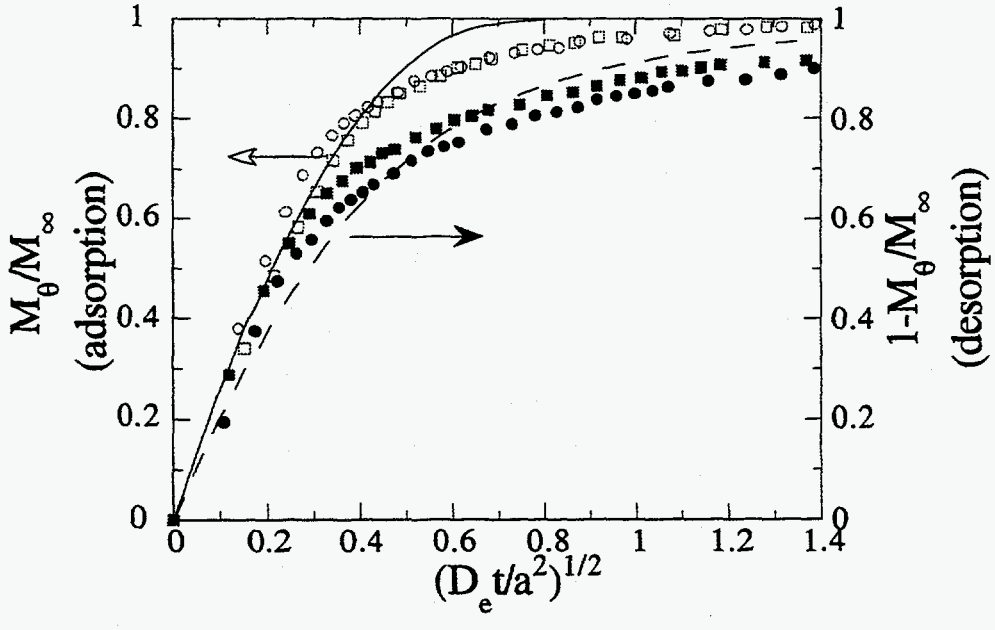
M_θ/M_∞ (adsorption)
$1-M_\theta/M_\infty$ (desorption)
$(D_e t/a^2)^{1/2}$
0
0.2
0.4
0.6
0.8
1
1.2
1.4

(c)

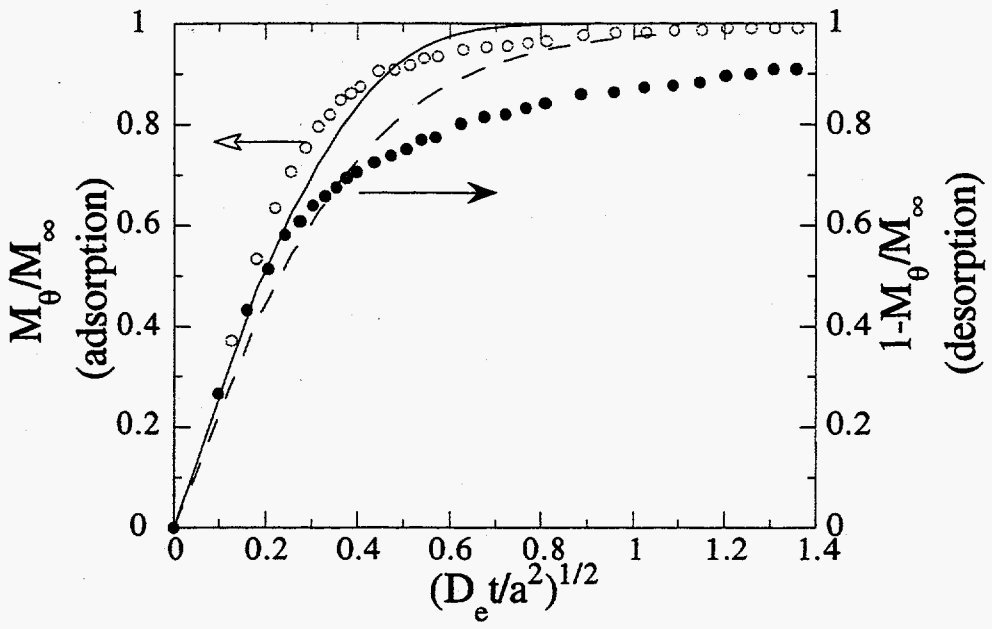

Figure 8. Sorption kinetics for water vapor onto (a) SSM, (b) McAFB and (c) sand, where M_θ/M_∞ is the cumulative mass gain relative to that at equilibrium, $(D_e t/a^2)^{1/2}$ is the square root of dimensionless time, D_e is the effective diffusivity (eq. 4), a is grain radius, and t is time. The circles represent data taken at RH=68% while the squares are for RH=85%. The open and filled symbols denote adsorption and desorption data, respectively. The fitted porous sphere model is shown as a solid line for adsorption and as a dashed line for desorption.

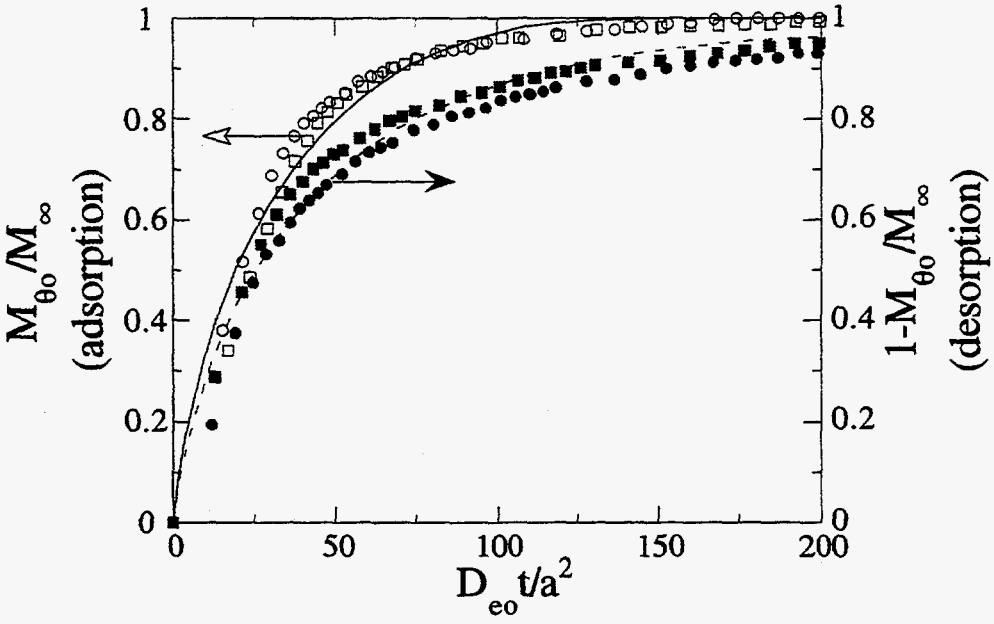

Figure 9. Sorption kinetics for water vapor onto McAFB where $M_{\theta o}/M_\infty$ is the cumulative mass gain relative to that at equilibrium, $(D_{eo}t/a^2)^{1/2}$ is the square root of dimensionless time, D_{eo} is the effective diffusivity (eq. 14) related to the pore with size r_{po}, a is grain radius, and t is time. The circles represent data taken at RH=68% while the squares are for RH=85%. The open and filled symbols denote adsorption and desorption data, respectively. The fitted parallel-path pore model is shown as a solid line for adsorption and as a dashed line for desorption.

Chapter III

Transport and Sorption of Water Vapor and Benzene within Dry Soil Organic Matter

ABSTRACT

To better understand gas-phase transport of organic contaminants in subsurface environments, the sorption behavior of water vapor and benzene within a model soil organic matter (SOM), peat, was studied. An electrobalance systems similar to that discussed in Chapter II, was employed to determine both the equilibrium sorption isotherm and sorption-desorption kinetics. For water vapor, the sorption isotherm was found to resemble that previously reported for this sample, with about 10-15% difference in sorption capacity. The sorption isotherm for benzene could not be determined, due to a failure to obtain reproducible sorption capacity. This failure may reflect structural changes in SOM upon exposure to benzene. In the kinetics study, strong asymmetries between sorption and desorption rates were observed for both water vapor and benzene. A dual diffusion model, including gas-phase pore diffusion within peat grains and solid-phase diffusion within microspheres of SOM, was used to interpret the asymmetric sorption rate data. Considering gas-phase pore diffusion only, the model resolved the asymmetry of sorption rates and described the experimental data very well for water vapor at three different concentrations. However, the pore diffusion model failed to capture the dominant feature of the experimental data for benzene. As a refinement, a model assuming that solid-phase intra-SOM diffusion is the rate-limiting mechanism produced a better description of the experimental data.

INTRODUCTION

Soil sorption is widely acknowledged to be one of the important factors governing the transport and fate of volatile organic compounds (VOCs) in subsurface systems (Weber et al., 1991). Sample applications in which sorption is important include soil venting operations (Johnson et al., 1988) and soil gas entry into buildings (Little et al., 1992). Typically, soil is considered as a dual sorbent, in which soil organic matter (SOM) acts as a partition medium and mineral surfaces act as a conventional adsorbent (Chiou and Shoup, 1985; Rutherford et al., 1992; Rutherford and Chiou, 1992; Chiou and Kile, 1994). Studies have shown that, for a water-saturated system, the sorption of organic compounds on mineral surfaces is suppressed by the presence of water and the sorption occurs mainly by partitioning into SOM (Karickhoff et al., 1979; Chiou and Shoup, 1985; Rutherford et al., 1992). In contrast, for a system with low moisture content, both sorption of VOCs onto mineral surfaces and partition into SOM may need to be considered.

To better understand the transport of VOCs in subsurface systems, it is important to gain knowledge of both sorption kinetics and equilibrium partitioning at the level of individual soil grains. Numerous studies have been conducted to investigate equilibrium sorption for both mineral surfaces and SOM, mostly in water-saturated systems (Karickhoff et al., 1979; Ball and Roberts, 1991a; Rutherford et al., 1992; and many others) and, in some cases, under unsaturated conditions (Chiou and Shoup, 1985; Rutherford and Chiou, 1992; Chapter II of this dissertation). In contrast, fewer studies have focused on sorption kinetics and these have been restricted to sorption in mineral-dominated systems (Wu and Gschwend, 1986; Weber and Miller, 1988; Ball and Roberts, 1991b; Harmon and Roberts, 1994; Chapter II of this dissertation). Therefore, there is a need to study the kinetic behavior for VOC sorption on SOM.

Several different forms of materials have been used as model SOM for studying VOC sorption: soil extracts, humic acid salt, cellulose, lignin (Garbarini and Lion, 1986),

peat, and muck (Rutherford et al., 1992; Rutherford and Chiou, 1992). Among these materials, peat, extensively studied by Chiou and coworkers (Rutherford et al., 1992; Rutherford and Chiou, 1992), is a reference sample for the International Humic Substances Society and, on this basis, was selected for this research. Kinetic studies for sorption to peat have been conducted for removing dyes (McKay and Allen; 1984), herbicides (Cloutier et al., 1985), and metals (Gosset et al., 1986; Allen et al., 1992) from wastewater. However, from our reading of the literature, no study has focused on the kinetics of sorption of VOCs to SOM (peat) in either aqueous or gaseous systems.

In this chapter, we explore the sorption equilibrium and kinetics for water vapor and benzene within individual dry peat grains. A Cahn-1000 electrobalance is used to determine both sorption isotherms and sorption kinetic curves. The experimental isotherm for water vapor is found to be similar to that reported in the literature; however, an isotherm for benzene could not be obtained because of a failure of the system to be reproducible. A dual diffusion model, which includes both gas-phase pore diffusion within peat grains and solid-phase diffusion within SOM microspheres, is employed to interpret the kinetic data. Assuming pore diffusion is the rate-limiting mechanism, the model fits the experimental data for water vapor very well using only one adjustable parameter, an effective diffusivity. The extracted effective diffusivity is then used to predict sorption kinetic data for other water vapor concentrations. Good agreement between the predictions and the data is observed. In contrast, the kinetic data for benzene do not conform to the predictions of the pore diffusion model even assuming that the isotherm is nonlinear. Instead, a model considering concentration-dependent diffusivity and solid-phase diffusion within the microspheres is found to better describe the experimental data.

THEORY

This section presents the theoretical sorption and transport models employed in this study. The model describing transport and sorption of water vapor and VOC molecules

within individual peat grains is based on our current understanding about the structure of soil organic matter. This model is used to simulate kinetic sorption curves and infer the intragranular pore diffusivity of water vapor from sorption experiments. The model is then used to describe the experimental sorption behavior for benzene to peat grains.

Physical Structure of Peat. Peat grains are represented as porous spheres containing a uniform distribution of soil organic matter (SOM) microparticles. The BET surface area reported in the literature (1.3-1.5 $m^2\ g^{-1}$) (Chiou and Kile, 1994) corresponds to about 36 times the nominal surface area of the peat grains, if the diameter and skeleton density of the grains are set at 1.0×10^{-4} m and 1.56×10^{6} g m^{-3}, respectively (see the Materials and Methods section). Taken together with the relatively smooth exterior surface shown in the scanning electron microscope (SEM) photomicrographs (Figure 1), this ratio suggests that most of the accessible surface area lies within the peat grains. Therefore, a porous structure is expected for the peat grains. SOM has been represented by others as an amorphous polymeric (macromolecular) substance (Chiou et al., 1983; Schwarzenbach et al., 1993). By contrast, we envision that SOM comprises polymeric microparticles that are uniformly distributed within peat grains with their surfaces in contact with the pore air. Through the internal pores of peat grains, the microparticles can react with (dissolve or release) the contaminant molecules in the bulk fluid.

As shown in Figure 2, our model assumes that each peat grain is a perfect porous sphere with constant diameter and is composed of many small particles of organic matter. Sorbate molecules are first transported from the bulk phase through a gas film to the grain. Within the grain, gas-phase diffusion in the pore air is accompanied by the sorption of sorbates to the SOM particles. A local equilibrium is assumed to be constantly maintained between the gas and sorbed phases at the surface of the microparticles (for simplicity, all microparticles are assumed to be spheres with uniform radii) with the isotherm being the same as the one obtained from a bulk experiment. Because of the high SOM content (about

86.4%) and low surface area in peat (about 1.3-1.5 $m^2\ g^{-1}$) (Chiou and Kile, 1994), any effects of mineral surfaces can be neglected in the model.

Sorbate Transport within Organic Microparticles. Transient diffusion of sorbate molecules within the microparticles can be described by

$$\frac{\partial q}{\partial t} = \frac{1}{r_m^2}\frac{\partial}{\partial r_m}\left(r_m^2 D_\mu \frac{\partial q}{\partial r_m}\right) \tag{1}$$

where q is the sorbed mass (mass of sorbate/mass of sorbent), r_m is the radial coordinate of the microsphere, t is time, and D_μ is the effective diffusivity of sorbate molecules in the SOM matrix. It is noted that D_μ may be a function of q for the case of a concentration-dependent diffusion coefficient (Paul, 1985).

The appropriate initial and boundary conditions for equation (1) are as follows:

$$q(0<r_m<1,\ t=0) = 0 \text{ (adsorption)}$$

$$\text{or} \quad q(0<r_m<1,\ t=0) = q_o \text{ (desorption)}$$

$$\partial q/\partial r_m(r_m=0,\ t) = 0 \tag{2}$$

$$q(r_m = a_m) = kC^n$$

where C is the gas-phase concentration within the pore (mass of sorbate/volume of air), q_o is the sorbed-phase concentration in equilibrium with imposed gas-phase concentration C_o, a_m is the radius of the microsphere, and k and n are empirical parameters for the Freundlich isotherm equation. These initial and boundary conditions state (a) that the sorbed mass is initially uniformly distributed throughout the microsphere, (b) that the sorbed mass is symmetrically distributed with respect to the center, and (c) that the sorbed mass is linked to the concentration in the pore air by assuming that the partitioning of sorbate molecules at the surface of the microspheres follows the Freundlich isotherm.

Sorbate Transport within Peat Grains. Considering transient diffusion and sorption, a mass balance on a small element of pore volume within a grain is combined with Fick's law to yield the following differential material balance:

$$\varepsilon_p \frac{\partial C}{\partial t} + (1-\varepsilon_p)\rho_p \frac{\partial q^*}{\partial t} = \frac{\varepsilon_p}{r^2}\frac{\partial}{\partial r}\left(r^2 D_p \frac{\partial C}{\partial r}\right) \tag{3}$$

where ε_p is the grain porosity, ρ_p is the density of the solid part of the sorbent, r is the radial coordinate of the grain, D_p is the effective gas diffusivity of sorbate molecules through the intraparticle pore space, and q^* is the total mass of sorbate in the microspheres, which can expressed as:

$$q^* = \frac{3}{a_m{}^3}\int_0^{a_m} r_m{}^2 q(r_m) dr_m \tag{4}$$

The initial and boundary conditions for equation (3) are:

$$C(0<r<1, t=0) = 0 \text{ (sorption)}$$

$$\text{or} \quad C(0<r<1, t=0) = C_o \text{ (desorption)}$$

$$\partial C/\partial r\,(r=0, t) = 0 \tag{5}$$

$$\frac{\partial C}{\partial r}\Big|_{r=a} = \frac{B}{a}(C_o - C_s)$$

where a is the radius of the peat grain, C_s is C at r=a, $B=k_f a/(D_p \varepsilon_p)$ is the mass-transfer Biot number, and k_f is the gas-film mass transfer coefficient. These initial and boundary conditions state (a) that the sorbate concentration is initially uniformly distributed throughout the grain, (b) that the sorbate concentration is symmetrically distributed with respect to the grain center, and (c) that the flux into or out of the grain must match the rate of mass transport across the external gas-film boundary.

The relative mass uptake for sorption (M_t/M_∞), or the loss for desorption ($1-M_t/M_\infty$), at a specific time can be found by integrating the mass sorbed over the entire

grain. By assuming that the sorbate mass is mostly in the sorbed-phase (microspheres), this yields

$$\frac{M_t}{M_\infty} = \frac{3}{a^3}\int_0^a r^2\left(\frac{q^*(r,t)}{q_o}\right)dr \qquad (6)$$

where M_t is the total mass sorbed at time t and M_∞ is the equilibrium mass sorbed at a gas-phase concentration of C_o.

The system described by equations (1)-(5) is analogous to a macrodiffusion and microdiffusion model used in zeolite (Ruthven and Loughlin, 1972) and activated carbon systems (Gray and Do, 1989). The relative importance of macropore and micropore diffusion resistance may be estimated by the magnitude of the parameter Ω (Ruthven and Loughlin, 1972; Gray and Do, 1989):

$$\Omega = \frac{(1-\varepsilon_p)\rho_p}{\varepsilon_p}\frac{(D_\mu)_{avg}}{D_p}\left(\frac{a}{a_m}\right)^2\frac{dq}{dC} \qquad (7)$$

where $(D_\mu)_{avg}$ is the average D_μ for the concentration range of interest. Ruthven and Loughlin (1972) and Gray and Do (1989) have shown that macropore diffusion (gas-phase pore diffusion in this study) will control the transport process if Ω is larger than about 20-30, while micropore diffusion (solid-phase SOM microsphere diffusion in this study) will govern the rate of uptake if Ω is less than about 0.2 for sorption and 0.01 for desorption.

MATERIALS AND METHODS

Sorbates and Sorbent. Water vapor and benzene were chosen as representative sorbates as they were used in our experimental study of mineral grains (Chapter II). Gas phase concentrations between 0.05 to 0.86 relative pressure (P/P_o) for water vapor and 0.10 to 0.40 for benzene were tested. The peat sample was provided by C.T. Chiou. It was from a batch previously used in equilibrium sorption studies for VOCs in aqueous systems (Rutherford et al., 1992) and for both water vapor and VOC sorption in vapor

systems (Rutherford and Chiou, 1992; Chiou and Kile, 1994). In the present study, a narrow size range between 60 and 80 US standard mesh (0.18-0.25 mm) was used in the sorption experiments. The BET surface area and the weight proportion of SOM were measured by Chiou and coworkers (Rutherford et al., 1992; Chiou and Kile, 1994) to be 1.3-1.5 $m^2\ g^{-1}$ and 86.4%, respectively. Efforts were made to determine the specific surface area, porosity and pore size distribution using a mercury intrusion method similar to that used in Chapter II. However, the results of the measurements were found to defy reality, apparently because of the fundamental properties of peat. The SOM in peat is thought to be polymer-like and is pliable in response to strong applied pressure. Therefore, mercury molecules may be able to penetrate the matrix of SOM and create additional pore space as the applied pressure increases (Chiou, 1994). In fact, our experimental results show that the surface area measured by this method is about 20 times higher than that from low-temperature nitrogen adsorption, indicating that the additional surface area is probably created by penetration of mercury into the SOM matrix. The skeleton density of peat was measured to be 1.56×10^6 g/m^3 using helium pycnometer (AccuPyc 1330, Micromeritics, Norcross, GA).

Sorption Experiments. Sorption experiments were performed with a Cahn-1000 electrobalance (Cahn Inc., Cerrito, CA) to determine both sorption kinetics and isotherms at 20°C. Because the experimental apparatus and procedures are very similar to those reported in Chapter II, only the differences are listed here. The mass of peat samples used in the experiments was in the range 10-50 mg. The time required to condition the sample was normally more than about 72 hours. The time to reach equilibrium for sorption was typically about 15 hours, while more than 72 hours was required to establish desorption equilibrium. Since sorption experiments of benzene on peat were conducted under near zero moisture condition, the effect of microbial decomposition of benzene within peat samples is neglected in this study, even though the experiments generally lasted for several days. The desired water vapor and benzene concentrations were obtained by

passing hydrocarbon-free (HC-free) air (Airco, Newark, CA) through gas bubblers filled with liquid water or benzene. The temperature of both generators was controlled within ±0.1°C of the preset temperature. The relative humidity was measured by a dew-point hygrometer (Model 911, EG&G, Waltham, MA). The relative pressure of benzene was determined by a gas chromatograph (GC) (HP-5890 II) equipped with a flame ionization detector (FID). In determining the relative pressure of benzene, a Tedlar bag (SKC, Fullerton, CA) was used to collect a gas sample before it entered the electrobalance. The gas sample was then diluted with HC-free air to an appropriate concentration for the GC/FID measurement.

RESULTS AND DISCUSSION

Equilibrium Sorption for Water Vapor. To investigate transport and sorption of water vapor within peat grains, the sorption isotherm of water vapor to peat was first measured. A sorption isotherm of water vapor to the same peat material was previously determined by Rutherford and Chiou (1992) up to P/P_o=0.75. They found noticeable curvature in the region of P/P_o=0-0.1 followed by an essentially linear rise to P/P_o=0.8 (actually 0.75 if based on the experimental data). In this study, experiments were performed up to P/P_o=0.86 and the resulting isotherm is shown in Figure 3. As shown in the figure, the shape of the isotherm for water to peat closely resembles that determined by Rutherford and Chiou (1992) except for RH>75%. In our measurement, the sorption capacity at P/P_o>0.75 is clearly higher than the values that fall on the linear line. Rutherford and Chiou (1992) suggested that the linear portion of the isotherm is attributed to the dissolution of water in the hydrated organic matter. It is suggested from our experimental results that, in addition to the dissolution mechanism, condensation may take place in the intragrain pores at high P/P_o. In fact, the sorption isotherm in this study is very similar to a type II isotherm in the BET classification normally found for hydrophilic polymers such as wool, silk and cellulosic materials (Barrie, 1968). It is also observed that

our sorption capacity measurements are about 10-15% lower than those obtained by Rutherford and Chiou (1992). Although the temperature (20°C) we used is different than that of Rutherford and Chiou (1992) (24°C), the temperature effect on solubility does not account for such a big difference. In fact, we also conducted a sorption experiment at 24°C, and observed no significant effect on the sorption capacity. We believe that the discrepancy may be a result of the differences between (a) measurement techniques, i.e. an electrobalance under vacuum and static conditions for Rutherford and Chiou (1992) versus an electrobalance under dynamic conditions in this study, and/or (b) subsamples used in two studies (we used peat samples with diameters between 0.18 and 0.25 mm, and Rutherford and Chiou used samples ground from the bulk batch).

Kinetics of Water Vapor Sorption. A typical set of sorption kinetic curves of water vapor to peat is shown in Figure 4. The sorption rate was found to be faster than the desorption rate for all three cases tested: P/P_o=0.23, 0.36 and 0.50. Although several other reasons may account for similarly asymmetric sorption and desorption rates, the experimental data were first analyzed using the gas-phase pore diffusion model with a nonlinear isotherm. A Freundlich isotherm was used in this analysis, as shown in Figure 3, and it agrees well with the experimental data up to about 65% RH. The mathematical formulation of the dual diffusion model, under the condition in which gas-phase pore diffusion control the overall rate of uptake, reduces to the porous sphere model presented in Chapter II. As in that chapter, a scheme similar to the least-squares method was applied to determine the best fit of the model to the experimental data using one or two adjustable parameters. Because the isotherm of water vapor to peat was obtained in advance, only one adjustable parameter, the effective diffusivity, D_e, is available for fitting the model. The effective diffusivity can be linked to other parameters by the following equation, derived in Chapter II:

$$D_e = \frac{\varepsilon_p}{(1-\varepsilon_p)\rho_p kn} D_p C_o^{1-n} \tag{8}$$

It is clearly shown in equation (8) that, if all the other parameters remain the same, the value of D_e will change as the imposed concentration (C_o) changes.

Figure 5 shows the experimental data at P/P_o=0.50 and the best fit found for the model. The pore diffusion model conforms to the data very well and the asymmetry between sorption and desorption is clearly resolved. According to equation (8), the D_e value extracted from one kinetic experiment can be used to estimate D_e for other water vapor concentrations. The D_e values, estimated from the experiment with P/P_o=0.50, were then used to predict sorption kinetic curves for P/P_o=0.23 and 0.36 as shown in Figure 6. Overall, the model predictions agree with the experimental data very well, regardless of the differences in applied water vapor concentration. The good agreement of model predictions with experimental data indicates that the assumption of pore diffusion control in this system is likely to be appropriate.

The pore diffusivity, D_p, can be calculated from the estimated D_e value using equation (8), provided that all the other quantities are independently known. All the required parameters (ρ_p, k, n and C_o), except the porosity, ε_p, were either measured or interpreted from the experimental data. Although ε_p remains unknown at this stage, it is probably safe to assume that $1-\varepsilon_p$ is close to 1. Using this approximation, the value of $\varepsilon_p D_p$ is calculated from equation (8) to be 2.4×10^{-8} m^2 s^{-1}. This $\varepsilon_p D_p$ value is similar to those for the three natural low-organic soils (from 4.3×10^{-9} to 1.4×10^{-7} m^2 s^{-1}) used in Chapter II.

To confirm that the assumption of gas-phase pore diffusion control was valid, the extracted $\varepsilon_p D_p$ value was used to estimate Ω from equation (7). Because of the shape of the isotherm, a lower concentration would have a larger slope for the isotherm (dq/dC) and thus, a larger value of Ω. Therefore, we used the slope at the highest water vapor concentration studied, P/P_o=0.5. The remaining parameters needed to calculate Ω are the average diffusivity of water vapor in soil organic matter, $(D_\mu)_{avg}$, and the radius of the microspheres, a_m. Assuming that the measured BET surface area of peat grains (~1.4 m^2

g^{-1}) is equal to the sum of the external surface area of all the microspheres, a_m can be estimated from the skeleton density of the grains (1.56×10^6 g m^{-3}) to be about 1.4×10^{-6} m (1.4 μm). This value is consistent with the characteristic length of microspheres (diameter ~ 3 μm) shown on the SEM photomicrograph of the peat grain surface (Figure 1). To ensure macropore diffusion control in this system, or $\Omega>20$, the $(D_\mu)_{avg}$ value needs to be larger than 6×10^{-15} m^2 s^{-1}. Since it appears that no literature value of water diffusivity within SOM is available, the diffusivity of water within two polymers, wool and nylon 6, is used to compare with the $(D_\mu)_{avg}$. Both wool and nylon 6 are polyamides, which have C=O and N-H groups similar to those that may be found in SOM (Chiou, 1994). The diffusivity of water vapor has been reported to be approximately 10^{-13} m^2 s^{-1} for both wool and nylon 6 (Barrie, 1968). This value is sufficiently large to effectively substantiate the assumption of gas-phase pore diffusion control.

Equilibrium Sorption for Benzene Vapor. Equilibrium sorption capacity of benzene vapor on peat was measured for partial pressures in the range P/P_o=0.1 to P/P_o=0.4. The experimental data are presented in Figure 7. The sorption capacities exhibit significant scatter. Although the sorption capacity is of the same order of magnitude as that determined by Rutherford and Chiou (1992), no definite isotherm can be obtained due to the lack of reproducibility in this experiment.

Substantial effort was made to try to improve the reproducibility of the sorption capacity data, including checking the sampling and analysis techniques for benzene vapor, recalibrating the electrobalance, extending the sorption-desorption time to ensure equilibrium, and increasing the mass of peat sample for each run. However, none of these approaches yielded more reproducible sorption capacity results. Since water has much more affinity to peat than benzene, small amounts of water vapor in the system, for example from the benzene source, may have had a strong effect on the measured benzene sorption capacity. An effort was made to eliminate dissolved water from the benzene source by purging HC-free air through the gas bubbler for a lengthy period after filling the

bubbler with benzene. The aging effect for the benzene/peat system due to the prior exposure of the peat to water vapor or benzene was also considered. However, no systematic differences were observed between the experiments conducted using fresh and aged peat samples.

The reasons for being not able to generate reproducible sorption capacity remain unclear. We suspect that the effect of water vapor may not have been completely eliminated by purging HC-free air through the benzene bubbler. In addition, there might have been other sources of water vapor in the system. Since the measurement technique employed by Rutherford and Chiou (1992) can only determine sorption capacity for the benzene-peat system, an additional experimental design and debugging effort is required to permit measurement of sorption capacity and sorption kinetics for a single sample.

Kinetics of Benzene Sorption. Despite the scatter in the sorption capacity data, sorption kinetics exhibit consistent behavior, with sorption rates always much faster than desorption rates. A typical sorption/desorption kinetic curve is shown in Figure 8. Since no isotherm was obtained in this study, the reasons for the observed sorption-desorption asymmetry are discussed qualitatively for the cases of both linear and nonlinear isotherms.

If the isotherm is nonlinear, the pore diffusion model may be able to describe the asymmetric behavior. Following the procedures used in modeling the sorption kinetics for water vapor on peat, the best fit model and the corresponding experimental data are shown in Figure 9 (a). Two parameters were adjusted in fitting the model: the effective diffusivity (D_e) and the Freundlich exponent (n); their values were found to be 1.2×10^{-12} m^2 s^{-1} and 0.2, respectively. Although the model captures the sorption/desorption asymmetry, it does not follow the experimental data closely, especially for the desorption case. Using the best fit values for the model, the $\varepsilon_p D_p$ value is calculated to be 2.7×10^{-11} m^2 s^{-1} from equation (8), if we assume that q is equal to about 5 mg/g at P/P_o=0.25 (see Figure 7). Although this value of q is only a rough estimation, we expect that the true $\varepsilon_p D_p$ value should be of

the same order of magnitude as estimated. The extracted $\varepsilon_p D_p$ value can be compared with that for the water vapor/peat system. For the diffusion of different molecular species in the same porous structure, a similar diffusional pathway is expected. Theoretically, if the diffusion of both water vapor and benzene within peat grains is controlled by pore diffusion only, the $\varepsilon_p D_p$ values for the two species should be roughly proportional to their molecular diffusivity in air and are therefore expected to be of the same order of magnitude. In fact, the $\varepsilon_p D_p$ value for benzene is about three orders of magnitude smaller than that for water vapor. Therefore, we believe that intragranular gas-phase pore diffusion is not likely to be the rate-limiting mechanism for benzene diffusion within peat grains in this study.

If the isotherm for benzene sorption by peat is linear as reported in the literature (Rutherford and Chiou, 1992), a concentration-dependent D_μ may be combined with the solid-phase diffusion model or the bimodal diffusion model (if both gas-phase pore diffusion and solid-phase intra-SOM diffusion are important) to generate results that are qualitatively similar to those presented in Figure 9 (a). For the sake of mathematical simplicity, only the solid-phase intra-SOM diffusion model will be considered here. For the diffusion of an organic vapor in a polymer, the penetrating molecules may change the structure of the polymer segments and cause their transport to become more rapid (Paul, 1985). Consequently, the diffusivity of the organic vapor may increase as the sorbed-phase concentration increases. Such a relationship may be described as follows (Paul, 1985):

$$D_\mu = D_{\mu o}\ e^{\gamma q} \tag{9}$$

where $D_{\mu o}$ is D_μ at q=0 and γ is an empirical parameter. Although the sorbed-phase concentration of benzene in peat may not be large enough to generate a structural change in the SOM segments, we tentatively assume that equation (9) is a good representation for the diffusivity of benzene in this system. Equation (9) is then combined with equation (1) to render the following dimensionless governing equation:

$$\frac{\partial Q}{\partial \theta_m} = \frac{1}{x_m^2}\frac{\partial}{\partial x_m}\left(x_m^2 \; e^{\Gamma Q} \; \frac{\partial Q}{\partial x_m} \right) \tag{10}$$

where $Q=q/q_o$, $\theta_m=(D_{\mu o}t)/a_m^2$, $x_m=r_m/a_m$, and $\Gamma=\gamma q_o$. Equation (10) along with appropriate initial and boundary conditions (equation (2) with n=1) was solved by a numerical method similar to that described in Chapter II. By adjusting two parameters: $(D_{\mu o}/a_m^2)$ and Γ, the models were fitted to the experimental data using the same procedures as for the gas-phase pore diffusion model. The best fits found for the models and their corresponding data are shown in Figure 9 (b), with $(D_{\mu o}/a_m^2)$ and Γ equal to 2.0×10^{-7} s^{-1} and 6.5, respectively. This model still resolves the asymmetry between sorption and desorption rates, while providing a better fit to the desorption data than does the pore diffusion model (Figure 9 a).

The average SOM diffusivity, $(D_\mu)_{avg}$, can be estimated from the following equation:

$$(D_\mu)_{avg} = D_{\mu o} \int_0^1 e^{\Gamma Q} \, dQ \tag{11}$$

With $\Gamma=6.5$, $(D_\mu)_{avg}$ is equal to about $100\times D_{\mu o}$. Using the same value of a_m as inferred for water vapor sorption on peat (1.4×10^{-6} m), $(D_\mu)_{avg}$ is approximately 4×10^{-17} m^2 s^{-1}. Compared with the $(D_\mu)_{avg}$ value we estimated for water vapor within SOM, the inferred value for benzene is two orders of magnitude smaller. This finding is consistent with the fact that polar molecules (water) have a higher diffusivity than nonpolar molecules in a hydrophilic polymer and that smaller molecules (water) would also tend to have a higher diffusivity.

To determine if the assumption of solid-phase intra-SOM diffusion control is valid, equation (7) is again used to calculate Ω. Assuming that the diffusional pathway for water vapor and benzene within the macropore of peat grains are the same, the $\varepsilon_p D_p$ value for benzene is estimated to be about 1.0×10^{-8} m^2 sec^{-1}. The Ω value is calculated to be about

0.004, based on the assumption that a linear isotherm prevails (n=1) with k=100 g cm^{-1} (approximately the average partition coefficient measured for $P/P_o<0.2$). This value of Ω suggests that the assumption that mass transport is limited by solid-phase intra-SOM diffusion is likely to be valid.

CONCLUSIONS

The sorption isotherm for water vapor on peat is found to be similar to that reported in the literature, whereas a reproducible isotherm for benzene could not be obtained. The gas-phase pore diffusion model is shown to resolve the asymmetry between sorption and desorption rates and conforms very well to the experimental data for water vapor at three different concentrations. In contrast, the solid-phase intra-SOM diffusion model with concentration-dependent diffusivity is found to conform fairly well to the experimental data for sorption kinetics of benzene on peat. As a first-order estimation, the average solid-phase diffusivity for benzene within the matrix of SOM (peat) is inferred to be about 4×10^{-17} m^2 s^{-1}.

APPENDIX I. REFERENCES:

Allen, S., Brown, P., McKay, G., and Flynn, O. (1992). "An evaluation of single resistance transfer models in the sorption of metal ions by peat." *J. Chem. Tech. Biotechnol.*, *54*, 271-276.

Ball, W.P., and Roberts, P.V. (1991a). "Long-term sorption of halogenated organic chemicals by aquifer material: 1. Equilibrium." *Environ. Sci. Technol.*, *25*, 1223-1236.

Ball, W.P., and Roberts, P.V. (1991b). "Long-term sorption of halogenated organic chemicals by aquifer material: 2. Intraparticle diffusion." *Environ. Sci. Technol.*, *25*, 1237-1249.

Barrie, J.A. (1968) "Water in polymers." In *Diffusion in Polymers*, Crank, J., and Park, G.S., ed., Academic Press, London, England, 259-313.

Chiou, C.T. (1994). Personal communication.

Chiou, C.T., and Kile, D.E. (1994) "Effects of polar and nonpolar groups on the solubility of organic compounds in soil organic matter." *Environ. Sci. Technol.*, *28*, 1139-1144.

Chiou, C.T., and Shoup, T.D. (1985). "Soil sorption of organic vapors and effects of humidity on sorptive mechanism and capacity." *Environ. Sci. Technol.*, *19*, 1196-1200.

Chiou, C.T., Porter, P.E., and Schmedding, D.W. (1983). "Partition equilibria of nonionic organic compounds between soil organic matter and water." *Environ. Sci. Technol.*, *17*, 227-231.

Cloutier, J.N., Leduy, A., and Ramalho, R.S. (1985). "Peat adsorption of herbicide 2,4-D from wastewaters." *Can. J. of Chem. Eng.*, *63*, 250-257.

Garbarini, D.R., and Lion, L.W. (1986). "Influence of the nature of soil organics on the sorption of toluene and trichloroethylene." *Environ. Sci. Technol.*, *20*, 1263-1269.

Gosset, T., Trancart, J.L., and Thevenot, D.R. (1986). "Batch metal removal by peat." *Water Research* , *20*, 21-26.

Gray, P.G., and Do, D.D. (1989). "Adsorption and desorption of gaseous sorbates on a bidispersed particle with Freundlich isotherm: I. Theoretical analysis." *Gas Sep. Purif.*, *3*, 193-200.

Harmon, T.C., and Roberts, P.V. (1994). "Comparison of intraparticle sorption and desorption rates for a halogenated alkene in a sandy aquifer material." *Environ. Sci. Technol.*, *28*, 1650-1660.

Johnson, P.C., Kemblowski, M.W., and Colthart, J.D. (1988). "Practical screening models for soil venting applications." *Proceedings of NWWA/API Conference on Petroleum Hydrocarbons and Organic Chemicals in Ground Water*, Houston, TX, pp. 521-546.

Karickhoff, S.W., Brown, D.S., and Scott, T.A. (1979). "Sorption of hydrophobic pollutants on natural sediments." *Water Research* , *13*, 241-248.

Little, J.C., Daisey, J.M., and Nazaroff, W.W. (1992). "Transport of subsurface contaminants into buildings: An exposure pathway for volatile organics." *Environ. Sci. Technol.*, *26*, 2058-2066.

McKay, G., and Allen, S.J. (1984). "Pore diffusion for dye adsorption onto peat in batch adsorbers." *Can. J. of Chem. Eng.*, *62*, pp. 340-345.

Paul, D.R. (1985) "Transport properties of polymers." In *ACS Symposium Series 285: Applied Polymers Science*, 2nd ed., American Chemical Society, Washington, D.C., pp. 253-275.

Rutherford, D.W., and Chiou, C.T. (1992). "Effect of water saturation in soil organic matter on the partition of organic compounds." *Environ. Sci. Technol.*, *26*, 965-970.

Rutherford, D.W., Chiou, C.T., and Kile, D.E. (1992). "Influence of soil organic matter composition on the partition of organic compounds." *Environ. Sci. Technol.*, *26*, 336-340.

Ruthven, D.M., and Loughlin, K.F. (1972)."The diffusional resistance of molecular sieve pellets." *Can. J. Chem. Eng.*, *50*, 550-552.

Schwarzenbach, R.P., Gschwend, P.M., and Imboden, D.M. (1993) *Environmental Organic Chemistry*. John Wiley and Sons, New York, N.Y., p. 269.

Weber, W.J., and Miller, C.T. (1988). "Modeling the sorption of hydrophobic contaminants by aquifer materials: I. Rates and equilibria." *Water Research, 22*, 457-464.

Weber, W.J., McGinley, P.M., and Katz, L.E. (1991). "Sorption phenomena in subsurface systems: Concepts, models and effects on contaminant fate and transport." *Water Research, 25*, 499-528.

Wu, S.-C., and Gschwend, P.M. (1986). "Sorption kinetics of hydrophobic organic compounds to natural sediments and soils." *Environ. Sci. Technol., 20*, 717-725.

APPENDIX II. NOMENCLATURE

a	radius of peat grain (m)
a_m	radius of soil organic matter (SOM) microsphere (m)
B	Biot number [$= (k_f a)\ (\varepsilon_p D_p)^{-1}$] (dimensionless)
C	gas-phase sorbate concentration (g m^{-3})
C_o	imposed, external gas-phase species concentration for kinetic studies (g m^{-3})
C_s	gas-phase concentration at external surface of peat grain (g m^{-3})
D_e	effective diffusivity ($m^2\ s^{-1}$)
D_p	pore diffusivity in peat grain ($m^2\ s^{-1}$)
D_μ	solid diffusivity in SOM microsphere ($m^2\ s^{-1}$)
$(D_\mu)_{avg}$	average solid diffusivity in SOM microsphere ($m^2\ s^{-1}$)
$D_{\mu o}$	solid diffusivity in SOM microsphere at zero sorbate concentration ($m^2\ s^{-1}$)
k	Freundlich isotherm parameter ((g g^{-1}) × (g m^{-3})$^{-n}$)
k_f	gas-film mass-transfer coefficient (m s^{-1})
M_t/M_∞	cumulative mass gain at time t relative to that in equilibrium with C_o (dimensionless)
M_θ/M_∞	cumulative mass gain relative to that in equilibrium with C_o (dimensionless)
n	Freundlich isotherm parameter (dimensionless)
q	(equilibrium) sorption capacity (g sorbate per g peat)
q_o	sorption capacity in equilibrium with C_o (g sorbate per g peat)
q^*	sorption capacity for SOM microsphere (g sorbate per g peat)
Q	normalized solid-phase species concentration [$= q\ q_o^{-1}$] (dimensionless)

r	radial coordinate in peat grain (m)
r_m	radial coordinate in peat microsphere (m)
t	time (s)
x_m	normalized radial coordinate in SOM microsphere [$=r_m\ a_m^{-1}$] (dimensionless)
Γ	normalized empirical parameter for the concentration-dependent diffusivity [$=\gamma\ q_o$] (dimensionless)
γ	empirical parameter in eq (9) for the concentration-dependent diffusivity (g peat per g sorbate)
ε_p	grain porosity (dimensionless)
θ	normalized time for individual grains [$= t\ D_e\ a^{-2}$] (dimensionless)
θ_m	normalized time for SOM microsphere [$= t\ D_{\mu o}\ a_m^{-2}$] (dimensionless)
ρ_p	solid density of peat grain (g m^{-3})
Ω	parameter for determining the rate-limiting mechanism in the dual diffusion model [see eq (7)] (dimensionless)

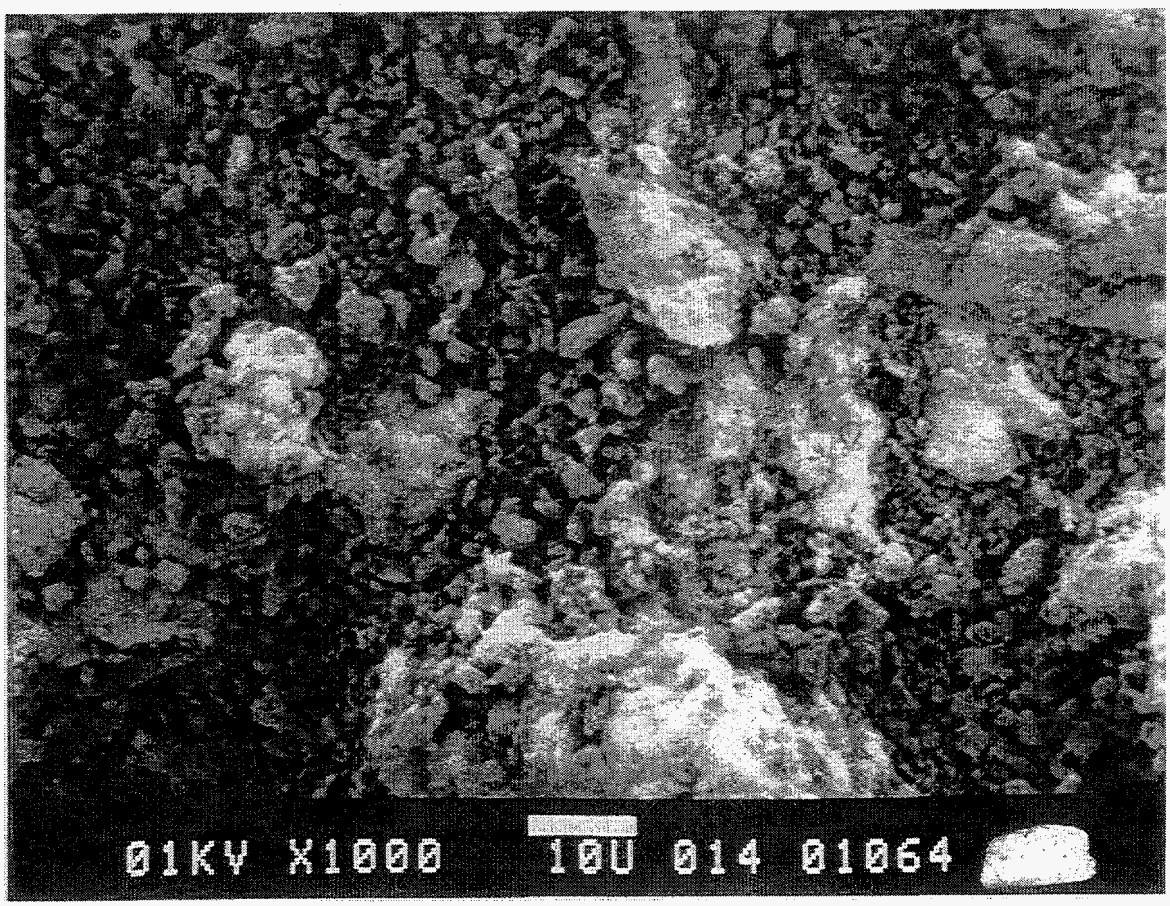

Figure 1. Scanning electron microscope (SEM) photomicrograph for peat grain surface. The grain diameter is about 200 μm and the "10U" bar represents a length of 10 μm. (Note that the granules have a characteristic dimension of ~ 3 μm.)

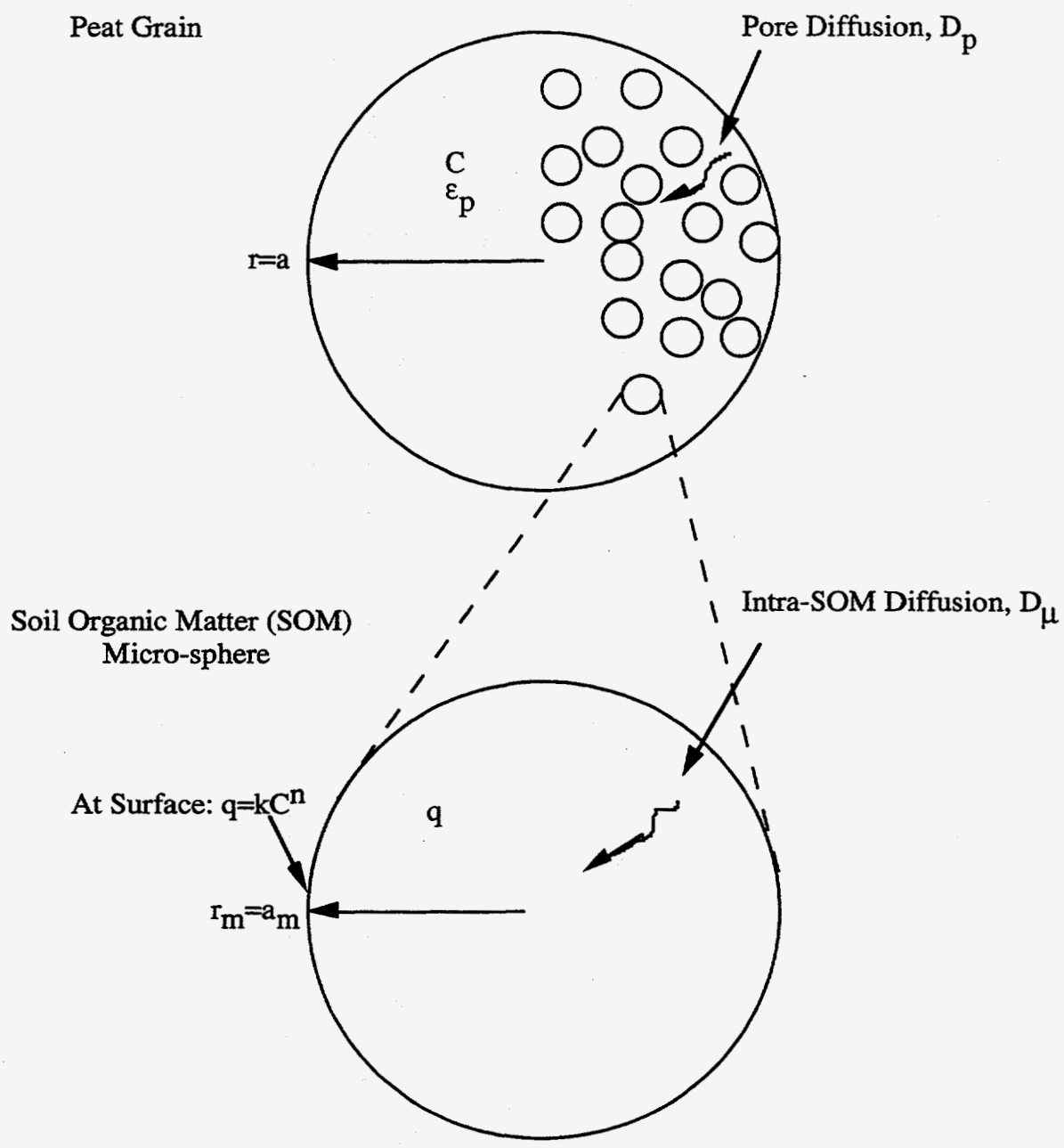

Figure 2. Schematic representation of the dual diffusion model used in this study. See symbols and text for parameter definitions.

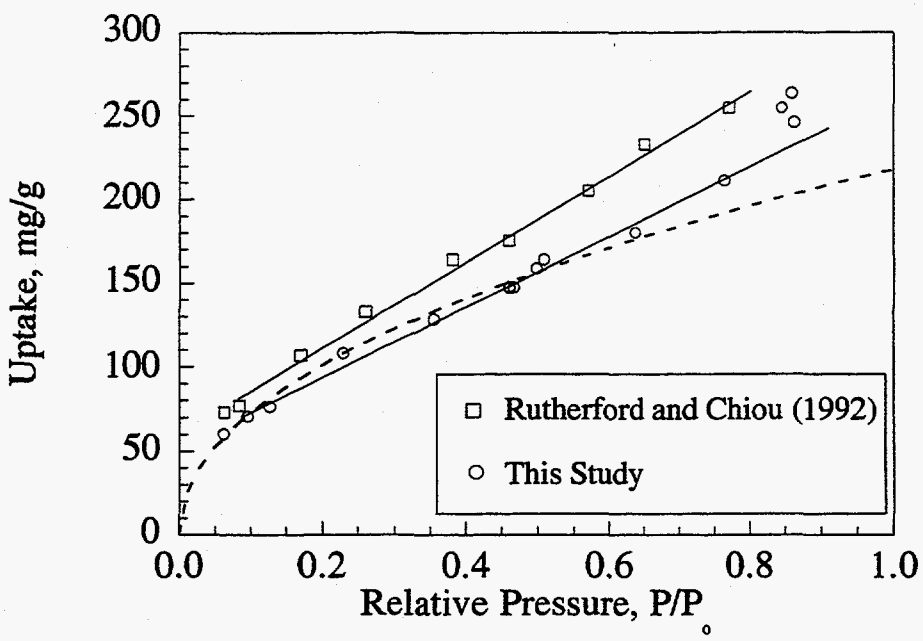

Figure 3. Sorption isotherm for water vapor on peat. The solid lines represent linear portions of the isotherms obtained by Rutherford and Chiou (1992) and this study. The dashed line represents a best fit for the data (from this study) up to RH=65% based on the Freundlich isotherm, $q=1500\ C^{0.48}$, where q is in mg/g and C is in mg/cm^3.

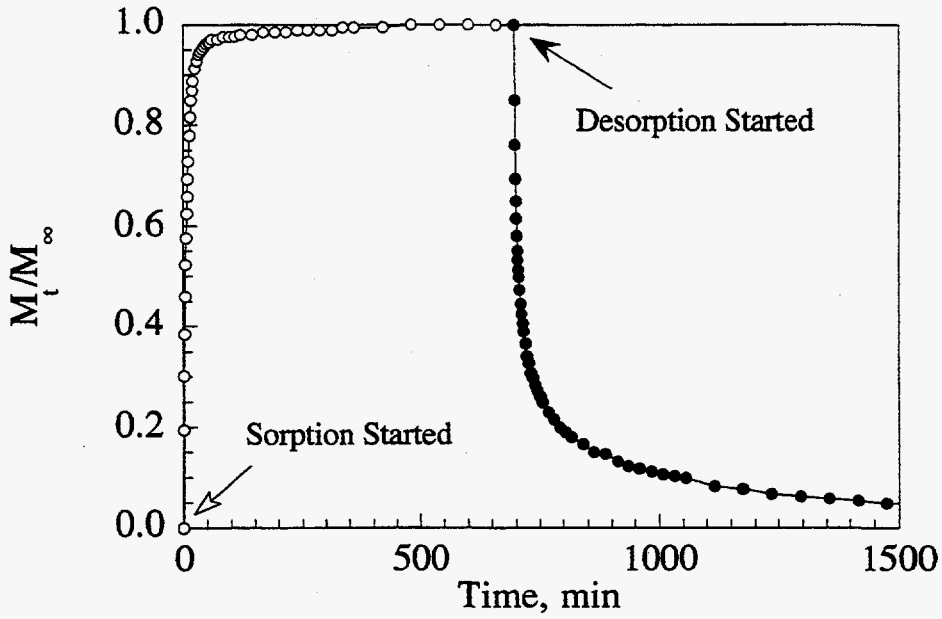

Figure 4. Typical experimental sorption kinetic curves for water vapor (50% RH) on dry peat grains. M_t/M_∞ is the cumulative mass gain at time t relative to that at equilibrium.

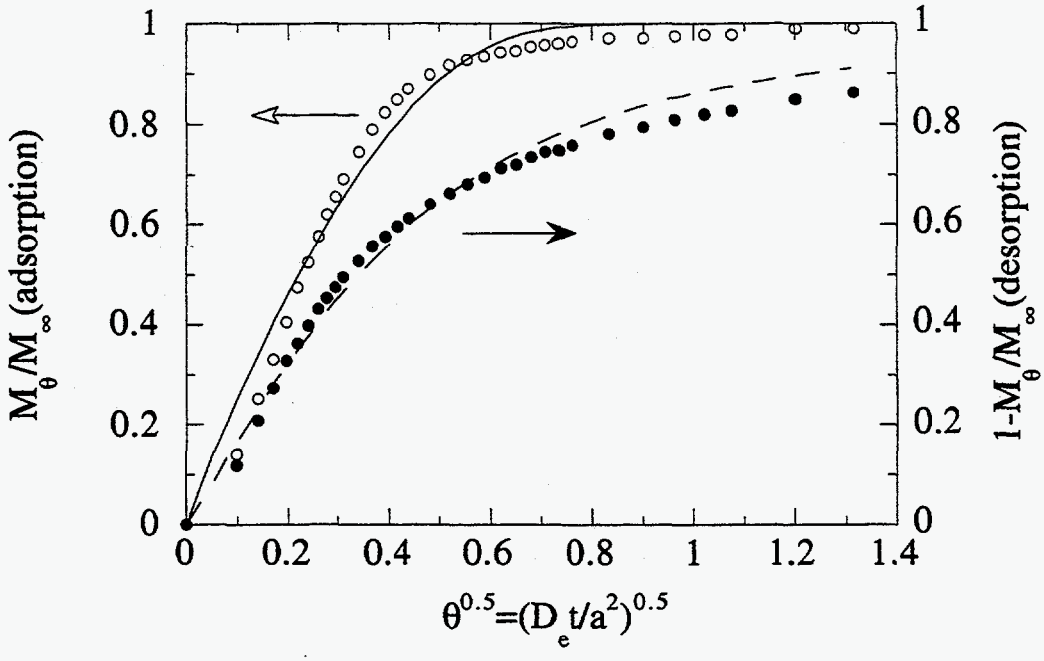

Figure 5. Sorption kinetics for water vapor at 50% RH on dry peat. See Appendix II for definition of parameters. The open and filled symbols denote experimental adsorption and desorption data, respectively. The fitted gas-phase pore diffusion model is shown as a solid line for sorption and as a dashed line for desorption. In the model, B is assumed to be ∞ (>300). The best fit value for D_e is 1.8×10^{-12} m^2 s^{-1}.

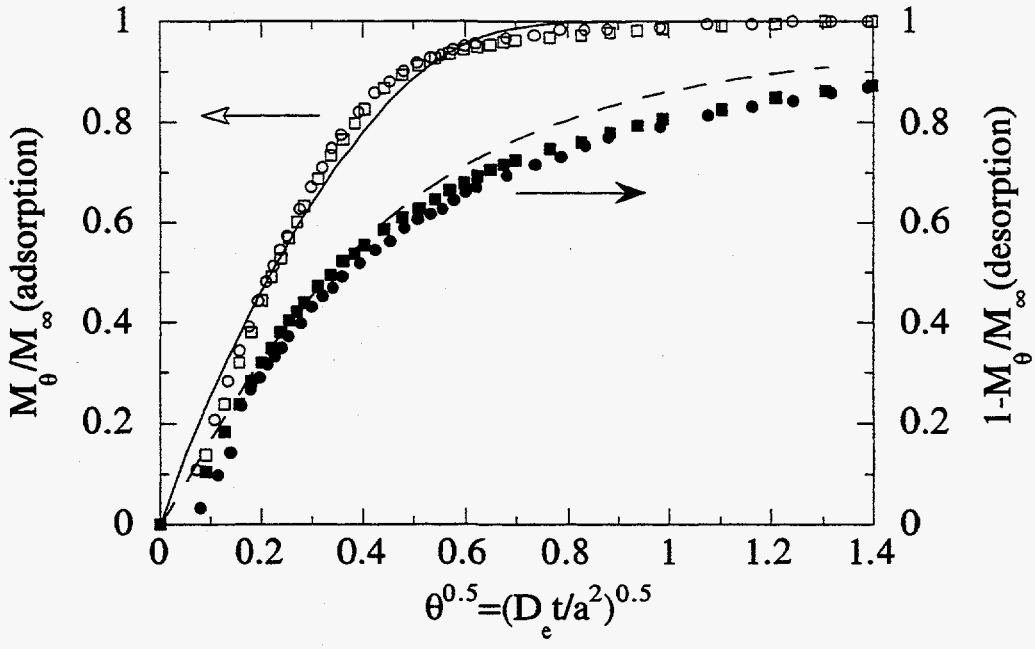

Figure 6. Sorption kinetics for water vapor at 23% and 36% RH on dry peat. See Appendix II for definition of parameters. The open and filled symbols denote experimental sorption and desorption data, respectively, while the circles and squares represent data at 23% and 36% RH, respectively. The predicted gas-phase pore diffusion model is shown as a solid line for sorption and as a dashed line for desorption. In the model, B is assumed to be ∞ (>300). The D_e values used for the prediction are calculated from equation (8) along with the D_e value extracted from the kinetic experiment for 50% RH (Fig. 5).

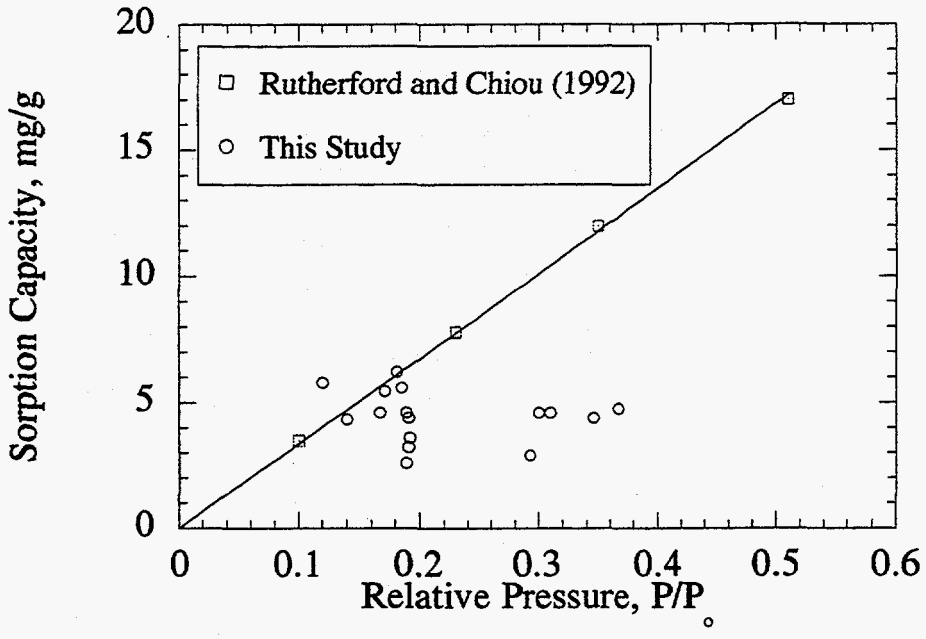

Figure 7. Sorption capacity for benzene on peat.

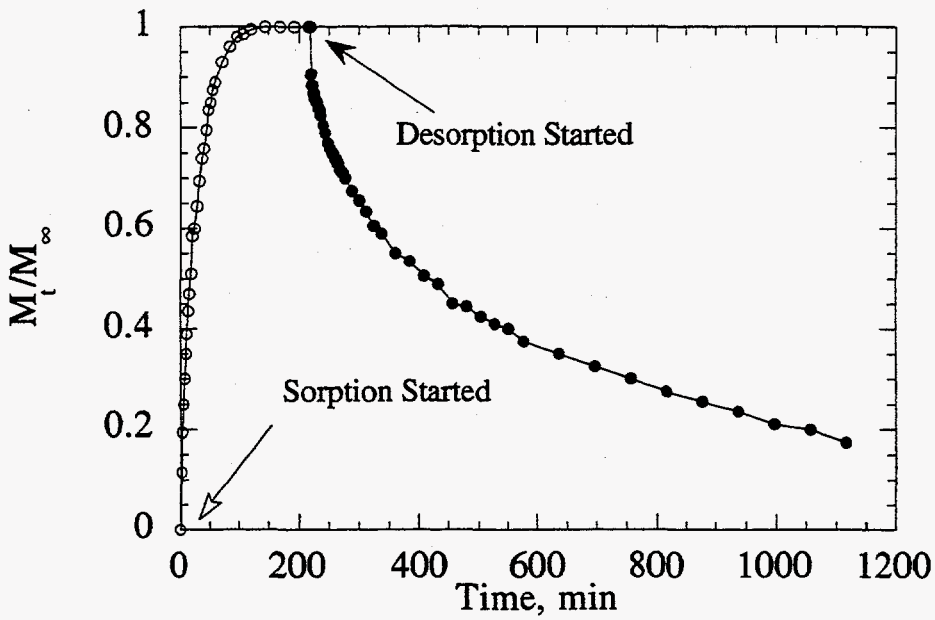

Figure 8. Typical experimental sorption kinetic curves for benzene (P/P_o=0.16) on dry peat grains. M_t/M_∞ is the cumulative mass gain at time t relative to that at equilibrium.

(a)

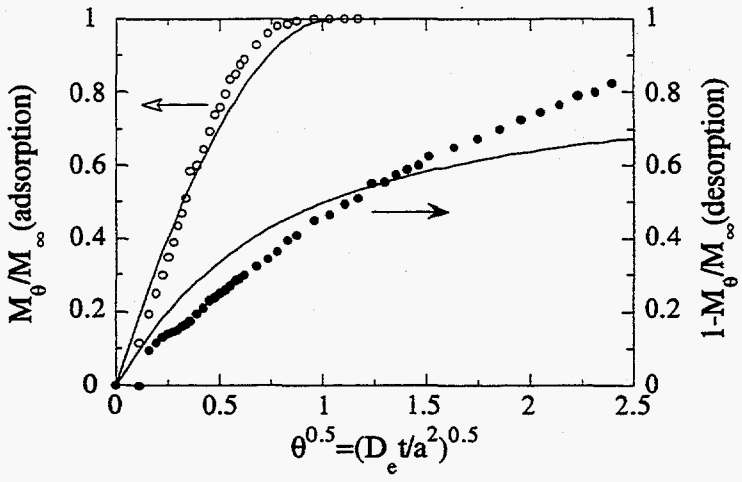

(b)

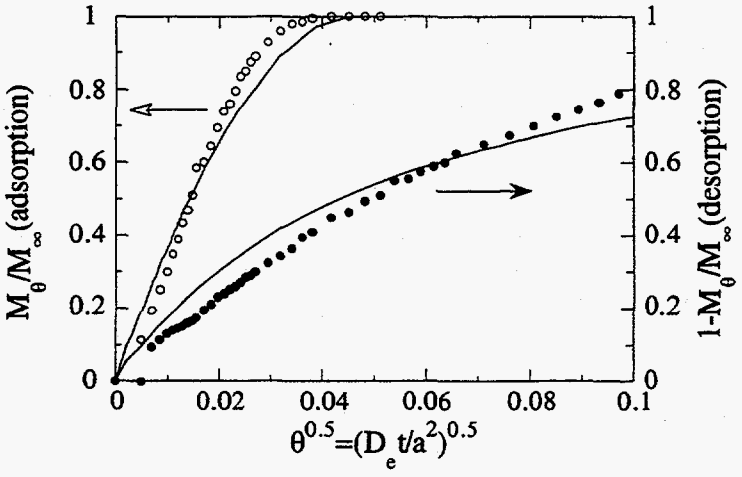

Figure 9. Sorption kinetics for benzene at $P/P_o=0.16$ on dry peat. See Appendix II for definition of parameters. The open and filled symbols denote experimental sorption and desorption data, respectively. The fitted models—(a) gas-phase pore diffusion model and (b) solid-phase intra-SOM diffusion model—are shown as a solid line for sorption and as a dashed line for desorption. In the models, (a) the best fit values for n and D_e are 0.20 and 1.2×10^{-12} m^2 s^{-1}, respectively, and (b) the best fit values for Γ and $(D_{\mu o}/a_m^2)$ are 6.5 and 2.0×10^{-7} s^{-1}, respectively.

Chapter IV

Gas-Phase Transport and Sorption of Benzene Through Soil Columns

ABSTRACT

To better understand the transport of gas-phase organic compounds through soil near buildings, we have studied the sorption kinetics of benzene on low-organic-content soil grains and its transport through soil columns under both dry and moist conditions. For dry soil, the adsorption/desorption kinetic data revealed strong asymmetry, with adsorption occurring faster than desorption. For the moist soil, adsorption and desorption kinetics were faster and symmetric. The degree of asymmetry in adsorption and desorption rates is governed by the shape of the sorption isotherm. Through the use of a porous sphere intragrain diffusion model, it is shown that a single kinetic experiment can be used to successfully predict the sorption isotherm. Transport through a soil column was interpreted by coupling an advection-diffusion-sorption (ADS) equation to describe contaminant movement external to the grains with the porous sphere intragrain diffusion model. Using the parameters for transport within grains and sorption as extracted from the kinetic experiments, the column breakthrough curves (BTCs) were successfully simulated.

INTRODUCTION

The fate of volatile organic compounds (VOCs) in subsurface environments is governed by many different mechanisms, such as partitioning between phases (sorption and volatilization), transformation (chemical and biological degradation) and transport phenomena (advection, diffusion, and dispersion). Among these mechanisms, sorption and transport phenomena may significantly affect the movement of contaminants in subsurface systems (Weber et al., 1991). To better understand the mechanisms associated with contaminant movement in subsurface environments, both transport and sorption phenomena need to be studied. Although transport and sorption of organic compounds on subsurface porous media (i.e., soil, sediment, and aquifer materials) have been studied extensively by many investigators, the system is very complicated, and problems remain to be resolved (van Genuchten et al., 1977; Karickhoff et al., 1979; Chiou and Shoup, 1985; Wu and Gschwend, 1986; Crittenden et al., 1986; Hutzler et al., 1986; Weber and Miller, 1988; Miller and Weber, 1988; Brusseau et al., 1989; Gierke et al., 1990; Ball and Roberts, 1991a and 1991b; Ong and Lion, 1991; Miller and Pedit, 1992; Harmon et al., 1992; Gierke et al., 1992; Young and Ball, 1994; Harmon and Roberts, 1994; Yiacoumi and Tien, 1994; Chapter II of this dissertation; and many others).

In studying the transport and sorption of VOCs in subsurface systems, both macroscopic models and microscopic models are normally considered (Weber et al., 1991). A macroscopic model incorporates the transport processes of contaminants in the macropore (external to soil grains) with an appropriate source-sink term, while a microscopic model describes the transport and equilibrium of contaminant within the soil grains.

The most widely used macroscopic transport model for laboratory and controlled field-scale investigations is probably the one dimensional advection-dispersion-sorption (ADS) equation (van Genuchten et al., 1977; Rao et al., 1979; Crittenden et al., 1986; Miller and Weber, 1988; Weber et al., 1991; Harmon et al., 1992; Young and Ball, 1994). As conveyed by its name, the ADS equation normally includes advection, dispersion and sorption terms. It is the sorption term in the equation that makes the transport behavior so

complicated. Depending on the relative time scales of macroscopic and microscopic transport, equilibrium partitioning may or may not adequately describe species partitioning between the macropores and the soil grains. If the time scale for transport within individual grains is much shorter than that for transport over the macroscopic length one is interested in, such as the length of a laboratory soil column, the local equilibrium assumption may be valid for the ADS equation. In contrast, if the time scale for grains is longer, an appropriate rate equation for describing transport of VOCs at the grain scale (the microscopic model) must be coupled through the sorption term to the ADS equation. Recent studies (Pignatello, 1991; Harmon et al., 1992) found that the local equilibrium assumption does not capture the observed subsurface transport of VOCs in many instances. Therefore, appropriate rate models must be considered at the microscopic scale to account for the discrepancy between the experimental findings and the predictions of local equilibrium models.

Many different models have been employed to describe the mass transfer processes associated with VOC sorption at the individual soil grain level (Wu and Gschwend, 1986; Weber and Miller, 1988; Ball and Roberts, 1991b; Miller and Pedit, 1992; Harmon and Roberts, 1994; Yiacoumi and Tien, 1994; Chapter II of this dissertation; and many others), and only a few are discussed here. First-order models, the so-called one-box and two-box models, have been proposed to simulate the sorption rates of experimental data. However, the one-box model cannot capture the dominant feature of the sorption rate data (Wu and Gschwend, 1986), while the two-box model requires 3 purely empirical fitted parameters (Wu and Gschwend, 1986; Yiacoumi and Tien, 1994). More fitted parameters are needed to resolve the asymmetry of sorption and desorption rates using first-order models. Recent studies show that intragranular diffusion models are the most likely physical description for VOC transport within individual soil grains (Wu and Gschwend, 1986; Weber and Miller, 1988; Ball and Roberts, 1991b; Miller and Pedit, 1992; Harmon and Roberts, 1994; Yiacoumi and Tien, 1994; Chapter II of this dissertation). Wu and Gschwend (1986), and Ball and Roberts (1991b) used a simple diffusion model to simulate the sorption rate data from their experiments. Weber and Miller (1988) and Miller and Pedit (1992) used surface

diffusion models to describe the transport of hydrophobic solutes within aquifer materials. Yiacoumi and Tien (1994) suggested that soil grains can be viewed as porous spheres with microparticles of soil organic matter (SOM) uniformly distributed. In their model, both diffusion within soil grains and within SOM are considered for an aqueous system. Most of the models developed previously used a linear isotherm to describe partitioning since the sorption capacity of the mineral surface is suppressed by water and only SOM is responsible for the sorption of VOCs (Chiou and Shoup, 1985). In fact, experimental findings (Weber and Miller, 1988; Young and Ball, 1994; Chapter II of this dissertation) have indicated that a nonlinear partitioning between the solid and fluid phases may exist for soil/aquifer materials with low organic carbon content. In Chapter II, we investigated the sorption kinetics of VOCs for dry, low-organic-carbon soil grains using a porous sphere model. The study indicated that, when dry, VOC sorption occurs entirely on mineral surfaces and the isotherm is nonlinear. In that study, pore diffusion was coupled with the nonlinear Freundlich isotherm to describe the transport of VOCs within individual dry soil grains.

Many researchers have successfully fitted the ADS equation discussed above to the experimental data from column or controlled field studies (van Genuchten et al., 1977; Rao et al., 1979; Hutzler et al., 1986; Gierke et al., 1990; Gierke et al., 1992). However, very few studies have used the model with independently determined parameters to predict the transport of VOCs through soil (Miller and Weber, 1988; Brusseau et al., 1989; Harmon et al., 1992; Young and Ball, 1994). Although Brusseau et al. (1989) sucessfully employed the multiprocess nonequilibrium model to predict column breakthrough curves (BTCs) for several cases, the model itself comprises too many input parameters and some of the parameters can not be determined independently. Thus far, most studies have been limited to transport and sorption in water-saturated systems (Rao et al., 1979; Hutzler et al., 1986; Miller and Weber, 1988; Harmon et al., 1992; Young and Ball, 1994); only a few have addressed unsaturated soil media (van Genuchten et al., 1977; Gierke et al., 1990; Gierke et al., 1992).

In this chapter, the gas-phase transport of benzene through both dry and moist soil columns is studied. We predict the transport behavior in laboratory columns using data obtained from sorption rate (kinetic) experiments. Sorption experiments were first performed using a differential adsorption bed (DAB) to obtain the sorption capacity and sorption kinetic curves for dry soil at one benzene concentration. The DAB data were then interpreted to obtain two parameters: the effective diffusivity of benzene within the soil grains and the exponent of the Freundlich isotherm, based on the porous sphere model (Chapter II). The equilibrium isotherm and column breakthrough curves (BTCs) for dry soil are predicted using these two parameters. Since the isotherm for moist soil can be approximated by a linear equation (Lin et al., 1995), only the effective diffusivity is needed for the BTC prediction. To test the predictions, breakthrough curves of soil columns were independently measured under both dry and moist conditions. The model predictions and the corresponding experimental data are found to agree very well.

THEORY

A one-dimensional model accounting for advection, dispersion, sorption and intragranular diffusion is employed to describe VOC movement through soil columns. As shown schematically in Figure 1, the model consists of two submodels: a transport model for the column (the ADS equation) and a diffusion model for individual soil grains (the porous sphere model). The mathematical formulations, and numerical procedures and solutions of the model are described in this section.

Transport and Sorption within Individual Soil Grains. As in Chapter II, this submodel assumes that the soil grains are perfect spheres of constant diameter with accessible sorption sites distributed uniformly within the grains. Considering transient diffusion and sorption, a mass balance on a small element of pore volume within the grain is combined with Fick's law to yield the following differential material balance:

$$\varepsilon_p \frac{\partial C}{\partial t} + (1-\varepsilon_p)\rho_p \frac{\partial q}{\partial t} = \frac{\varepsilon_p}{r^2}\frac{\partial}{\partial r}\left(r^2 D_p \frac{\partial C}{\partial r}\right) \qquad (1)$$

where q is the sorbed mass (mass of sorbate/mass of sorbent), C is the gas-phase concentration (mass of sorbate/volume of air), ε_p is the intragrain porosity, ρ_p is the density of the solid part of the sorbent, r is the radial coordinate of the sphere, t is time, and D_p is the gas diffusivity of sorbate molecules through the intraparticle pore space. Although the adsorbed-phase diffusive flux may approach the gas-phase flux under certain circumstances, the problem is simplified by considering gaseous diffusion as the only means of VOC transport within the soil grains. The close agreement between model results and measurements, as shown in Chapter II, substantiates this assumption for the system considered here.

Since the sorbed-phase is strongly favored (the mass of gas phase sorbate is always less than 1% of the sorbed mass in our systems), the first term in eq 1 can be neglected without loss of accuracy. Within the pores, instantaneously attained local equilibrium, following the Freundlich equation, is assumed to describe the partitioning between gas and sorbed phases:

$$q = k\, C^n \tag{2}$$

where k and n are empirical parameters, and now different from Chapter II.

Combining eqs (1) and (2), converting the equation into dimensionless form, and assuming that D_p is constant with respect to r, we find

$$\frac{\partial Q}{\partial \theta} = Q^{1-n}\, \frac{1}{x^2}\frac{\partial}{\partial x}\left(x^2 \frac{\partial Q}{\partial x}\right) \tag{3}$$

where $Q=C/C_o$, $x=r/a$, $\theta=t\, D_e/a^2$, a is the grain radius, C_o is the imposed external gas-phase concentration, and

$$D_e = \frac{\varepsilon_p\, D_p}{(1-\varepsilon_p)\, \rho_p\, nk} C_o^{\,1-n} \tag{4}$$

is an effective diffusivity. Mathematically, eq (3) corresponds to the diffusion equation in spherical coordinates with radial symmetry and with a concentration-dependent diffusion

coefficient, Q^{1-n}. It is this coefficient that links the degree of asymmetry in the rates of sorption and desorption to the parameter n that appears in the Freundlich isotherm (eq 2).

The kinetic intragrain sorption experiments begin with the soil in equilibrium with zero gaseous VOC concentration. Then the soil is challenged with a step increase in the gas-phase sorbate concentration and the total amount sorbed is monitored as a function of time until steady-state is achieved. Desorption data are generated by suddenly reducing the gas-phase sorbate concentration to zero while periodically monitoring the total amount sorbed. The appropriate initial and boundary conditions for the adsorption phase of the experiment, incorporating the effects of external film-resistance, are as follows:

$$Q(0<x<1,\ \theta=0) = 0$$

$$\frac{\partial Q}{\partial x}\Big|_{x=1} = B(1-Q_S) \qquad (5)$$

$$\partial Q/\partial x(x=0,\theta) = 0$$

For the desorption phase, the corresponding initial and boundary conditions are:

$$Q(0<x<1,\ \theta=0) = 1$$

$$\frac{\partial Q}{\partial x}\Big|_{x=1} = B(-Q_S) \qquad (6)$$

$$\partial Q/\partial x(x=0,\theta) = 0$$

where Q_s represents Q at surface (x=1), $B=k_f\, a/(D_p\, \varepsilon_p)$ is the mass-transfer Biot number, and k_f is the gas-film mass transfer coefficient. These initial and boundary conditions state (a) that the sorbed mass is initially uniformly distributed throughout the grain, (b) that the flux into or out of the grain must match the rate of mass transport across the external gas-film boundary, and (c) that the center of the grain must represent an extremum with respect to the local amount sorbed.

The relative mass uptake for adsorption (M_θ/M_∞), or the loss for desorption ($1-M_\theta/M_\infty$), at a specific time can be found by integrating the mass sorbed over the entire grain. This yields

$$\frac{M_\theta}{M_\infty} = 3\int_0^1 x^2 Q^n(x,\theta)dx \qquad (7)$$

where M_θ is the total mass sorbed at time θ and M_∞ is the equilibrium mass sorbed at a gas-phase concentration of C_o.

Predicting the Benzene Sorption Isotherm for Dry Soil. Each specific value of the Freundlich exponent, n, produces a unique pair of normalized adsorption and desorption curves (i.e. M_θ/M_∞ and $1-(M_\theta/M_\infty)$ vs. θ) in the porous sphere model. The shape of these curves in response to one imposed concentration, C_o, can thus be used to predict the n value of an isotherm. From our reading of the literature, it appears that the only previous suggestion that one can predict an isotherm from the asymmetry of sorption kinetic curves is due to Gray and Do (1989). They suggested that one can determine the sorption isotherm from the ratio of half-period for adsorption (M_θ/M_∞) to the half-period for desorption ($1-M_\theta/M_\infty$). In the present study, the full set of adsorption and desorption kinetic data are taken into account in predicting the Freundlich exponent, n, thus improving the accuracy of the prediction. A parameter-estimation scheme, which is similar to the least-squares method, is employed to determine the n value from the best fit of the model to the experimental data. In this scheme, D_e and n are systematically varied, and the difference in M_θ/M_∞ (or $1-M_\theta/M_\infty$) between the experimental data points and the corresponding model predictions are squared and summed. The n value that generates the smallest sum-of-squares error is taken as the exponent in the Freundlich equation. Once n is determined, the parameter k in the Freundlich isotherm is calculated from C and the steady-state value of q (Equation 2), as obtained in the course of the kinetic experiment.

Breakthrough Curves for Dry Soil Columns. An advection-dispersion-sorption (ADS) equation (Weber et al., 1991) is used to describe transport of benzene through soil columns. Consider a gas stream containing a dilute concentration of a single sorbate as it flows through a column packed with soil grains. Assuming constant

temperature and flow velocity, the material-balance equation for the soil column can be expressed as follows (Ruthven, 1984):

$$\frac{\partial C_b}{\partial t} = D_L \frac{\partial^2 C_b}{\partial z^2} - u\frac{\partial C_b}{\partial z} - (\frac{1-\varepsilon}{\varepsilon})\rho_b \frac{\partial M}{\partial t} \tag{8}$$

where C_b is the gas-phase concentration in the column pores (external to the soil grains), z is the axial coordinate for the column, u is the interstitial fluid velocity (i.e., the volumetric flow rate divided by the cross-sectional pore area), D_L is the dispersion coefficient, ε is the porosity and ρ_b is the grain density of the soil. Note that M is the sorbed mass of sorbate per mass of soil and can be evaluated as

$$M = \frac{3}{a^3}\int_0^a r^2 q(r)dr \tag{9}$$

The last term in Equation (8) can be expressed in relation to the gas-phase concentration in the pores between grains by matching fluxes at the grain boundaries. Using a film model for mass transfer in the gas phase, the following relationship holds (Ruthven, 1984):

$$\rho_b \frac{\partial M}{\partial t} = \frac{3k_f}{a}(C_b - C_s) \tag{10}$$

where C_s is the gas-phase sorbate concentration at external surface of soil grain.

Combining equations (8) and (10), and recasting the result in terms of dimensionless parameters yields

$$\frac{\partial Q_b}{\partial \theta_b} = \frac{1}{Pe}\frac{\partial^2 Q_b}{\partial y^2} - \frac{\partial Q_b}{\partial y} - 3\ St\ (Q_b - Q_s) \tag{11}$$

where $Q_b = C_b/C_o$, $Q_s = C_s/C_o$, $\theta_b = ut/L$, $Pe = uL/D_L$ is a Peclet number, $y = z/L$, $St = (1-\varepsilon)k_f L/(\varepsilon a u)$ is a Stanton number, and L is the length of column.

BTCs can be obtained by simultaneously solving eqs (3) and (11) subject to appropriate initial and boundary conditions for individual soil grains (as in eq (5) except $\partial Q/\partial x(x=1) = B(Q_b-Q_s)$) and those for the column:

$$Q_b(0<y<1,\ \theta_b=0) = 0$$

$$Q_{bi} - Q_b|_{y=0} = -\frac{1}{Pe}\frac{\partial Q_b}{\partial y}|_{y=0} \qquad (12)$$

$$\partial Q_b/\partial y(y=1,\theta_b) = 0$$

where $Q_{bi}= C_{bi}/C_o$, and C_{bi} is the imposed gas-phase concentration at the inlet of the soil column. Normally, Q_{bi} is 1 for the case of adsorption and is 0 for desorption. These conditions respectively state that (a) the column pores are initially free of sorbate, (b) the advective flux of sorbate into the column at the leading edge is balanced by the advective and dispersive fluxes away from the leading edge, and (c) the concentration at the outlet of the column is continuous.

Transport through Moist Soil Columns. The sorption capacity of mineral grains is greatly reduced when moist rather than dry. The lower sorption capacity speeds the approach to equilibrium for sorption within individual porous grains. If the time scale to achieve sorption equilibrium within the soil grain is much less than that for transport through the soil column, local equilibrium can be assumed to describe the partitioning of sorbate between the column pores and their adjacent soil grains. In addition, for the adsorption of a volatile organic compound onto moist soil, a linear isotherm is normally expected to describe the gas-phase/sorbed-phase partitioning. With the assumption of local equilibrium and a linear isotherm, eq (11) can be reduced to this form:

$$R\frac{\partial Q_b}{\partial \theta_b} = \frac{1}{Pe}\frac{\partial^2 Q_b}{\partial y^2} - \frac{\partial Q_b}{\partial y} \qquad (13)$$

where $R=(1-\varepsilon)\rho_b\, k_d\, \varepsilon^{-1}+1$ is the retardation factor, ρ_b is the bulk soil grain density, and $k_d=q/C$ is the partition coefficient for a linear isotherm.

Eq (13), with eq (12) describing initial and boundary conditions ($Q_{bi} = 1$), has been solved analytically by Brenner (1962) to yield the gaseous species concentration at the column outlet :

$$Q_{b|y=1} = 1 - \sum_{j=1}^{\infty} \frac{2\,\beta_j \sin(\beta_j) \exp\left(\frac{Pe}{2} - \frac{Pe\,\theta_b}{4R} - \frac{\beta_j^2 \theta_b}{Pe\,R}\right)}{\beta_j^2 + \frac{Pe}{4} + Pe} \tag{14}$$

where β_j are the positive roots of

$$Pe\,\beta_j \cot(\beta_j) - \beta_j^2 + \frac{Pe^2}{4} = 0 \tag{15}$$

Another analytical solution for the same equation has been presented by Hashimoto et al. (1964); because of space limitations, it is not reproduced here. Van Genuchten and Parker (1984) showed that eq (14) can be reduced to the following form when Pe is larger than 5 (Lapidus and Amundson, 1952):

$$Q_{b|y=1} = \frac{1}{2}\left(\operatorname{erfc}\left(\left(\frac{Pe}{4}\frac{R}{\theta_b}\right)^{\frac{1}{2}}\left(1 - \frac{\theta_b}{R}\right)\right) + \exp(Pe)\operatorname{erfc}\left(\left(\frac{Pe}{4}\frac{R}{\theta_b}\right)^{\frac{1}{2}}\left(1 + \frac{\theta_b}{R}\right)\right)\right) \tag{16}$$

This expression is a solution of eq (13) with initial and boundary conditions as follows:

$$\begin{aligned} &Q_b(0<y<1,\ \theta_b=0) = 0 \\ &Q_b(y=0, \theta_b)=1 \\ &Q_b(y=\infty, \theta_b) = 0 \end{aligned} \tag{17}$$

Numerical Solution Procedures. Similar systems of governing equations plus boundary and initial conditions have been solved by Crittenden et al. (1986), Gray and Do (1989), and Yao and Tien (1992, 1994) using orthogonal collocation (OC) (Finlayson, 1980). The OC method converts the nonlinear partial differential equations into a set of

time-dependent, nonlinear, ordinary differential equations which can be integrated by commercially available software, such as the International Mathematics and Scientific Library (IMSL). For our work, the model equations and their boundary and initial conditions were solved using an approach similar to Yao and Tien (1992, 1994) with modification of the isotherm equation and the boundary conditions. For sorption kinetics, Yao and Tien (1992) found that 5 or 6 collocation points sufficed to generate a nearly exact solution. In the present study, 7 collocation points were used in the numerical solutions. The resulting solutions compare well with the analytical solution for the case of a linear isotherm and $B=\infty$, and with the results of analysis based on the finite-difference method for a nonlinear Freundlich isotherm (Chapter II). For the case of BTC prediction, 4 collocation points in the radial (x) direction and 10 in the axial (y) direction were used in the numerical solutions. Test cases in which axial and radial collocation points were added did not change the solution significantly in our system. The model results were also checked against the analytical solution provided by Rasmuson and Neretnieks (1980) for the case of a linear isotherm (n=1).

MATERIALS AND METHODS

Sorbate and Sorbent. Benzene was chosen as a representative VOC as it is commonly found at contaminated sites and was used in our previous study of the kinetics of VOC uptake by individual soil grains (Chapter II). In the present study, gas-phase concentrations in the range of 100-1000 ppm, i.e. about 2-3 orders of magnitude lower than the saturated vapor pressure, were used. The synthetic soil matrix (SSM) (USEPA, 1988), prepared by the US Environmental Protection Agency, was selected as a representative soil. The properties of SSM have been previously determined (Chapter II) and, for convenience, are briefly summarized here. SSM is a low organic carbon soil (about 0.25 % by mass) with a surface area of 8 $m^2\ g^{-1}$, as measured by low-temperature nitrogen adsorption as well as by mercury intrusion. The grain density (ρ_p) is 2.61×10^6

g m^{-3}, and the grain porosity (ε_p) is 0.15. To simplify interpretation of the experimental data, we used a narrow range of grain sizes, 20-30 U.S. standard mesh (0.60-0.86 mm).

Kinetic Experiments. In the soil sorption experiments described in Chapter II, we employed an electrobalance to determine sorption isotherms and kinetics for VOCs in dry soils. However, the nature of that apparatus precludes its direct use for multicomponent systems, such as VOC sorption by moist soil. Since the sorption capacity of water vapor by mineral surfaces is very much higher than that for benzene, even a small fractional change in sorbed water vapor mass would confound attempts to determine benzene sorption based on total mass change. Therefore, an experimental technique more appropriate for multicomponent systems, the differential adsorption bed (DAB) (Carlson and Dranoff 1985; Mayfield and Do, 1991), was employed in this study to determine sorption equilibria and kinetics.

In the DAB system, a gas stream containing predetermined concentrations of sorbates flows through a short column packed with sorbent (the adsorption bed). The flow rate through the sorbent bed is sufficiently high so that at all times the rate of sorbate uptake by the sorbent is small compared with the rate of sorbate supply by the gas stream. Under this condition, each sorbent grain within the bed can be considered to be exposed to the sorbate concentration at the column inlet. Thus, the bed behaves as a "differential" sorbent unit and the sorption kinetics of individual grains can be investigated.

The DAB apparatus is shown schematically in Figure 2. All materials that contact the gas flow were either stainless steel or Teflon. Five stainless-steel columns, 4 cm × 0.65 cm ID, were each filled with ~ 3 g of soil and arranged in parallel inside a wooden cabinet whose internal temperature was maintained at 20.0±0.5 °C. The concentrations of benzene and water vapor in the gas stream supplied to the columns were controlled by varying the flowrate ratios of a benzene standard, high purity hydrocarbon-free (HC-free) air, and HC-free air passing through a water-vapor generator (a temperature-regulated gas bubbler). Experimental results indicate that a flow rate of 1-2 L min^{-1} is sufficient to ensure proper DAB operation.

The general procedure for a DAB experiment consists of three main steps: (1) adsorption, (2) thermal desorption and collection, and (3) analysis. During the adsorption step, a gas stream containing known concentrations of water vapor and benzene was passed through the column. By varying the duration of this step, sorbate mass retained by the sorbent can be obtained as a function of exposure time. Desorption curve data were generated by exposing columns to the sorbate gas for sufficient time to establish equilibrium, then switching to high flow rate gas at zero VOC concentration (but the proper humidity) for a predetermined time.

In the second step, the temperature of the columns was increased and high-purity nitrogen gas was passed through the columns to a set of Tedlar sampling bags by means of peristaltic pumps at a flow rate of 10-20 mL min^{-1}. The flow rate of gas through each column was determined using a soap bubble flow meter at the end of the thermal desorption process. Tests conducted to determine the necessary duration and temperature for the thermal desorption process revealed that less than 5% of the sorbed mass remained on the column after two hours at 80 °C. Consequently, the desorption process was always conducted for more than two hours with the column temperature maintained at 80-100 °C. The volume in each bag was calculated by multiplying the flow rate through each column by the total time that the pumps were on.

In the third step, the sorbate concentration in each bag was determined using a gas chromatograph (GC) equipped with a flame ionization detector (FID). The sorbed mass for each run was determined as the product of the sorbate concentration and gas volume in the corresponding sampling bag.

Column Experiments. Two different approaches were employed to measure breakthrough curves (BTCs) of benzene through soil columns. For high-flow conditions, a positive pressure system was employed in which pressure-regulated cylinders were used to induce flow through soil columns (Figure 3). In contrast, a negative pressure system in which a peristaltic pump was used to draw flow from a gas sampling bag through the soil column was employed for low flow conditions (Figure 4).

The column for the high-flow runs was made of stainless steel with a length of 7.6 cm and an inner diameter of 2.3 cm. The column temperature was maintained at 20.0±1.0 °C. Air flow through the dry-soil column was maintained at 5.0 $cm^3\ s^{-1}$ (±5%) by rotameters with high-resolution stainless steel valves; for the moist soil column, flow was regulated at 3.3 $cm^3\ s^{-1}$ (±3%) by means of a mass flow controller. Both the rotameters and the mass flow controllers were checked periodically either using a flow calibrator or a soap bubble meter.

Before each experimental run, HC-free air, at 33% RH for the case of moist soil columns, was used to purge the column for sufficient time so that only negligible residual benzene could be detected by the gas chromatograph. The water vapor content upstream and downstream of the moist soil column was checked periodically using a dew-point hygrometer. Once column conditioning was complete, a step increase to a predetermined benzene concentration was maintained at the column inlet. The benzene concentration in the column effluent was monitored by continuously diverting a small aliquot of air flow through a six-port valve system with a 0.25 cm^3 sampling loop. By switching the valve periodically, the air in the sampling loop passed through a gas chromatograph equipped with a flame ionization detector (FID), and the concentration was measured. The column was considered to be saturated when the effluent concentration became equal to the imposed concentration. After reaching saturation, the moist air/benzene flow was replaced by a benzene-free air flow at the same RH. Effluent monitoring was continued to obtain the desorption part of the BTCs. For the dry soil case, only the adsorption part of the BTCs was measured. It is noted that, since the moisture contents in these systems were very low (33% RH at most), microbial decay of benzene is excluded in this study.

The sorption capacity was calculated from the following relationship, derived from mass balance:

$$q_o = \frac{Q_f}{w}\int_0^{\infty}(C_o - C_{b1})dt \qquad (18)$$

where Q_f is the air flow rate through the column (volume/time), w is the mass of soil in the column, and C_{b1} is the gaseous benzene concentration at the column outlet.

The experimental procedures and apparatus for the low-flow runs are similar to those for the high flow runs except that the flow was induced by a peristaltic pump drawing air from a 5-layer sampling bag through the soil column and the GC sampling loop. (The 5-layer sampling bag was used instead of a Tedlar bag because water vapor can easily diffuse through the membrane of a Tedlar bag.) Two runs were conducted for moist soil with this system. The air flow rates, which were checked periodically using a soap bubble meter at both the soil column and at the outlet of the peristaltic pump, were 0.13 $cm^3\ s^{-1}$ (±3%) and $2.2 \times 10^{-3}\ cm^3\ s^{-1}$ (±3%), respectively.

To prepare the gas stream, a predetermined amount of deionized water was first injected into the bag using a 50-μL microsyringe. Then a predetermined volume of either HC-free air or gas from a benzene standard cylinder was added to the bag to obtain the desired moisture content. The benzene and water vapor concentration in the bag were checked before and after each experiment to ensure that the concentrations were constant through the experimental periods.

RESULTS AND DISCUSSION

Sorption Experiments. The porous sphere model with two adjustable parameters—the effective diffusivity (D_e) and the exponent in the Freundlich isotherm (n)—was fit to the experimental sorption kinetic data for benzene at 590 ppm to dry soil. The Biot number (B) was calculated from the Ranz-Marshall correlation for single particles (Wakao and Funazkri, 1978). The experimental data and the best model fit are shown to be in good agreement (Figure 5). The extracted D_e and n values are found to be 1.3×10^{-10} $m^2\ s^{-1}$ and 0.35, respectively.

Using the approach we described in the theory section, the extracted n value and the sorption capacity measured from this one kinetic experiment were used to predict the sorption isotherm for benzene to dry SSM. The predicted adsorption isotherm is compared in Figure 6 with the sorption capacities measured from column experiments and the

isotherm measured from an electrobalance (Chapter II). Excellent agreement (typically within 4%) was found in comparing the isotherm inferred from the DAB kinetic experiment with that determined from the column experiments. However, a systematic discrepancy in sorption capacities of about a factor of 2 was observed between the current study and the previous electrobalance measurements. Based on the D_e value and isotherm parameters we extracted from the DAB data, along with the porosity and grain density of SSM, the pore diffusivity, D_p, is estimated to be 3.0×10^{-7} m^2 s^{-1} from eq (4). A tortuosity factor (τ) of 16 was inferred from the D_p value and is about 60% higher than that from the electrobalance study. The reason for these discrepancies is not clear. It is possible that sample heterogeneity contributes, since only about 0.05 g of soil sample (~ 100 grains) was used in the electrobalance experiments, whereas about 3 g of soil was used in the DAB experiment.

The sorption capacities measured for 340 ppm and 700 ppm of benzene to moist SSM at 33% RH show that the isotherm is linear with a partition coefficient, k_d, of 72×10^{-6} m^3 g^{-1}. The sorption isotherms determined from the DAB experiments for both dry and moist soil, and the extracted D_p value for dry soil are used in the following BTC predictions.

Breakthrough Curve Predictions. The porous sphere model (eq 3) was coupled with the mass balance equation for transport through a soil column (eq 11) to predict column BTCs using the extracted isotherm and D_p values from the DAB experiments as input parameters. The predictions were then compared with the experimental BTCs.

The model input parameters for all BTC predictions are summarized in Table 1. The Biot number was calculated from the modified Ranz-Marshall correlation developed by Wakao and Funazkri (1978). Although that correlation is only valid for Re>3, numerical analysis revealed that reducing k_f and B by a factor of 10 for our system only changed the breakthrough curves by a few percent. The axial dispersion coefficient, D_L, was estimated from the Edwards-Richardson correlation (Edwards and Richardson, 1968) as modified for small particles by Langer et al. (1978):

$$D_L = 0.73\ D_a + \frac{0.149\ u}{1 + 9.7(\frac{D_a}{2\ ua})} \qquad (19)$$

where D_a is the molecular diffusivity of the sorbate in air. This equation embodies two mechanisms that contribute to axial dispersion: molecular diffusion (the first term) and mechanical dispersion (the second term). As advection in a system diminishes, axial dispersion is dominated by molecular diffusion. Considering typical ε values for soil (0.3-0.5), the D_L value calculated from eq (19) under low flow conditions is almost identical to that calculated from the Millington correlation (Millington, 1959) as typically used in subsurface transport (Karimi et al., 1987; Gierke et al., 1992; Little et al., 1992).

The BTC predictions and the corresponding experimental data for dry soil with advection-dominated transport are shown in Figure 7. The models show good agreement with experimental data over a range of benzene concentrations: the time required for the outlet concentration to rise to 50% of the inlet value is predicted to within about 5% in each case. These results demonstrate that the model can predict BTCs based on measurements of adsorption and desorption kinetics, not only at the concentration used in the kinetic experiment, but also at significantly higher or lower concentrations.

Having obtained successful results for dry soil, the model was then used to predict BTCs for a moist soil column. Three flow regimes were chosen to simulate real flow conditions in the environment: an advection-dominated condition (Pe>100), an intermediate flow condition (Pe~10), and a diffusion-dominated condition (Pe<0.2). These different flow regimes may be considered to represent different environmental engineering applications. For a typical soil venting operation, commonly used in site remediation, the pore velocities may be as high as 0.01 m s^{-1} (Johnson et al., 1988). The flow velocity in the advection-dominated case (u=0.022 m s^{-1}) is chosen to be similar to this value. Soil gas is acknowledged as a potential source for elevated indoor radon (Nazaroff et al., 1987) and VOC concentrations (Little et al., 1992). The effective transport velocities through soil into houses, often driven by the small pressure difference between indoor and outdoor air, may exceed 2.8×10^{-4} m s^{-1} (Nazaroff et al., 1987). The flow velocity in the intermediate

case ($u = 8.4 \times 10^{-4}$ m s^{-1}) is of the same order of magnitude. Finally, diffusional transport, which could be the major transport mechanism for VOC movement near uncontrolled landfill sites (Karimi et al., 1987), is represented by the third case. It is noted that, because the sorption capacity of water vapor at 33% RH corresponds to a liquid water content that would fill only 2% of the pore space, both ε_p and D_p for the moist soil are assumed to be the same as those measured for dry soil.

Crittenden et al. (1986) proposed an equation to determine which mechanisms would control the spreading of the mass transfer zone (BTCs) for chemical transport within a soil column. For a strong sorbate, the equation can be modified for our system as

$$PD = \frac{Pe\ B}{15\ St} \quad \text{and} \quad PF = \frac{B}{5} \tag{20}$$

where PD represents the amount of BTC spreading due to pore diffusion relative to that from dispersion, and PF represents the amount of BTC spreading due to pore diffusion relative to that from gas-film transfer. Small values of PD and PF indicate that the mass transfer processes for BTC spreading are controlled by dispersion and gas-film resistances, respectively. Both PD and PF values are shown in Table 1. All the PF values shown in Table 1 are larger than about 40, suggesting that gas-film resistance is not important at all in our system. The large PD values (> 40) indicate that axial dispersion is not important for the advection-dominated cases, while the small PD value (< 0.02) for the slow flow condition reveals that axial dispersion may be responsible for the spreading of BTC for this condition.

The model predictions and their corresponding data for the advection case are shown in Figure 8. Both the coupled (intragranular and ADS) diffusion model and the (local) equilibrium model for individual soil grains are considered in the predictions. The diffusion models conform very well to the experimental BTCs, while the equilibrium models do not accurately capture key features of the data. Considering the large values of both PD and PF in Table 1, it is not surprising that pore diffusion seems to dominate the spreading of the BTC in this case. The superior predictions of the diffusion model

demonstrates that the local equilibrium assumption is not appropriate under the given flow-rate and sorption conditions.

For the intermediate case (Pe=9.9), the model predictions and data are shown in Figure 9. Both diffusion and equilibrium models predict essentially the same results and are in good agreement with the experimental BTCs. Considering the large value of PF and small value of PD (Table 1), BTC spreading is likely to be controlled by the hydrodynamic dispersion of the gas in the macropores. Therefore, the local equilibrium assumption is apparently valid for this case and for slower flow conditions. As the flow rate becomes lower, the PD value will become even smaller, and thus, the assumption of local equilibrium should hold for the diffusion case.

Finally, the predicted BTCs are compared with the experimental data for the slowest flow condition. Because the time to reach saturation is very long in this case (more than two months, according to the models), the column inlet was exposed to elevated benzene for 146 hours, and then switched back to benzene-free moist air for desorption. Brenner (1962) suggested, if Pe approaches zero, that a column can be treated as a constant flow stirred tank reactor (CFSTR). The corresponding solution for eq (11) becomes

$$Q_{b|y=1} = 1 - \exp(-\frac{\theta_b}{R}) \tag{21}$$

The CFSTR model is found to predict almost identical results with the equilibrium model for column BTCs in this case. As in Figure 10, both models successfully predict the data over the month-long experimental period.

SUMMARY

The porous sphere model, which accounts for intragranular diffusive transport coupled with adsorption to the pore walls, yields predictions that conform well to the experimental kinetic data for adsorption and desorption of benzene on dry SSM mineral grains. Using this model, the parameters of the Freundlich isotherm describing equilibrium adsorption can be extracted from kinetic adsorption/desorption data obtained for a single

sorbate concentration. Furthermore, the same model and parameters can be combined with the advection-dispersion-sorption equation to successfully predict column breakthrough curves (BTCs). The model predictions agreed well with experimental BTC for dry soil under strong advective flow conditions, and for moist soil with strong, moderate, and weak advective flow. A model based on the assumption of local equilibrium was shown to work equally well for the moderate and weak advective conditions, but not for the strong advective flow cases.

APPENDIX I. REFERENCES

Ball, W.P., and Roberts, P.V. (1991a). "Long-term sorption of halogenated organic chemicals by aquifer material: 1. Equilibrium." *Environ. Sci. Technol., 25*, 1223-1236.

Ball, W.P., and Roberts, P.V. (1991b). "Long-term sorption of halogenated organic chemicals by aquifer material: 2. Intraparticle diffusion." *Environ. Sci. Technol., 25*, 1237-1249.

Brenner, H. (1962). "The diffusion model for longitudinal mixing in beds of finite length: Numerical values." *Chem. Eng. Sci., 17*, 229-243.

Brusseau, M.L., Jessup, R.E., and Rao, P.S.C. (1989). "Modeling the transport of solutes influenced by multiprocess nonequilibrium." *Water Resources Res., 25*, 1971-1988

Carlson, N.W., and Dranoff, J.S. (1985). "On the adsorption of ethane by 4A zeolite pellets." *Ind. Eng. Chem. Process Des. Dev., 24*, 1300-1302.

Chiou, C.T., and Shoup, T.D. (1985). "Soil sorption of organic vapors and effects of humidity on sorptive mechanism and capacity." *Environ. Sci. Technol., 19*, 1196-1200.

Crittenden, J.C., Hutzler, N.J., Geyer, D.G., Oravitz, J.L., and Friedman, G. (1986). "Transport of organic compounds with saturated groundwater flow: Model development and parameter sensitivity." *Water Resources Res., 22*, 271-284.

Edwards, M.F., and Richardson, J.F. (1968). "Gas dispersion in packed beds." *Chem. Eng. Sci., 23*, 109-123.

Finlayson, B.A. (1980). *Nonlinear Analysis in Chemical Engineering.* McGraw-Hill, New York, N.Y.

Gierke, J.S., Hutzler, N.J., and Crittenden, J.C. (1990). "Modeling the movement of volatile organic chemicals in columns of unsaturated soil." *Water Resources Res., 26*, 1529-1547.

Gierke, J.S., Hutzler, N.J., and McKenzie, D.B. (1992). "Vapor transport in unsaturated soil columns: Implications for vapor extraction." *Water Resources Res.*, *28*, 323-335.

Gray, P.G., and Do, D.D. (1989). "Adsorption and desorption of gaseous sorbates on a bidispersed particle with Freundlich isotherm: I. Theoretical analysis." *Gas Sep. Purif.*, *3*, 193-200.

Harmon, T.C., and Roberts, P.V. (1994). "Comparison of intraparticle sorption and desorption rates for a halogenated alkene in a sandy aquifer material." *Environ. Sci. Technol.*, *28*, 1650-1660.

Harmon, T.C., Semprini, L., and Roberts, P.V. (1992). "Simulating solute transport using laboratory-based sorption parameters." *J. Env. Eng., ASCE*, *118*, 666-689.

Hashimoto, I., Deshpande, K.B., and Thomas, H.C. (1964). "Peclet numbers and retardation factors for ion exchange columns." *Ind. Eng. Chem. Fundam.*, *3*, 213-218.

Hutzler, N.J., Crittenden, J.C., Gierke, J.S., and Johnson, A.S. (1986). "Transport of organic compounds with saturated groundwater flow: Experimental results." *Water Resources Res.*, *22*, 285-295.

Johnson, P.C., Kemblowski, M.W., and Colthart, J.D. (1988). "Practical screening models for soil venting applications." *Proceedings of NWWA/API Conference on Petroleum Hydrocarbons and Organic Chemicals in Ground Water*, Houston, TX, pp. 521-546.

Karickhoff, S.W., Brown, D.S., and Scott, T.A. (1979). "Sorption of hydrophobic pollutants on natural sediments." *Water Research* , *13*, 241-248.

Karimi, A.A., Farmer, W.J., and Cliath, M.M. (1987). "Vapor-phase diffusion of benzene in soil." *J. Environ. Qual.*, *16*, 38-43.

Langer, G., Roethe, A., Roethe, K.-P., and Gelbin, D. (1978). "Heat and mass transfer in packed beds: III. Axial mass dispersion." *Int. J. Heat Mass Transfer*, *21*, 751-759.

Lapidus, L., and Amundson, N.R. (1952). "Mathematics of adsorption in beds: IV. The effect of longitudal diffusion in ion exchange and chromatographic columns." *J. Phys. Chem.*, *56*, 984-988.

Lin, T.F., Van Loy, M.D., and Nazaroff, W.W. (1995). "Gas-phase transport and sorption of benzene through soil columns." In preparation.

Little, J.C., Daisey, J.M., and Nazaroff, W.W. (1992). "Transport of subsurface contaminants into buildings: An exposure pathway for volatile organics." *Environ. Sci. Technol.*, *26*, 2058-2066.

Mayfield, P.L.J., and Do D.D. (1991). "Measurement of the single-component adsorption kinetics of ethane, butane, and pentane onto activated carbon using a differential adsorption bed." *Ind. Eng. Chem. Res.*, *30*, 1262-1270.

Miller, C.T., and Pedit, J.A. (1992). "Use of a reactive surface-diffusion model to describe apparent sorption-desorption hysteresis and abiotic degradation of lindane in a subsurface material." *Environ. Sci. Technol.*, *26*, 1417-1427.

Miller, C.T., and Weber, W.J. (1988). "Modeling the sorption of hydrophobic contaminants by aquifer materials: II. Column reactor systems." *Water Research*, *22*, 465-474.

Millington, A.V. (1959). "Gas diffusion in porous media." *Science*, *130*, 100-102.

Nazaroff, W.W., Lewis, S.R., Doyle, S.M., Moed, B.A., and Nero, A.V. (1987). "Experiments on pollutant transport from soil into residential basements by pressure-driven airflow." *Environ. Sci. Technol.*, *21*, 459-466.

Ong, S.K., and Lion, L.W. (1991) "Effects of soil properties and moisture on the sorption of trichloroethylene vapor." *Water Research*, *25*, 29-36.

Pignatello, J.J. (1991). "Desorption of tetrachloroethene and 1,2-dibromo-3-chloropropane from aquifer sediments." *Environ. Toxi. Chem.*, *10*, 1399-1404.

Rao, P.S.C., Davison, J.M., Jessup, R.E., and Selim, H.M. (1979). "Evaluation of conceptual models for describing nonequilibrium adsorption-desorption of pesticides during steady-flow in soils." *Soil Sci. Soc. Am. J., 43*, 22-28.

Rasmuson, A., and Neretnieks, I. (1980). "Exact solution of a model for diffusion in particles and longitudinal dispersion in packed beds." *AIChE J., 26*, 686-690.

Ruthven, D.M. (1984). *Principles of Adsorption and Adsorption Processes*. John Wiley and Sons, New York, N.Y.

U.S. Environmental Protection Agency, Risk Reduction Engineering Laboratory, Release Control Branch (1988). *Synthetic Soil Matrix (SSM-SARM) User's Manual.* Edison, N.J.

van Genuchten, M.Th., and Parker, J.C. (1984). "Boundary conditions for displacement experiments through short laboratory soil columns." *Soil Sci. Soc. Am. J., 48*, 703-708.

van Genuchten, M.Th., Wierenga, P.J., and O'Connor, G.A. (1977). "Mass transfer studies in sorbing porous media: III. Experimental evaluation with 2,4,5-T." *Soil Sci. Soc. Am. J., 41*, 278-285.

Wakao, N., and Funazkri, T. (1978). "Effect of fluid dispersion coefficients to particle-to-fluid mass transfer coefficients in packed bed." *Chem. Eng. Sci., 33*, 1375-1384.

Weber, W.J., and Miller, C.T. (1988). "Modeling the sorption of hydrophobic contaminants by aquifer materials: I. Rates and equilibria." *Water Research, 22*, 457-464.

Weber, W.J., McGinley, P.M., and Katz, L.E. (1991). "Sorption phenomena in subsurface systems: Concepts, models and effects on contaminant fate and transport." *Water Research, 25*, 499-528.

Wu, S.-C., and Gschwend, P.M. (1986). "Sorption kinetics of hydrophobic organic compounds to natural sediments and soils." *Environ. Sci. Technol., 20*, 717-725.

Yao, C., and Tien, C. (1992). "Approximation of intraparticle mass transfer in adsorption processes: II. Nonlinear systems." *Chem. Eng. Sci., 47*, 465-473.

Yao, C., and Tien, C. (1994). "Approximate solution of intraparticle diffusion equations and their application to continuous-flow stirred tank and fixed-bed adsorption calculations." *Sep. Technol.*, *4*, 67-80.

Yiacoumi, S., and Tien, C. (1994). "A model of organic solute uptake from aqueous solutions by soils." *Water Resources Res.*, *30*, 571-580.

Young, D.F., and Ball, W.P. (1994). "*A priori* simulation of tetrachloroethene transport through aquifer material using an intraparticle diffusion model." *Environmental Progress*, *13*, 9-20.

APPENDIX II. NOMENCLATURE

a	radius of soil grain (m)
B	Biot number [= $(k_f a)$ $(\varepsilon_p D_p)^{-1}$] (dimensionless)
C	gas-phase sorbate concentration (g m^{-3})
C_b	gas-phase species concentration in intergranular pores within column (g m^{-3})
C_{bl}	gas-phase species concentration at the outlet of column (g m^{-3})
C_{bi}	imposed gas-phase species concentration at inlet of soil column (g m^{-3})
C_o	imposed, external gas-phase species concentration for adsorption (g m^{-3})
C_s	gas-phase concentration at external surface of soil grain (g m^{-3})
D_a	molecular diffusivity of sorbate in bulk air (m^2 s^{-1})
D_e	effective diffusivity (m^2 s^{-1})
D_L	dispersion coefficient (m^2 s^{-1})
D_p	pore diffusivity in soil grain (m^2 s^{-1})
k	Freundlich isotherm parameter ((g g^{-1}) × (g m^{-3})$^{-n}$)
k_d	partition coefficient for linear isotherm ((g g^{-1}) × (g m^{-3}))
k_f	gas-film mass-transfer coefficient (m s^{-1})
L	length of column (m)
M_θ/M_∞	cumulative mass gain relative to that in equilibrium with C_o (dimensionless)
n	Freundlich isotherm parameter (dimensionless)
PD	BTC spreading from pore diffusion relative to dispersion [= PeB $(15St)^{-1}$] (dimensionless)
Pe	Peclet number [= u L D_L^{-1}] (dimensionless)
PF	BTC spreading from pore diffusion relative to gas-film transfer [= B / 5] (dimensionless)

q	(equilibrium) sorption capacity (g sorbate per g soil)
q_o	sorption capacity in equilibrium with C_o (g sorbate per g soil)
Q	normalized gas-phase species concentration [$= C\ C_o^{-1}$] (dimensionless)
Q_b	normalized gas-phase species concentration in column [$= C_b\ C_o^{-1}$] (dimensionless)
Q_{bi}	normalized gas-phase species concentration at column inlet [$= C_{bi}\ C_o^{-1}$] (dimensionless)
Q_f	air flow rate in column ($m^3\ s^{-1}$)
Q_s	normalized gas-phase species conc. on grain surface [$= C_s\ C_o^{-1}$] (dimensionless)
R	retardation factor for linear isotherm [$= (1-\varepsilon)\ \rho_b\ k_d\ \varepsilon^{-1} + 1$] (dimensionless)
r	radial coordinate in soil grain (m)
St	Stanton number [$= (1-\varepsilon)\ k_f L\ (\varepsilon a u)^{-1}$] (dimensionless)
t	time (s)
u	interstitial fluid velocity ($m\ s^{-1}$)
w	mass of soil in column (g)
x	normalized radial coordinate in soil grain [$= r\ a^{-1}$] (dimensionless)
y	normalized axial coordinate in column [$= z\ L^{-1}$] (dimensionless)
z	axial coordinate in column (m)
β_j	positive roots in eq 13 (dimensionless)
ε	bulk porosity in soil column (dimensionless)
ε_p	grain porosity (dimensionless)
θ	normalized time for transport within individual grains [$= t\ D_e\ a^{-2}$] (dimensionless)
θ_b	normalized time for transport through column [$= u\ t\ L^{-1}$] (dimensionless)
ρ_b	bulk density of soil grain ($g\ m^{-3}$)
ρ_p	solid density of soil grain ($g\ m^{-3}$)

Table 1. Parameters Used to Predict Breakthrough Curves for Dry and Moist Soil Columns.

Parameter	symbol (unit)	Dry Column	Moist Column	Moist Column
Corresponding Figure	-	7	8	9
Column Length	L (m)	0.076	0.076	0.076
Interstitial Fluid Velocity	u ($m\ s^{-1}$)	0.034	0.022	8.4×10^{-4}
Bulk Porosity in Column	ε (-)	0.36	0.37	0.37
Effective Diffusivity	D_e ($m^2\ s^{-1}$)	1.9×10^{-10}†	2.8×10^{-10}	2.8×10^{-10}
Freundlich Exponent	n (-)	0.35	1.0	1.0
Gas-film Mass Transfer Coefficient	k_f ($m\ s^{-1}$)	0.047	0.042	0.027
Peclet Number	Pe (-)	150	150	9.9
Stanton Number	St (-)	540	690	12000
Biot Number	B (-)	360	330	210
BTC Spreading Parameter	PD (-)	67	48	0.012
BTC Spreading Parameter	PF (-)	72	66	42

†for 1000 ppm benzene.

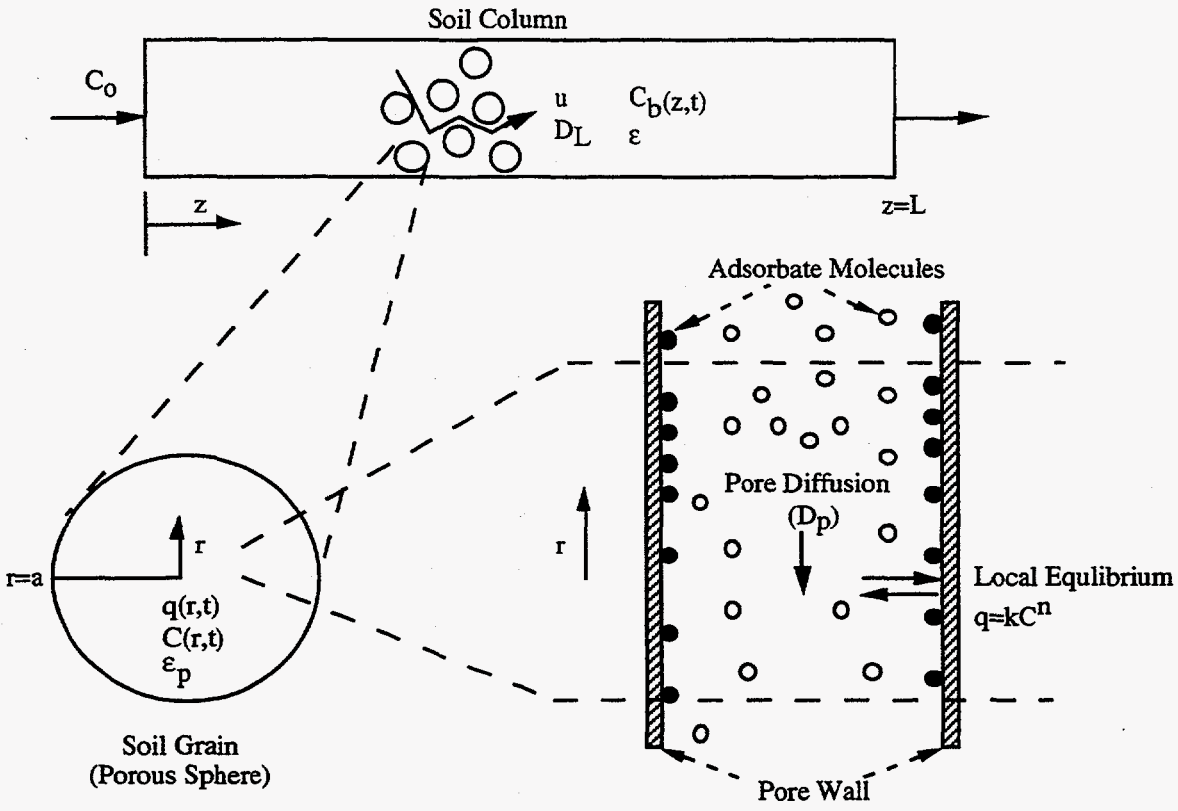

Figure 1. Schematic representation of macroscopic and microscopic models used in this study. See symbols and text for parameter definitions.

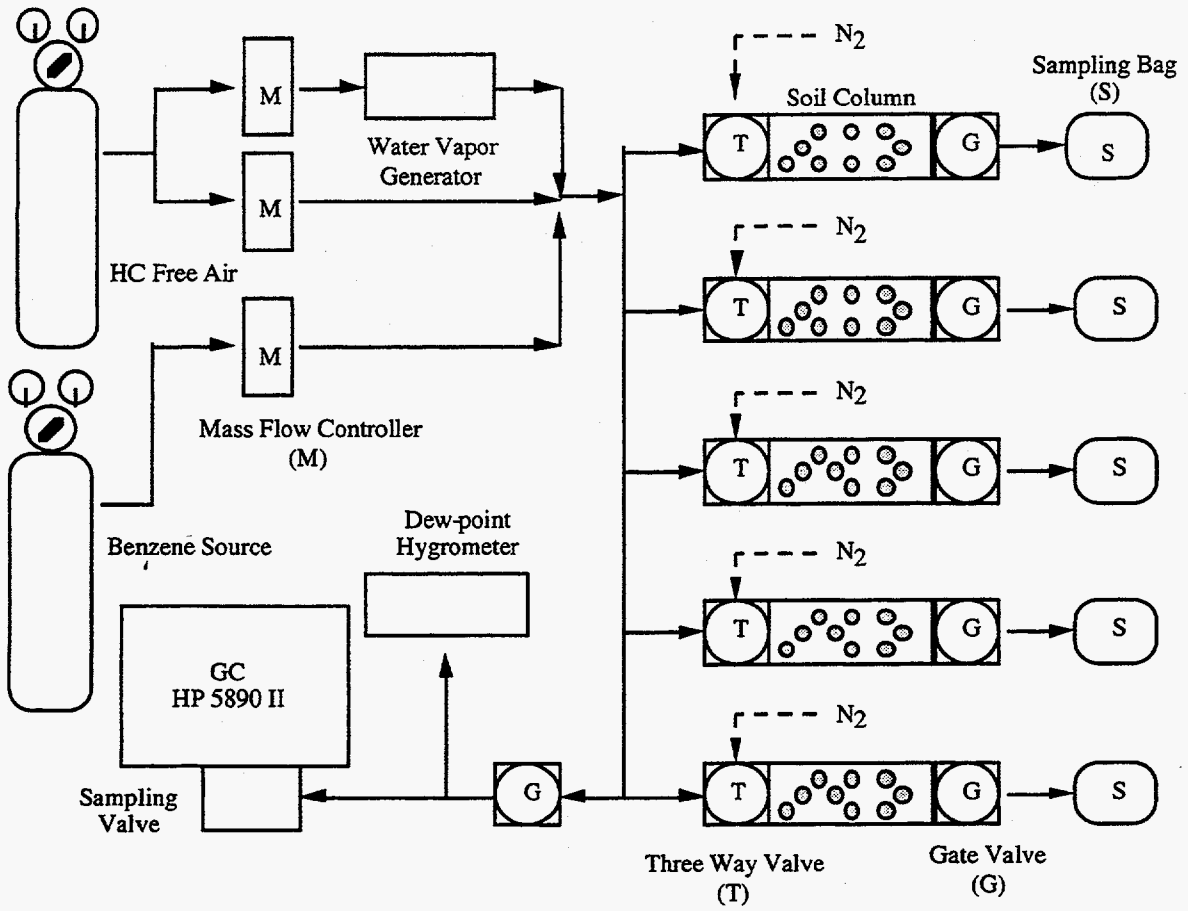

Figure 2. Schematic diagram of the differential adsorption bed (DAB) system.

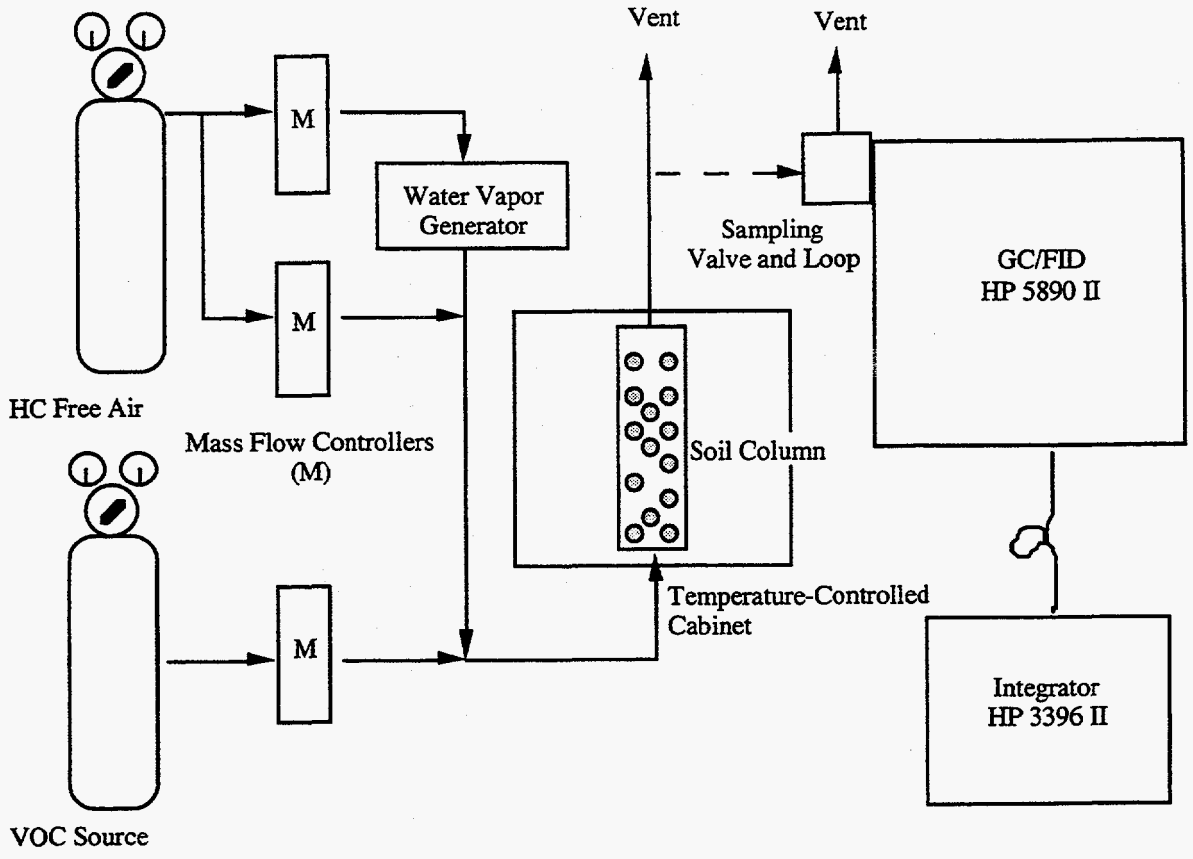

Figure 3. Schematic diagram of the column system used for high flow conditions.

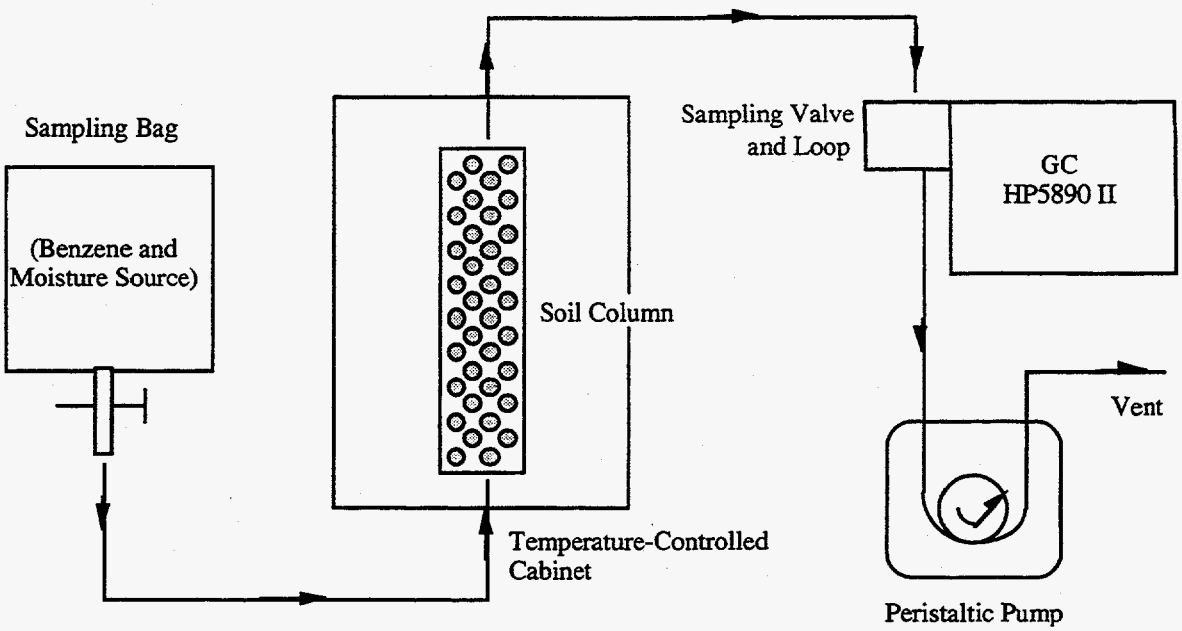

Figure 4. Schematic diagram of the column system used for low flow conditions.

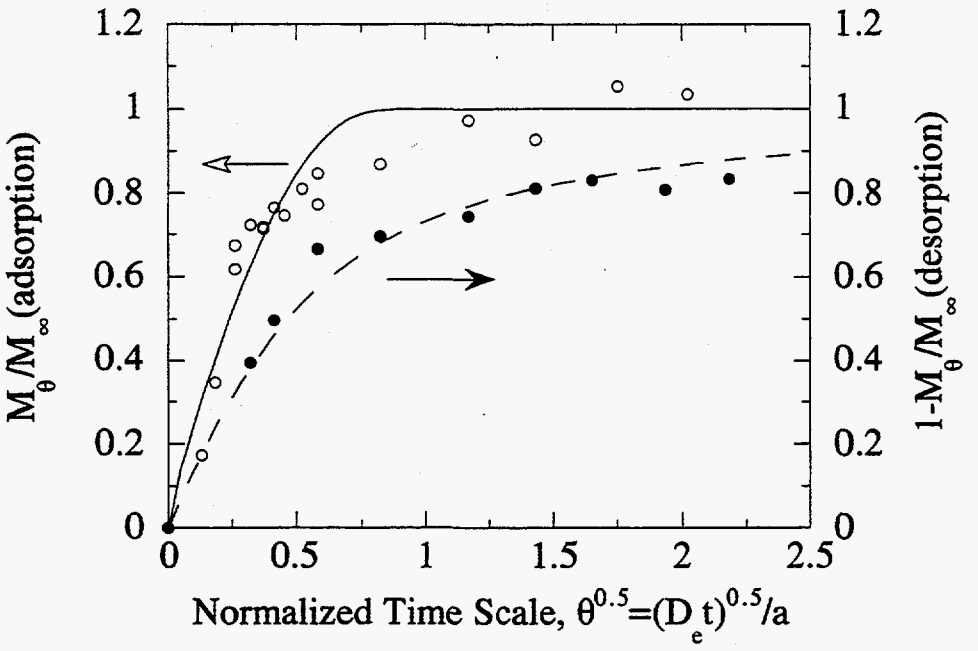

Figure 5. Sorption kinetics for benzene at 590 ppm on dry SSM (synthetic soil matrix) grains. M_θ/M_∞ is the cumulative mass gain relative to that at equilibrium, $(D_e t)^{0.5}/a$ is the square root of dimensionless time, D_e is the effective diffusivity (Equation 4), a is grain radius, and t is time. The open and filled symbols denote experimental adsorption and desorption data, respectively. The fitted porous sphere model is shown as a solid line for adsorption and as a dashed line for desorption. In the model, B is calculated to be ∞ (>300). The best fit values for n and D_e are 0.35 and 1.3 $\times 10^{-10}$ m^2 s^{-1}, respectively.

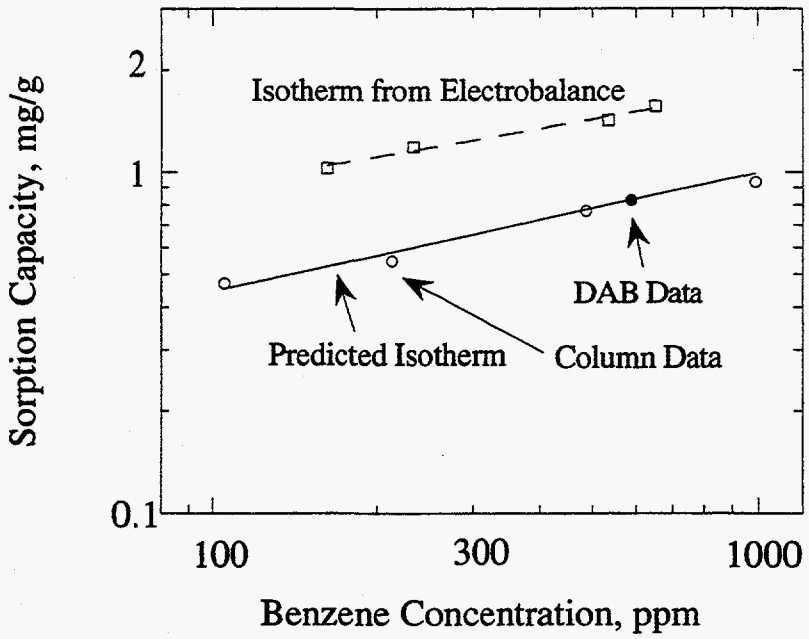

Figure 6. Predicted and experimental sorption isotherms of benzene on dry SSM (synthetic soil matrix). The solid line represents the predicted isotherm, based on DAB (differential adsorption bed) experiments conducted at 590 ppm for benzene. The open and filled circles represent experimental data measured by column and DAB systems, respectively, while the squares represent experimental data obtained from an electrobalance system.

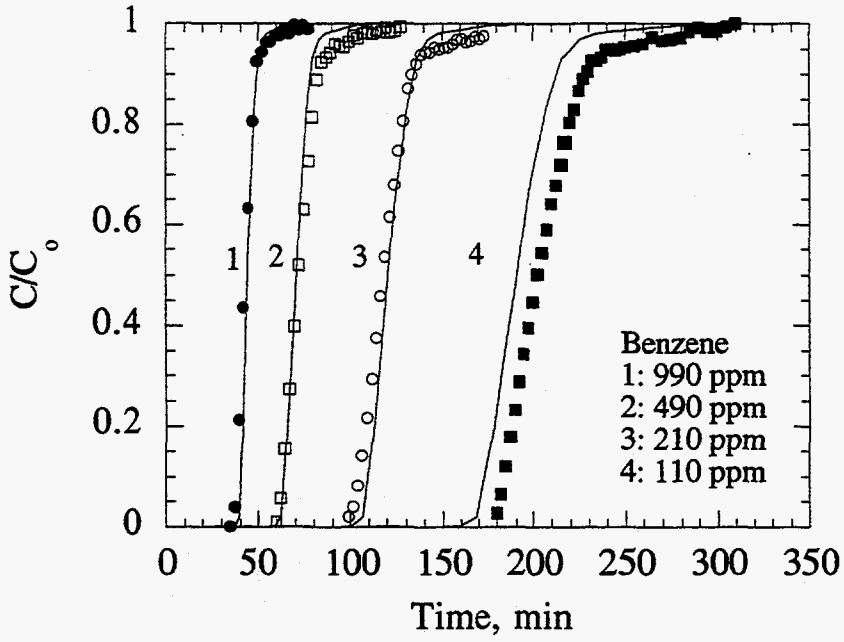

Figure 7. Predicted and experimental breakthrough curves (BTCs) for benzene through a dry soil column. The discrete symbols denote experimental data, while the predictions based on the advection-dispersion-sorption (ADS) equation coupled with the porous sphere model are shown as solid lines. The only experimental data used to generate the predictions result from a single kinetic adsorption-desorption experiment conducted at a benzene concentration of 590 ppm. The parameters used to predict experimental BTCs are listed in Table 1.

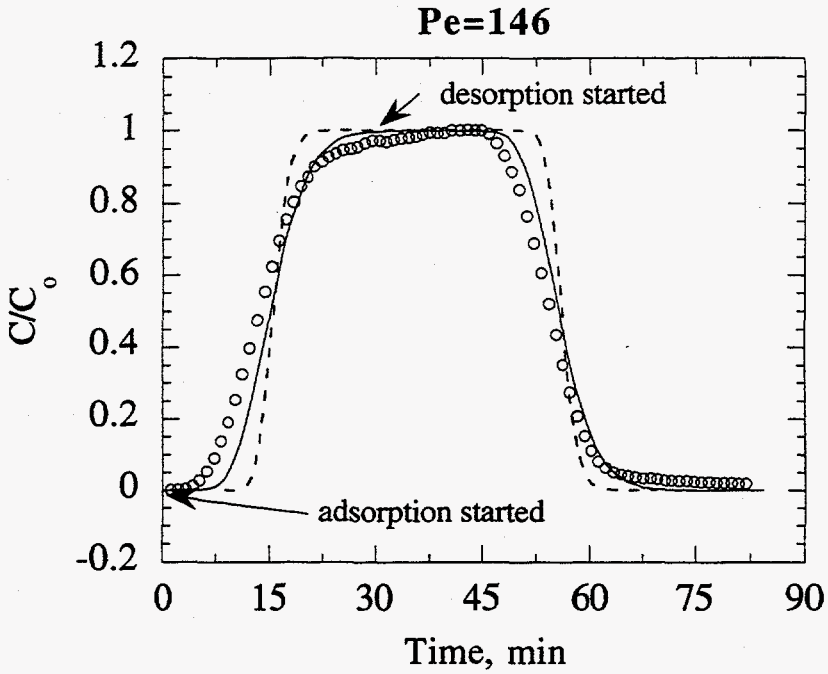

Figure 8. Predicted and experimental breakthrough curves (BTCs) for benzene through a moist soil column under a high flow condition. The open symbols denote experimental data. The predictions based on the advection-dispersion-sorption (ADS) equation coupled with the porous sphere model are shown as a solid line, whereas those based on the equilibrium model are shown as a dashed line. The parameters used to predict experimental BTCs are listed in Table 1.

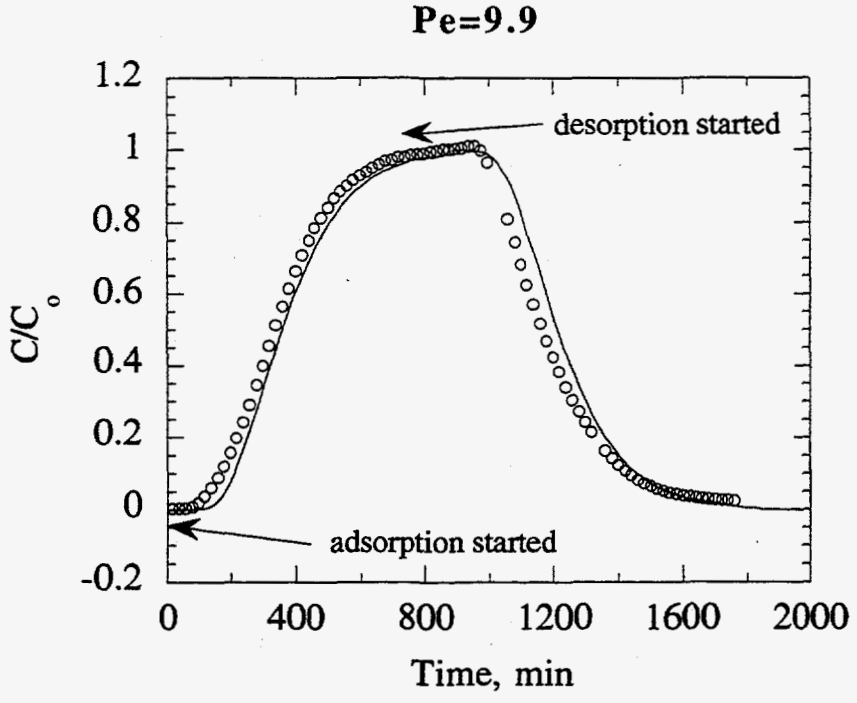

Figure 9. Predicted and experimental breakthrough curves (BTCs) for benzene through a moist soil column under an intermediate flow condition. The open symbols denote experimental data, while the predictions based on the advection-dispersion-sorption (ADS) equation coupled with the porous sphere model is shown as a solid line. The ADS equation based on an assumption of local equilibrium within the column yields almost identical predictions. The parameters used to predict experimental BTCs are listed in Table 1.

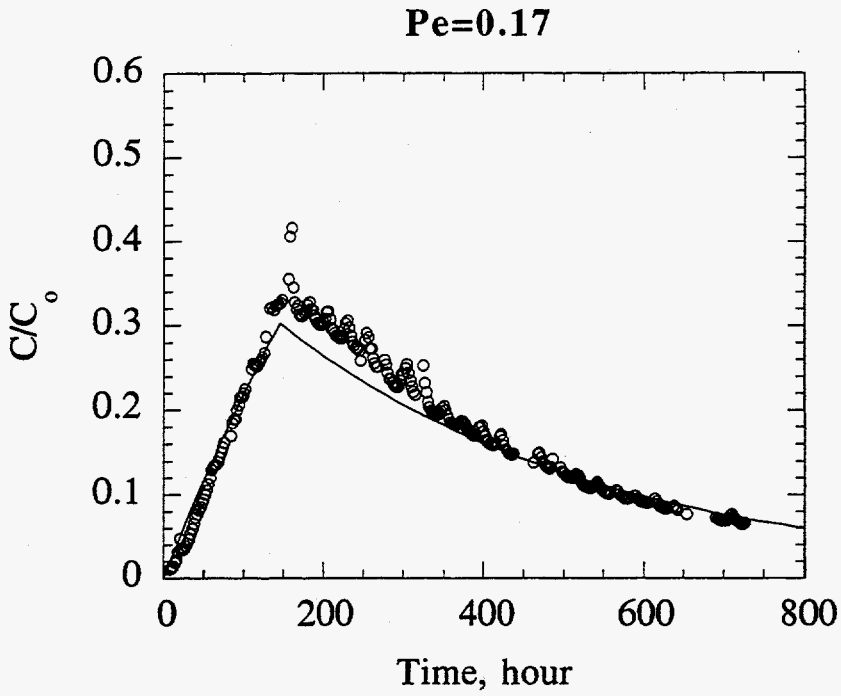

Figure 10. Predicted and experimental breakthrough curves (BTCs) for benzene through a moist soil column under a low flow condition. The open symbols denote experimental data, while predictions based on either the ADS equation assuming local equilibrium or the constant flow stirred tank reactor (CFSTR) model are shown as a solid line.

Chapter V

Gaseous Transport and Sorption in Activated Carbon: 1. Predicting the VOC Sorption Isotherm and Breakthrough Curves from a Single Kinetic Experiment*

ABSTRACT

The relationships among adsorption-desorption kinetics, equilibrium partitioning, and fixed-column breakthrough curves are elucidated for airborne benzene and vinyl chloride on activated carbon grains and fibers. An electrobalance is used to measure adsorption/desorption kinetics and to obtain equilibrium partitioning data; column experiments are conducted to determine additional equilibrium partitioning data and to measure breakthrough curves. A porous sphere/cylinder intragrain diffusion model, coupled with a Freundlich isotherm to describe equilibrium partitioning, conforms closely to the experimental kinetic data for both adsorption and desorption. In addition, it is shown that the sorption isotherm may be accurately predicted based on the asymmetry between adsorption and desorption rates measured in a single kinetic experiment. The parameters extracted from the kinetic experiment, when combined with the appropriate transport equations, can be used to accurately forecast column breakthrough curves.

---

* This chapter is taken from a paper: Lin, T.-F., Little, J.C., and Nazaroff, W.W. (1995). "Gaseous transport and sorption in activated carbon: 1. Predicting the VOC sorption isotherm and breakthrough curves from a single kinetic experiment." Submitted to *J. Env. Eng., ASCE.* Minor changes have been made to fit the format of this dissertation.

INTRODUCTION

Activated carbon adsorption is a proven method for removing volatile organic compounds (VOCs) from air. Both granular activated carbon (GAC) and activated carbon fibers (ACF) are used in a variety of engineered applications. A thorough understanding of the mechanisms controlling transport and sorption of VOCs within activated carbon systems is desirable as a basis for designing reliable and efficient sorbent-based separation devices. Also, since water vapor is a common constituent in gas-phase adsorption systems, there is a need to better understand water vapor sorption dynamics on activated carbon.

Recent research on sorption by dry soil grains (Chapter II) revealed that pore diffusion governs the rate at which gas-phase species reach the intragranular soil surfaces. The effective rate of diffusion into the soil grains is limited by strong, nonlinear local sorption between the gas-phase in the pores and the internal grain surface. A porous sphere model that couples intragrain diffusion with an experimentally measured Freundlich isotherm provided good resolution of the asymmetry in the rates of adsorption and desorption. That work demonstrated a close coupling between the extent of asymmetry in the kinetic curves and the degree of nonlinearity in the Freundlich isotherm.

The structural similarity between porous soil grains and activated carbon suggested that similar mechanisms may be controlling in both systems, and several related studies (Garg and Ruthven, 1972; Ruthven and Derrah, 1972; Gray and Do, 1989a, 1989b) support this inference. However, no prior studies have specifically addressed the relationship between adsorption/desorption kinetics and equilibrium partitioning during sorption of VOCs and water vapor by activated carbon. This study addresses that relationship. In this chapter, the scheme proposed in Chapter IV for predicting adsorption isotherms and breakthrough curves (BTCs) is used. Based on sorbent characterization data, only one kinetic experiment is needed to extract all the parameters for the prediction. To test this approach for sorbents used in engineered control systems, experimental data are

presented for the specific cases of vinyl chloride on both granular activated carbon (GAC) and activated carbon fibers (ACF), and for benzene on GAC. In Chapter VI, a similar investigation is conducted for the case of water vapor on GAC. That chapter addresses some challenges distinct from those considered here that arise due to (a) the relative importance of surface diffusion for transport of water vapor within GAC pores and (b) the observation of hysteresis in the equilibrium partitioning.

In conventional methods for designing an adsorption system, several separate experiments must be conducted to fully characterize the important kinetic and equilibrium properties of the sorbate-sorbent system. In this chapter, a simple and rapid experimental procedure, slightly modified from Chapter IV, is proposed. When properly interpreted, such an experiment can yield all of the important kinetic and equilibrium parameters for the given sorbent-sorbate system. The procedure is applied to several sorbate-sorbent combinations for which equilibrium partitioning is well described by a Freundlich isotherm. However, the procedure should be applicable with modest or no alteration to other sorbate-sorbent systems provided that (a) the sorbent is porous, and (b) the equilibrium isotherm has a known shape that can be described by no more than two parameters. In this procedure, an electrobalance experiment is first conducted to simultaneously obtain kinetic adsorption/desorption curves and the sorption capacity at a predetermined gas-phase concentration. A model of transport and sorption within single grains is then fit to the experimental data to extract two parameters: the effective diffusivity of the sorbate in the sorbent pores and the exponent of the Freundlich isotherm. The equilibrium sorption isotherm and column breakthrough curves are predicted based on these two parameters. To test the predictions, we independently measured the sorption isotherm and breakthrough curves (BTCs) at different imposed gas-phase concentrations. The model predictions and the corresponding experimental data are shown to agree well.

THEORY

This section presents the theoretical sorption and transport models employed in this study. The model describing transport and sorption of VOC molecules within individual carbon grains or fibers is based on the effort, described in Chapter II, to develop a porous sphere model for VOC sorption within dry soil grains. This model is used to infer pore diffusivity and one isotherm parameter from a kinetic experiment. The single grain/fiber model is then coupled with an axially dispersed plug-flow transport model (also known as the advection-dispersion-sorption equation) to predict the BTCs for column experiments. Since similar mathematical formulations, and numerical procedures and solutions have been described in detail in Chapter IV, only a brief summary of the theory is made here.

Individual Grain/Fiber Transport and Sorption. Our model assumes that the carbon grains are perfect spheres with constant diameter and that the carbon fibers are perfect cylinders, again with a constant diameter and with a length that is much greater than the diameter. Adsorption sites are assumed to be uniformly distributed within the grains or fibers. Considering transient diffusion and sorption, a mass balance on a small element of pore volume within the grain or fiber is combined with Fick's law to yield the following differential material balance:

$$\varepsilon_p \frac{\partial C}{\partial t} + (1-\varepsilon_p)\rho_p \frac{\partial q}{\partial t} = \frac{\varepsilon_p}{r^m}\frac{\partial}{\partial r}\left(r^m D_p \frac{\partial C}{\partial r}\right) \tag{1}$$

where q is the sorbed mass (mass of sorbate/mass of sorbent), C is the gas-phase concentration (mass of sorbate/volume of air), ε_p is the grain porosity, ρ_p is the density of the solid part of the sorbent, r is the radial coordinate of the sphere or cylinder, t is time, D_p is the effective gas diffusivity of sorbate molecules through the intraparticle pore space, and m is a shape factor equal to 1 for a cylindrical sorbent and 2 for a sphere. Although surface diffusion might be important under some circumstances in activated carbon systems (Gray and Do, 1990), the problem is simplified by considering gaseous diffusion as the only

means of VOC transport within the activated carbon grains or fibers. The close agreement between model predictions and measurements substantiates this assumption for the systems considered here.

In sorption of VOCs by activated carbon, the sorbed-phase is strongly favored and so the first term in Equation (1) can be neglected without loss of accuracy. Within the pores, instantaneously attained local equilibrium, following the Freundlich equation, is assumed to describe the partitioning between gas and sorbed phases:

$$q = kC^n \tag{2}$$

where k and n are empirical parameters. For the sake of mathematical simplicity, it is noted that temperature change due to adsorption/desorption processes is ignored in this study. Therefore, k, n and Dp are assumed to be constant for each adsorbent/adsorbate combination.

Combining Equations (1) and (2) and assuming D_p is constant with respect to r, we find

$$\frac{\partial C}{\partial t} = D_e (C / C_o)^{1-n} \frac{1}{r^m} \frac{\partial}{\partial r}\left(r^m \frac{\partial C}{\partial r} \right) \tag{3}$$

where

$$D_e = \frac{\varepsilon_p D_p}{(1-\varepsilon_p)\rho_p n k} C_o^{\,1-n} \tag{4}$$

is an effective diffusivity and C_o is the imposed external gas-phase concentration. Converting Equation (3) into dimensionless terms, yields

$$\frac{\partial Q}{\partial \theta} = Q^{1-n} \frac{1}{x^m} \frac{\partial}{\partial x}\left(x^m \frac{\partial Q}{\partial x} \right) \tag{5}$$

where $Q=C/C_o$, $x=r/a$, $\theta=tD_e/a^2$, and a is the grain radius. Mathematically, Equation (5) corresponds to the diffusion equation in spherical or cylindrical coordinates with radial symmetry and with a concentration-dependent diffusion coefficient, Q^{1-n}. It is this coefficient that links the degree of asymmetry in the rates of adsorption and desorption to the parameter n that appears in the Freundlich isotherm (Equation 2). Based on this property, the sorption isotherm of benzene on dry soil (Chapter IV) was successfully predicted from a single kinetic experiment. A similar technique is used in this study for the isotherm determination for VOCs on activated carbon.

The kinetic experiments begin with the sorbent in equilibrium with constant gaseous VOC concentration (typically zero). Then the sorbent is challenged with a step increase in the gas-phase sorbate concentration and the total amount sorbed is monitored as a function of time until steady-state is achieved. Desorption data are generated by suddenly reducing the gas-phase sorbate concentration to zero while continuing to monitor the total amount sorbed. The appropriate initial and boundary conditions for the adsorption phase of the experiment, incorporating the effects of external film-resistance, are as follows:

$$Q(0<x<1,\ \theta=0) = C_i/C_o$$

$$\frac{\partial Q}{\partial x}\Big|_{x=1} = B(1-Q_S) \qquad (6)$$

$$\partial Q/\partial x(x=0,\theta) = 0$$

For the desorption period, the corresponding initial and boundary conditions are:

$$Q(0<x<1,\ \theta=0) = 1$$

$$\frac{\partial Q}{\partial x}\Big|_{x=1} = B(-Q_S) \qquad (7)$$

$$\partial Q/\partial x(x=0,\theta) = 0$$

where C_i represents the initial concentration of adsorbate in gas-phase immediately before the step increase, Q_s represents Q at the grain or fiber surface (x=1), $B=k_f a/(D_p\varepsilon_p)$ is the mass-transfer Biot number, and k_f is the gas-film mass transfer coefficient. These initial

and boundary conditions state (a) that the sorbed mass is initially uniformly distributed throughout the grain or fiber, (b) that the flux into or out of the grain or fiber must match the rate of mass transport across the external gas-film boundary, and (c) that the center of the grain or fiber must represent an extremum with respect to local amount sorbed.

The relative mass uptake for adsorption (M_θ/M_∞), or the loss for desorption ($1-M_\theta/M_\infty$), at a specific time can be found by integrating the mass sorbed over the entire grain or fiber. This yields

$$\frac{M_\theta}{M_\infty} = (m+1)\int_0^1 x^m Q^n(x,\theta)dx \tag{8}$$

where M_θ is the total mass sorbed at time θ and M_∞ is the equilibrium mass sorbed at a gas-phase concentration of C_o.

Breakthrough Curves. Consider a gas stream containing a dilute concentration of a single sorbate as it flows through a column packed with sorbent. Assuming constant temperature and flow velocity, the material-balance equation for the sorbent column can be expressed as follows (cf. equations (8) and (10) in Chapter IV):

$$\frac{\partial C_b}{\partial t} = D_L\frac{\partial^2 C_b}{\partial z^2} - u\frac{\partial C_b}{\partial z} - (m+1)\left(\frac{1-\varepsilon}{\varepsilon}\right)\frac{k_f}{a}(C_b - C_s) \tag{9}$$

where C_b is the gas-phase concentration in the column pores (external to the soil grains), z is the axial coordinate for the column, u is the interstitial fluid velocity (i.e., the volumetric flow rate divided by the cross-sectional pore area), D_L is the dispersion coefficient and ε is the column porosity. Equation (9) can be rendered dimensionless:

$$\frac{\partial Q_b}{\partial \theta_b} = \frac{1}{Pe}\frac{\partial^2 Q_b}{\partial y^2} - \frac{\partial Q_b}{\partial y} - (m+1)\ St\ (Q_b - Q_s) \tag{10}$$

where $Q_b = C_b/C_o$, $\theta_b = ut/L$, $Pe = uL/D_L$ is a Peclet number, $y = z/L$, $St = (1-\varepsilon)k_f L/(\varepsilon a u)$ is a Stanton number, and L is the length of column.

BTCs can be obtained by simultaneously solving Equations (5), (6), and (10) subject to appropriate initial and boundary conditions for the column:

$$Q_b(0<y<1,\ \theta_b=0) = 0$$

$$1 - Q_b|_{y=0} = -\frac{1}{Pe}\frac{\partial Q_b}{\partial y}|_{y=0} \qquad (11)$$

$$\partial Q_b/\partial y(y=1,\theta_b) = 0$$

These conditions respectively state that (a) the column pores are initially free of sorbate, (b) the advective flux of sorbate into the column at the leading edge is balanced by the advective and dispersive fluxes away from the leading edge, and (c) the concentration at the outlet of the column is continuous.

MATERIALS AND METHODS

Adsorbates and Adsorbents. Benzene and vinyl chloride (VC) were chosen as representative VOCs as they are commonly found at contaminated environmental sites and are highly toxic. Gas-phase concentrations in the range of 100-1500 ppm were tested. GAC from Calgon (CAL) and ACF from American Kynol (ACF-1605-15) were selected as representative adsorbents. Manufacturers' data for the physical properties of the GAC and ACF are listed in Table 1. For GAC, the average diameter was estimated by us from the geometric mean of 100 grains measured by an optical microscope. For ACF, we used the middle of the range of fiber diameters as specified by the manufacturer.

Kinetic Experiments. Sorption experiments were performed with a Cahn-1000 electrobalance (Cahn Inc., Cerrito, CA) enabling the determination of both adsorption/desorption kinetics and sorption capacities. The electrobalance, which can weigh to a precision of ±1 μg providing careful control is exercised, was maintained at 20.0±0.2°C inside a temperature-controlled cabinet as shown in Figure 1.

For each experimental run, a sample of about 0.01 g of oven-dried (24 hrs at 105 °C) activated carbon was placed in a single layer of grains or fibers on the mesh pan inside

the electrobalance. The sample was conditioned by passing high purity hydrocarbon-free (HC-free) air (Airco, San Leandro, CA) through the electrobalance. The total hydrocarbon content (as methane) in the high purity air was less than 0.1 ppm while water vapor was less than 3 ppm. Generally the sample weight reached a constant level within 12 hours for GAC and within 1 hour for ACF. The overall sample weight change during the conditioning period was less than 0.1%.

On reaching constant weight, the HC-free air passing through the sample side was replaced by a mixture of a VOC and HC-free air. The VOC concentration in air was determined by material balance using the respective flow rates of benzene or VC standard (Scott Specialty Gases, Fremont, CA) and HC-free air. The mass of activated carbon plus sorbed VOC on the sample pan was continuously plotted on a chart recorder (Fisher, Model D-500, Austin, TX). Typically, after a few hours of exposure to the VOC, the sample mass became constant. The steady-state mass change relative to HC-free air represents the sorption capacity of the sorbent at the given VOC concentration. The VOC-air mixture was then replaced by clean HC-free air and a desorption curve was recorded.

One kinetic experiment was conducted for each of three sorbate-sorbent combinations. For vinyl chloride on activated carbon fibers and granular activated carbon, the adsorption/desorption response was measured for a step change from 0 to 490 ppm and back. For benzene on granular activated carbon, kinetics were measured for a step change between 150 ppm and 300 ppm. The results from these experiments were used to predict sorption isotherms and, for the case of VC/GAC, column breakthrough curves. These predictions were then compared with corresponding experimental measurements.

Column Experiments. Experimental BTCs were determined for columns packed with granular activated carbon using vinyl chloride as the target VOC (see Figure 2). The columns were made of stainless steel with respective lengths of 7.6 cm and 15.2 cm and an inside diameter of 2.3 cm. The column temperature was maintained at 20.0±0.2 °C throughout the experiments. Mass flow controllers (Model FC-280, Tylan, San Diego,

CA) regulated the air flow through the columns to 80 $cm^3\ s^{-1}$ (±3%). The mass flow controllers were checked periodically using a flow calibrator (Model DryCal DC-1, Bios, Pompton Plains, NJ).

Before each experimental run, HC-free air was used to purge the column for sufficient time so that only a negligible amount of residual VOC could be detected by a gas chromatograph (GC). Once column conditioning was complete, a step increase to a predetermined VOC concentration was supplied and maintained at the column inlet. The column effluent was periodically sampled by diverting a small aliquot of the air flow through a six-port valve system (HP 18900F) with a 0.25 cm^3 sampling loop. By switching the valve periodically, the air in the sampling loop passed through a gas chromatograph (GC, HP-5890 II) equipped with a flame ionization detector (FID), and the VOC concentration was measured. The column was considered to be saturated, and the experiment was terminated when the effluent concentration became equal to the imposed concentration at the inlet. The BTC for each run was obtained by plotting the effluent concentration-time history, and the sorption capacity was calculated from the following equation, derived from mass balance:

$$q = \frac{Q_f}{w}\int_0^\infty (C_o - C_b(L,t))\ dt \qquad (12)$$

where Q_f is the volumetric air flow rate through the column, w is the mass of GAC in column, and $C_b(L,t)$ is the time-dependent gas-phase species concentration at the column outlet.

RESULTS AND DISCUSSION

Sorption Kinetics. Typical adsorption/desorption kinetic data for vinyl chloride onto granular activated carbon are shown in Figure 3. As expected, the experimental curves were found to be asymmetric with adsorption occurring more rapidly than desorption. Similar results with varying degrees of asymmetry were found for

benzene/GAC and vinyl chloride/ACF. This type of asymmetry, with faster adsorption than desorption, implies for the Freundlich isotherm that the value of n is less than one.

The porous sphere/cylinder model was used to interpret the data from the sorption kinetic experiments. For vinyl chloride sorption onto GAC and ACF, two parameters were adjusted: the effective intragranular diffusivity, D_e, and the Freundlich exponent, n. For the case of benzene sorption onto GAC, the Freundlich isotherm parameters were obtained by measuring the equilibrium sorption capacity at two concentrations, 150 ppm and 300 ppm, and only D_e was obtained by fitting a model to the kinetic data. The Biot number used in the model was calculated from the Ranz-Marshall correlation for single particles (Wakao and Funazkri, 1978). Figures 4 and 5 show the experimental kinetic data and the best fit models. It should be emphasized that a single value for D_e is used for both adsorption and desorption for each of the sorbate-sorbent combinations. The models conform closely to the experimental data and the asymmetry in adsorption and desorption rates is well resolved. The close fits of the models to the experimental data suggests that the porous sphere/cylinder model captures the dominant features of adsorption and desorption kinetics of VOCs onto activated carbons.

Sorption Isotherms. Isotherms are predicted for VC sorption to both GAC and ACF from the single kinetic adsorption/desorption experiment, and for benzene to GAC based on kinetics in response to a change in gas phase concentration between 150 and 300 ppm plus the measured sorption capacity at these two concentrations. The procedures for making these predictions are the same as those presented in Chapter IV.

The predicted adsorption isotherms, summarized in Table 2, are compared with the sorption capacities measured from both electrobalance and column experiments (Figure 6). Excellent agreement (typically within 4%) was obtained when compared to equilibrium data from the electrobalance, whereas somewhat higher predictive errors (5% on average with a maximum of 13%) were obtained for adsorption capacity measured in the column experiments. The achievement of good agreement even across measurement methods

justifies significant confidence in the use of this predictive procedure, particularly considering that the measurement approaches are fundamentally different (mass change versus material balance using Equation (12)) and the sample mass used in the two procedures was vastly different (by three orders of magnitude).

Breakthrough Curves. To further test the applicability of the porous sphere/cylinder model, it was combined with the mass balance equation for transport through a fixed-bed column (Equations (10) and (11)) to predict the breakthrough curves for vinyl chloride through GAC columns. The predictions were then compared with measured BTCs.

The model input data are listed in Table 3. The Biot number was calculated from the modified Ranz-Marshall correlation (Wakao and Funazkri, 1978), and the axial dispersion coefficient, D_L, was estimated from the Edwards-Richardson correlation (Edwards and Richardson, 1968) as modified for small particles by Langer et al. (1978).

With one exception, the model predictions conform very well to the corresponding experimental data, as shown in Figure 7. The model only shows fair to good agreement with data from the low concentration run (190 ppm); this reflects the discrepancy between prediction and measurement for sorption capacity. It is significant to note that the model successfully predicts the BTCs, not only at the concentration used in the kinetic experiment, but also at higher or lower concentrations.

Engineering Application: Constant Pattern Behavior. Considerable mathematical effort is required to solve Equations (5), (6), (10) and (11). For engineering purposes, the simpler constant-pattern solution can be used as a design tool to predict the BTCs for fixed-bed adsorption systems (Fleck, et al. 1973; Garg and Ruthven, 1973; Hashimoto et al., 1977; Hand et al., 1984; Ruthven, 1984).

For a favorable isotherm (i.e., $n < 1$), the concentration front near the leading edge of the column first expands as a result of axial dispersion or mass-transfer resistance. However, as the front travels along the column, its shape will "self-sharpen" because of the

opposing influence on the front velocity of the equilibrium isotherm (Yang, 1987). In time, the shape of the concentration front will attain a constant pattern, at which point the concentration profiles in the gas and solid phases become coincident (Garg and Ruthven, 1973) and the mass-balance equation for the sorbent column reduces to

$$\frac{C_b}{C_o} = \frac{M_\theta}{M_\infty} \tag{13}$$

Once a constant pattern is achieved, the mathematical analysis is greatly simplified, since only one partial differential equation needs to be solved instead of two. Under constant-pattern conditions, the concentration profile within the mass-transfer zone of the column is obtained from the solution of Equations (5), (8), and (13). The breakthrough time for the column can be estimated from the sorption capacity. Using the shape of the breakthrough curve and the breakthrough time, the effluent concentration profile from an sorbent bed can be predicted.

A numerical solution for Equations (5), (8) and (13) was developed by Fleck et al. (1973). Since the results of their study were presented in a figure, which is not easy to interpret, a separate numerical solution of the three governing equations was generated for the present study. The numerical scheme was similar to the adsorption case for the porous sphere/cylinder model (see Chapter II and IV), with appropriate modification of the boundary condition at the surface of the sorbent grain. The treatment of that boundary condition was similar to that of Garg and Ruthven (1973) for constant pattern BTCs and pore diffusion control, although those authors used a Langmuir isotherm. The results of our numerical solution were found to be very close to those of Fleck et al. (1973).

A comparison between the full model and the constant pattern approach showed that for St > ~20 (in our system, with B = 33 and n = 0.55), the predictions are essentially identical. Since the distance required to attain a constant-pattern concentration front is very small (about 5 cm in our column experiments) relative to the length of practical adsorption systems (Ruthven, 1984), the constant-pattern model represents a relatively simple and

useful way to predict BTCs using the equilibrium isotherm obtained from a single kinetic experiment.

SUMMARY

The porous sphere/cylinder models conform closely to the experimental data for adsorption of volatile organic compounds on GAC and ACF. The models assume that local equilibrium between the pore wall and the adjacent pore air is established instantaneously during intraparticle diffusional transport of sorbate molecules. Furthermore, this equilibrium is assumed to be the same as that measured for the bulk sample. The asymmetry between adsorption and desorption rates can be used to predict the adsorption isotherm, and then the breakthrough curves can be predicted using the parameters extracted from a single kinetic experiment, even when different imposed gas-phase concentrations are used. The simpler, constant-pattern approach for predicting the BTC yielded predictions that were essentially the same as for the full numerical solution.

APPENDIX I. REFERENCES

Edwards, M.F., and Richardson, J.F. (1968). "Gas dispersion in packed beds." *Chem. Eng. Sci., 23*, 109-123.

Fleck, R.D., Kirwan, D.J., and Hall, K.R. (1973). "Mixed-resistance diffusion kinetics in fixed-bed adsorption under constant pattern conditions." *Ind. Eng. Chem. Fundam., 12*, 95-99.

Garg, D.R., and Ruthven, D.M. (1972). "The effect of the concentration dependence of diffusivity on zeolite sorption curves." *Chem. Eng. Sci., 27*, 417-423.

Garg, D.R., and Ruthven, D.M. (1973). "Theoretical prediction of breakthrough curves for molecular sieve adsorption columns: I. Asymptotic solutions." *Chem. Eng. Sci., 28*, 791-798.

Gray, P.G., and Do, D.D. (1989a). "Adsorption and desorption of gaseous sorbates on a bidispersed particle with Freundlich isotherm: I. Theoretical analysis." *Gas Sep. Purif., 3*, 193-200.

Gray, P.G., and Do, D.D. (1989b). "Adsorption and desorption of gaseous sorbates on a bidispersed particle with Freundlich isotherm: II. Experimental study of sulphur dioxide sorption on activated carbon particles." *Gas Sep. Purif., 3*, 201-208.

Gray, P.G., and Do, D.D. (1990). "Adsorption and desorption dynamics of sulphur dioxide on a single large activated carbon particle." *Chem. Eng. Comm., 96*, 141-154.

Hand, D.W., Crittenden, J.C., and Thacker, W.E. (1984). "Simplified models for design of fixed-bed adsorption systems." *J. Env. Eng., ASCE, 110*, 440-456.

Hashimoto, K., Muira, K., and Tsukano, M. (1977). "Experimental verification of design methods for liquid phase fixed-bed adsorbers." *J. Chem. Eng. Japan, 10*, 27-34.

Langer, G., Roethe, A., Roethe, K.-P., and Gelbin, D. (1978). "Heat and mass transfer in packed beds: III. Axial mass dispersion." *Int. J. Heat Mass Transfer, 21*, 751-759.

Ruthven, D.M. (1984). *Principles of Adsorption and Adsorption Processes*. John Wiley and Sons, New York, N.Y.

Ruthven, D.M., and Derrah, R.I. (1972). "Sorption in Davison 5A molecular sieves." *Can. J. Chem. Eng., 50*, 743-747.

Wakao, N., and Funazkri, T. (1978). "Effect of fluid dispersion coefficients on particle-to-fluid mass transfer coefficients in packed beds." *Chem. Eng. Sci., 33*, 1375-1384.

Yang, R.T. (1987). *Gas Separation by Adsorption Processes*. Butterworths, Stoneham, MA.

APPENDIX II. NOMENCLATURE

a	radius of carbon grain or fiber (m)
B	Biot number [= $(k_f a)$ $(\varepsilon_p D_p)^{-1}$] (dimensionless)
C	gas-phase sorbate concentration (g m^{-3})
C_b	gas-phase species concentration in intergranular pores within column (g m^{-3})
C_i	initial gas-phase species concentration in sorbent pores (g m^{-3})
C_o	imposed, external gas-phase species concentration for kinetic studies and inlet concentration for column studies (g m^{-3})
C_s	gas-phase concentration at external surface of carbon grain or fiber (g m^{-3})
D_e	effective diffusivity (m^2 s^{-1})
D_L	dispersion coefficient (m^2 s^{-1})
D_p	pore diffusivity in carbon grain or fiber (m^2 s^{-1})
k	Freundlich isotherm parameter ((g g^{-1}) × (g m^{-3})$^{-n}$)
k_f	gas-film mass-transfer coefficient (m s^{-1})
L	length of column (m)
m	geometry factor: 1 for cylindrical system, 2 for spherical system
M	cumulative mass gain due to sorption (g sorbate per g sorbent)
M_θ/M_∞	cumulative mass gain relative to that in equilibrium with C_o (dimensionless)
n	Freundlich isotherm parameter (dimensionless)
Pe	Peclet number [= $uL\ D_L^{-1}$] (dimensionless)
q	(equilibrium) sorption capacity (g sorbate per g sorbent)
Q	normalized gas-phase species concentration [= $C\ C_o^{-1}$] (dimensionless)
Q_b	normalized gas-phase species concentration in column [= $C_b\ C_o^{-1}$] (dimensionless)
Q_f	air flow rate in column (m^3 s^{-1})

Q_s	normalized gas-phase species conc. on grain surface [= C_s C_o^{-1}] (dimensionless)
r	radial coordinate in carbon grain or fiber (m)
St	Stanton number [= (1-ε) $k_f L$ (εau)$^{-1}$] (dimensionless)
t	time (s)
u	interstitial fluid velocity (m s^{-1})
w	mass of GAC in column (g)
x	normalized radial coordinate in carbon grain or fiber [= r a^{-1}] (dimensionless)
y	normalized axial coordinate in column [= z L^{-1}] (dimensionless)
z	axial coordinate in column (m)
ε	bulk porosity in carbon column (dimensionless)
ε_p	grain porosity (dimensionless)
θ	normalized time for individual grains or fibers [= t D_e a^{-2}] (dimensionless)
θ_b	normalized time for column [= u t L^{-1}] (dimensionless)
ρ_b	bulk density of carbon grain (g m^{-3})
ρ_p	solid density of carbon grain or fiber (g m^{-3})

Table 1. Properties of Activated Carbon Samples

Property	Granular Activated Carbon[†]	Activated Carbon Fibers[‡]
Approximate Shape	Sphere	Cylinder
Size	12-40 US mesh	9-10 μm
Average Diameter	0.17[a](0.15[b]) cm	9.5 μm
Porosity, ε_p	0.65	0.5
BET Surface Area, m^2/g	900-1100	1500
Carbon Density, g/cm^3	2.1	2.0

[†]Data from Calgon Carbon Corp. [‡]Data from American Kynol, Inc. [a]For column experiments, geometric mean of 100 grains. [b]For kinetic experiments, geometric mean of all the grains (13) used in the experiments.

Table 2. Predicted Isotherm and Errors for VOC Adsorption on Activated Carbons.

Adsorbent	VOC	Experimental Method	Predicted Isotherm[a] $q=kC^n$	Error of Prediction[b] average (range),%
GAC	benzene	electrobalance	$q = 0.20\ C^{0.30}$	3.6 (+3.3~+3.8)
GAC	vinyl chloride	electrobalance	$q = 0.025\ C^{0.55}$	3.7 (-1.8~+7.1)
GAC	vinyl chloride	column	$q = 0.025\ C^{0.55}$	5.2 (-1.1~+13)
ACF	vinyl chloride	electrobalance	$q = 0.047\ C^{0.55}$	3.6 (-2.6~+6.2)

[a] q is adsorbed mass (g sorbate per g sorbent) and C is gas-phase sorbate concentration (g m^{-3}). [b] Error is defined as (q of prediction - q of measurement)/(q of measurement).

Table 3. Parameters Used to Predict Breakthrough Curves.

Parameter	Symbol (unit)	Long Column	Short Column
Column Length	L (m)	0.152	0.076
Interstitial Fluid Velocity	u ($m\ s^{-1}$)	0.528	0.504
Bulk Porosity in Column	ε (-)	0.36	0.39
Effective Diffusivity (for 1500 ppm)	D_e ($m^2\ s^{-1}$)	4.95×10^{-10}	4.95×10^{-10}
Gas-film Mass Transfer Coefficient	k_f ($m\ s^{-1}$)	0.103	0.100
Peclet Number	Pe (-)	112	57
Stanton Number	St (-)	62	28
Biot Number	B (-)	33	33

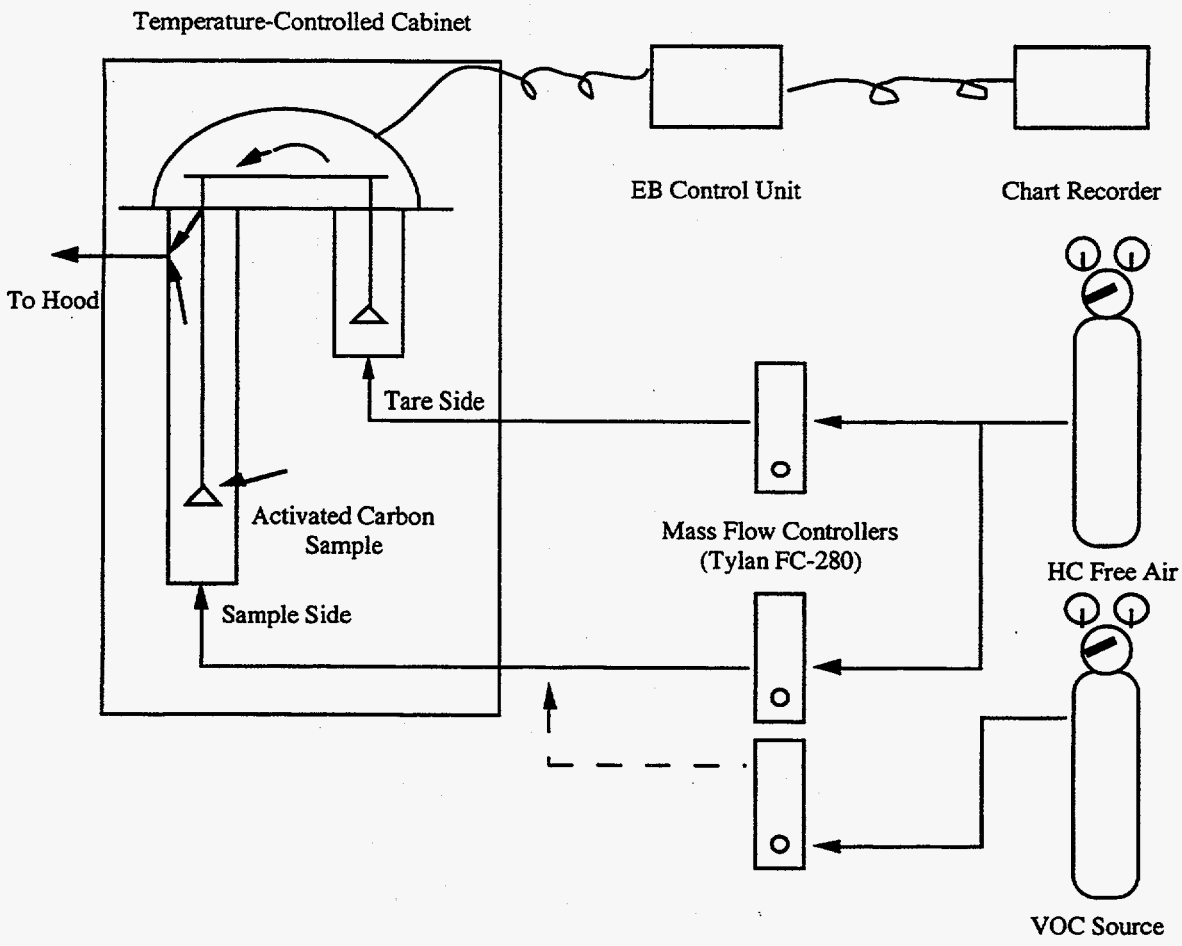

Figure 1. Schematic diagram of the electrobalance (EB) system.

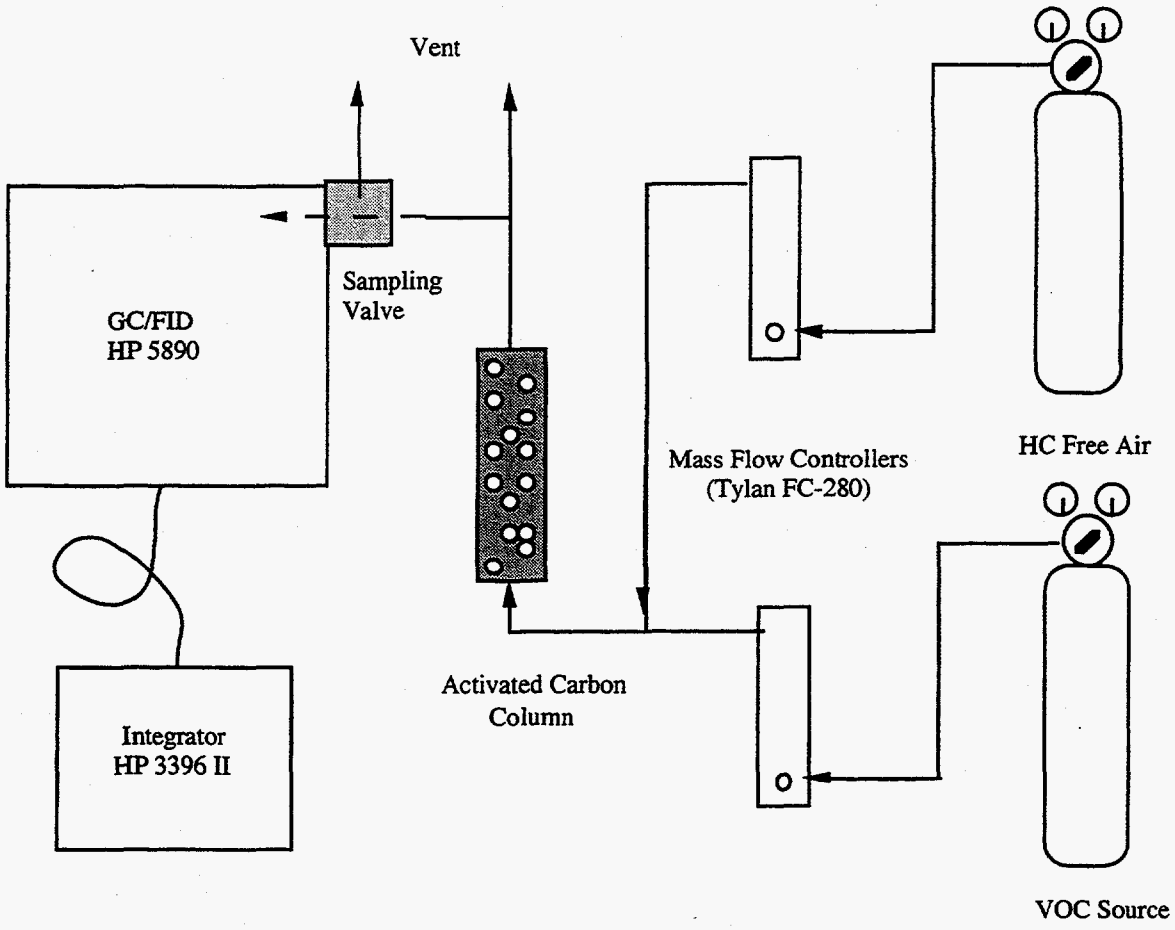

Figure 2. Schematic diagram of the column system.

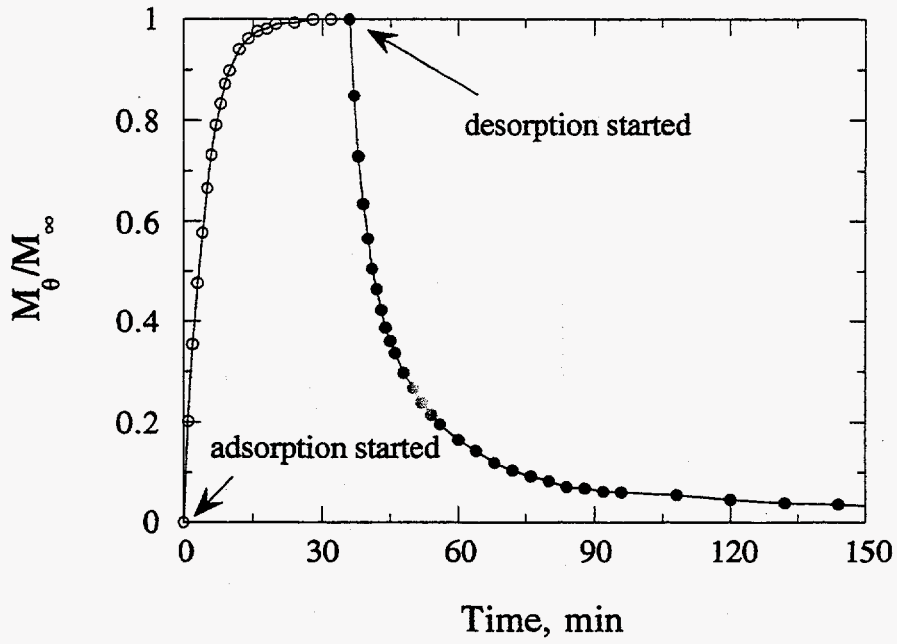

Figure 3. Typical experimental sorption kinetic curves for vinyl chloride (490 ppm) on activated carbon grains.

(a)

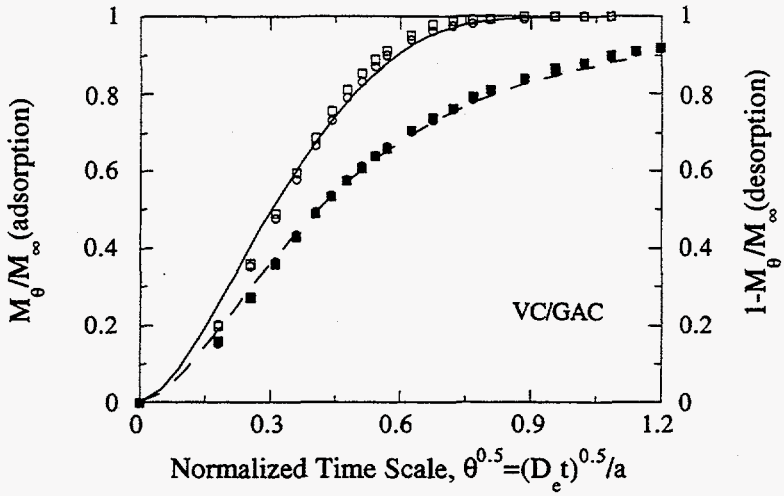

(b)

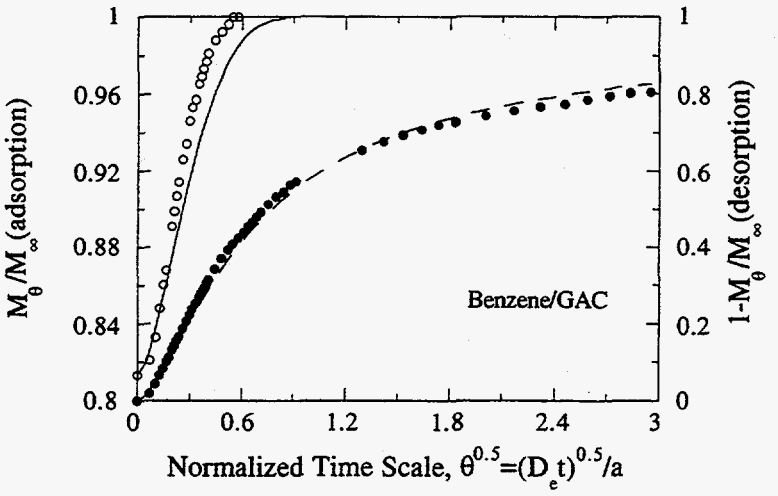

Figure 4. Sorption kinetics for granular activated carbon where (a) represents response to vinyl chloride at 490 ppm and (b) represents response to benzene at 300 ppm. See Appendix II for definition of parameters. The open and filled symbols denote experimental adsorption and desorption data, respectively. The fitted porous sphere model is shown as a solid line for adsorption and as a dashed line for desorption. In the model, B is calculated to be 8. The best fit value for n is 0.55 for vinyl chloride, while the D_e values are 3.0×10^{-10} m^2 s^{-1} for vinyl chloride and 2.6×10^{-11} m^2 s^{-1} for benzene.

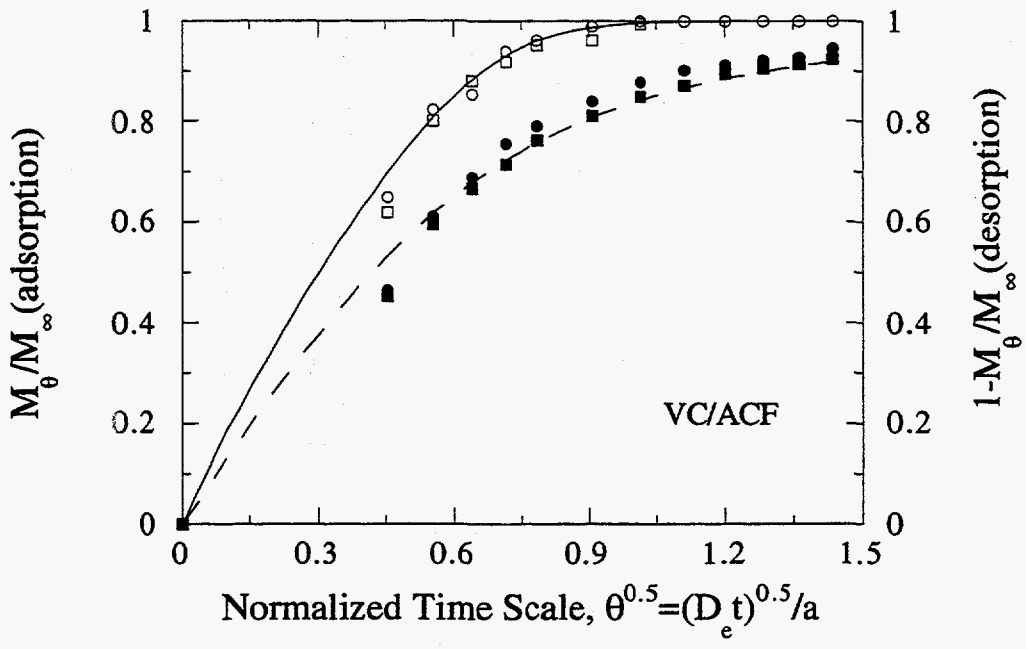

Figure 5. Sorption kinetics for vinyl chloride at 490 ppm on activated carbon fibers. See caption to Figure 4 for symbol and parameter definitions. In the model, B is calculated to be ∞ (>200), while the best fit value for n is 0.55 and for D_e is 3.9×10^{-13} m^2 s^{-1}.

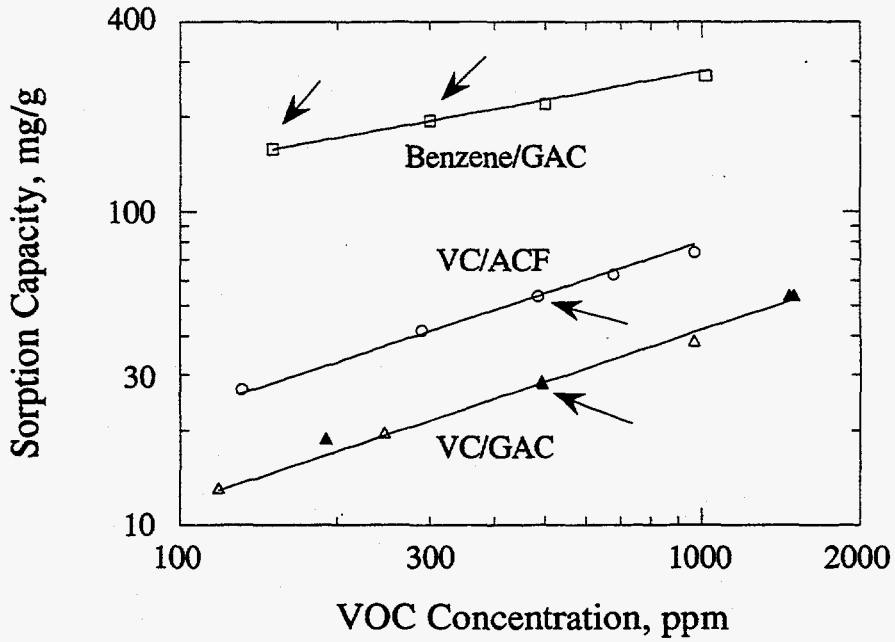

Figure 6. Predicted and experimental sorption isotherms of VOCs on activated carbons. The lines represent predicted isotherms, based on electrobalance kinetic experiments (identified by arrows) conducted at 490 ppm for vinyl chloride and 300 ppm for benzene (the sorption capacity of benzene, measured at 150 ppm, was also used in isotherm prediction). The open and filled symbols represent experimental data measured by electrobalance and column systems, respectively.

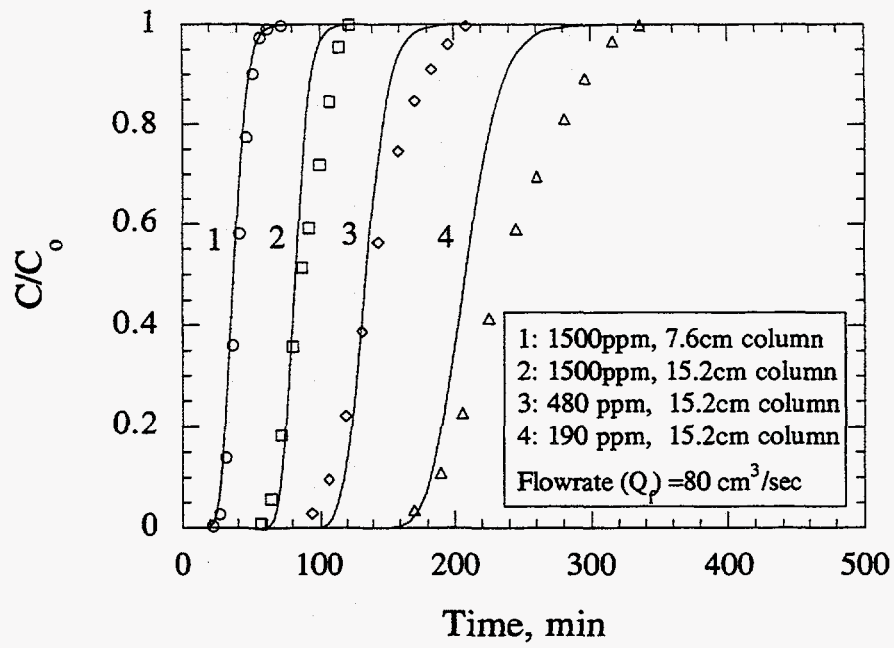

Figure 7. Predicted and experimental breakthrough curves (BTCs) for vinyl chloride through granular activated carbon columns. The open symbols denote experimental data, while the predictions based on the dispersed plug flow equation coupled with the porous sphere model are shown as solid lines. The only experimental data used to generate the predictions result from a single kinetic adsorption-desorption experiment conducted at a vinyl chloride concentration of 490 ppm. The parameters used to predict experimental BTCs are listed in Table 3.

Chapter VI

Gaseous Transport and Sorption in Activated Carbon: 2. Linking Kinetic Behavior with the Equilibrium Isotherm for Water Vapor*

ABSTRACT

Control of of organic vapors by adsorption on activated carbon can be impacted by the presence of water vapor in the gas stream. As a foundation to better understand this issue, we have studied the transport and sorption of water vapor within activated carbon grains. Adsorption/desorption kinetics and equilibrium partitioning of water between gas and sorbed phases were determined at relative humidities (RH) in the range 0 to 86% and at 20 °C using an electrobalance. A model that accounts for transport within grains by pore and surface diffusion is used to interpret the sorption kinetic data. The model assumes instantaneously attained local equilibrium between sorbed and gas phases within the pores based on a piecewise-linear isotherm measured for a small ensemble of activated carbon grains. Despite the complicated observed shape of the isotherms, including hysteresis, the model conforms well to all of the experimental data, and the asymmetry between adsorption and desorption rates is well resolved. The model results indicate that gas-phase diffusion dominates transport through the pores at RH $\leq$ 60%. Surface diffusion is found to be important at higher values of RH.

---

* This chapter is taken from a paper: Lin, T.-F., and Nazaroff, W.W. (1995). "Gaseous transport and sorption in activated carbon: 2. Linking kinetic behavior with the equilibrium isotherm for water vapor." Submitted to *J. Env. Eng., ASCE*. Minor changes have been made to fit the format of this dissertation.

INTRODUCTION

Activated carbon (AC) adsorption is a proven method for removing volatile organic compounds (VOCs) from an air stream. For example, AC adsorption units are used to remove VOCs from air stripper off-gas (Crittenden et al., 1988) and to reduce VOC concentrations in indoor air (Liu, 1993). Commonly, water vapor is present at substantial levels in the air streams. Although activated carbon has a higher affinity for VOCs than for water vapor, the presence of water vapor can reduce the VOC sorption capacity (Crittenden et al., 1988; Rudisill et al., 1992) and may certainly change the kinetics of sorption processes, especially at higher values of relative humidity (RH). Therefore, it is desirable to understand both the kinetics and equilibrium of water vapor adsorption onto activated carbon as a basis for designing more effective adsorption units.

Many investigations have addressed the relationship between sorption kinetics and equilibrium for different sorbent/sorbate combinations (Ruthven and Derrah, 1972; Garg and Ruthven, 1972; Gray and Do, 1989a, 1989b, 1990 and 1991; Desai et al., 1992; Chapter II of this dissertation). These studies have revealed that adsorption rates are faster than desorption rates whenever the sorption isotherms are convex (diminishing slope with increasing gas-phase concentration). Several different models have been used to resolve the asymmetry between adsorption and desorption kinetics. Ruthven and coworkers studied the sorption of light-weight hydrocarbons onto zeolites (Ruthven and Derrah, 1972; Garg and Ruthven, 1972) using micropore and macropore diffusion models, and the sorption of water vapor onto activated alumina (Desai et al., 1992) using a macropore and surface diffusion model. Gray and Do (1989a, 1989b, 1990 and 1991) have investigated sorption of sulfur dioxide and carbon dioxide onto activated carbon particles; their model descriptions account for gas-phase diffusion through macropores and micropores as well as surface diffusion. In Chapter II, VOC and water vapor transport within dry soil grains was described using a pore diffusion model. In Chapter V, a pore diffusion model was used to

link the adsorption/desorption kinetics with equilibrium partitioning behavior of VOCs on both activated carbon grains and fibers. All of these investigations have used either Langmuir, Freundlich or BET isotherms to describe the equilibrium partitioning between the gas and sorbed phases, and none of the studies has addressed the adsorption of water vapor sorption onto activated carbon. The nature of the water vapor/activated carbon system is different from the systems previously investigated. The sorption isotherm reveals hysteresis and has too complex a shape to be well described by any of the basic isotherm equations.

In this chapter, the relationship between adsorption/desorption kinetics and equilibrium partitioning of water vapor on activated carbon (AC) grains is investigated. First, the adsorption and desorption isotherms, and adsorption and desorption kinetic curves of water vapor onto AC grains were measured by an electrobalance at RH between 0% and 86% and at 20 °C. A model that accounts for both pore and surface diffusion was coupled with the experimentally determined piecewise-linear isotherm to interpret the experimental kinetic data. The models conform well with the experimental data and the model results serve as a basis for inferring the relative importance of surface diffusion versus gas-phase diffusion within the AC grains.

THEORY

The transport and sorption of water vapor within individual AC grains is described using a similar approach to those previously presented to account for VOC and water transport/sorption in soil grains (Chapter II) and VOC in activated carbon (Chapter V). Briefly, the AC grains are assumed to be porous spheres with adsorption sites uniformly distributed throughout their volume. Transport within a grain occurs by both gas-phase diffusion through the pores and surface diffusion along the pore walls (only gas-phase diffusion was considered in the prior chapters). Local equilibrium between gas and sorbed phases is maintained within the pores, as described by the experimental isotherm measured for the grain as a whole.

A mass balance equation can thus be written to describe transient diffusion and sorption of water vapor within carbon grains. In writing this equation, we neglect accumulation of water vapor in the grain pores as negligible compared with accumulation of sorbed water vapor. Thus,

$$(1-\varepsilon_p)\rho_p\frac{\partial q}{\partial t}=\frac{1}{r^2}\frac{\partial}{\partial r}\left(r^2\left(\varepsilon_p D_p\frac{\partial C}{\partial r}+(1-\varepsilon_p)D_s\,\rho_p\frac{\partial q}{\partial r}\right)\right) \tag{1}$$

where q is the sorbed mass (mass of sorbate per mass of adsorbent), C is the gas-phase species (H_2O) concentration (mass of adsorbate per volume of air), ε_p is the grain porosity, ρ_p is the density of the solid part of the adsorbent, r is the radial coordinate, t is time, D_p is the effective gas diffusivity of sorbate molecules through the intraparticle pore space, and D_s is the effective surface diffusivity for migration of sorbed H_2O molecules along the pore surface.

Within the pores, the local equilibrium partitioning between gas and sorbed phases follows an experimentally determined isotherm, which can be generically expressed as

$$q = f(C) \tag{2}$$

Hysteresis is experimentally observed in the adsorption of water vapor on activated carbon (Sing et al., 1985). Consequently, q is not uniquely a function of C, but also depends on the path by which C is attained. This complication causes no fundamental difficulty so long as it is borne in mind in the analysis that follows.

Equations (1) and (2) can be combined, yielding

$$\frac{\partial C}{\partial t}=\frac{1}{f'(C)}\frac{1}{r^2}\frac{\partial}{\partial r}\left(r^2\left(\frac{\varepsilon_p D_p}{(1-\varepsilon_p)\rho_p}\frac{\partial C}{\partial r}+D_s f'(C)\frac{\partial C}{\partial r}\right)\right) \tag{3}$$

Because of the complex shape of the adsorption isotherm between water vapor and AC when a broad range of relative humidities is considered (0 to 86% in this case), the

experimental equilibrium partitioning data were approximated by a piecewise-linear isotherm:

$$q_i = b_i + k_i C_i \tag{4}$$

where the subscript i represents the values in the ith region, k_i is the slope of the isotherm segment between C_i and C_{i-1}, and b_i is the ith intercept value, chosen to ensure continuity across linear segments. The piecewise-linear isotherm was used by Leigh and Smith (1993) to approximate adsorption and transport of sorbates for nonlinear Freundlich and Langmuir isotherms. They found that a 5-region, piecewise-linear isotherm is sufficient to model the nonlinear isotherms. For the present paper, more than 13 segments were used to describe the isotherm over the range $0 \leq RH \leq 86\%$.

Assuming D_p is constant, Equation (3) is transformed to the following form when expressed in dimensionless quantities for the case of a piecewise-linear isotherm:

$$\frac{\partial Q}{\partial \theta} = \frac{1}{k_i'} \frac{1}{x^2} \frac{\partial}{\partial x} \left(x^2 \left(\frac{\partial Q}{\partial x} + \frac{D_s}{D_e} k_i' \frac{\partial Q}{\partial x} \right) \right) \tag{5}$$

where

$$D_e = \frac{\varepsilon_p D_p}{(1-\varepsilon_p)\rho_p k_{io}} \tag{6}$$

is the effective pore diffusivity, $Q=C/C_o$ is the normalized gas-phase concentration, $\theta=D_e t/a^2$ is dimensionless time, $x=r/a$ is a dimensionless radial coordinate, a is the carbon grain radius, $k_i'=k_i/k_{io}$ is a normalized isotherm slope, and k_{io} is the slope of the final isotherm segment that extends up to $C = C_o$. The appropriate initial and boundary conditions for a step increase in gas-phase concentration (adsorption), starting with the AC grain in equilibrium with RH = 0, and accounting for external gas-film transport resistance are as follows:

$$Q(0<x<1,\ \theta=0)=0$$

$$(1+\frac{D_s}{D_e}k_i')\frac{\partial Q}{\partial x}\Big|_{x=1} = B(1-Q_s) \qquad (7)$$

$$\partial Q/\partial x(x=0,\theta) = 0$$

In this set of equations, B (= $[k_f\ a]/[\varepsilon_p\ D_p]$) is the mass-transfer Biot number, where k_f is the gas-film mass-transfer coefficient, which can be calculated from the Ranz-Marshall correlation for single particles (Wakao and Funazkri, 1978). The Biot number was calculated to be 40 for each of the kinetic experiments conducted in this study. For a step decrease in gas-phase concentration (desorption) to RH = 0 from a condition in which the AC grain is in equilibrium at a fixed RH, the initial and boundary conditions are as follows:

$$Q(0<x<1,\ \theta=0)=1$$

$$(1+\frac{D_s}{D_e}k_i')\frac{\partial Q}{\partial x}\Big|_{x=1} = B(-Q_s) \qquad (8)$$

$$\partial Q/\partial x(x=0,\theta) = 0$$

These conditions state (a) that gaseous concentration of water vapor is initially uniform throughout the grain; (b) that the flux through the grain surface is continous at the outer edge of the grain; and (c) that the center of the grain represents an extremum in gas-phase water vapor concentration with respect to position.

The relative mass uptake for adsorption (M_θ/M_∞), or loss for desorption ($1-M_\theta/M_\infty$), at a specific time can be found by solving Equation (5), subject to boundary/initial conditions given by Equation (7) or (8), and converting the result to dimensional form as C(r). The sorbed mass can then be determined as a function of position from the isotherm, Equation (4). The total sorbed mass as a function of time is then obtained by numerically evaluating the following integral:

$$\frac{M_\theta}{M_\infty} = 3\int_0^1 x^2 \frac{q(x,\theta)}{q_o} dx \qquad (9)$$

where M_θ is the mass uptake at dimensionless time θ and M_∞ is the equilibrium mass uptake at a gas-phase concentration C_o. This system of equations was solved by the orthogonal collocation method (Finlayson, 1980), with seven collocation points, as described in Chapter IV. Solutions were also generated with additional collocation points and no significant change was observed.

If surface diffusion is negligible in the intraparticle mass-transfer process, Equation (5) is reduced to the form of the pore diffusion model (cf., Equation (5) of Chapter V):

$$\frac{\partial Q}{\partial \theta} = \frac{1}{k_i'} \frac{1}{x^2} \frac{\partial}{\partial x}\left(x^2 \frac{\partial Q}{\partial x}\right) \qquad (10)$$

The corresponding boundary conditions at surface of the grain are then the same as given in Equations (6) and (7) of Chapter V.

For the case of a linear isotherm (which is observed to prevail for low RH) and constant surface diffusivity, the governing model equation is the linear form (n=1) of the porous sphere model (Equation (5) of Chapter V) except that the dimensionless time (θ) becomes $\theta'=(D_e+D_s)t/a^2$. In this case, if intraparticle diffusion controls the overall mass transfer processes (i.e., $B \rightarrow \infty$) the exact solution of relative mass uptake (or loss) can be obtained analytically as follows (Crank, 1975):

$$\frac{M_\theta}{M_\infty} (\text{or } 1 - \frac{M_\theta}{M_\infty}) = 1 - \frac{6}{\pi^2} \sum_{j=1}^{\infty} \frac{1}{j^2} \exp(-j^2 \pi^2 \theta') \qquad (11)$$

This analytical equation was used in the present work to validate the numerical solutions.

MATERIALS AND METHODS

Adsorbates and Adsorbents. Water vapor (0% < RH < 86%) was selected as the target adsorbate, while GAC from Calgon (CAL) was chosen as a representative

adsorbent. Manufacturer's data for the adsorbent are listed in Table 1 of Chapter V and summarized here. The BET surface of this GAC is about 1000 m^2/g. The porosity (ε_p) and solid density (ρ_p) are about 0.65 and 2.1 g/cm^3, respectively. The average diameter of the carbon grains used in the sorption experiment was 0.15 cm.

Sorption Experiments. Sorption experiments were performed with a Cahn-1000 electrobalance (Cahn Inc., Cerrito, CA), maintained at 20 °C, enabling the determination of both adsorption/desorption kinetics and equilibrium adsorption capacities. The materials and procedures used in this experiment are similar to those used in Chapter V. (See Figure 1 of that chapter.) Two compressed-gas cylinders of HC-free air were used to generate the test air stream. Air flow from one cylinder was passed through a water vapor generator and blended with air flow from the second cylinder to produce desired water vapor concentrations. A gas bubbler filled with deionized water was used as the water vapor generator; its temperature was maintained by a temperature-controlled water bath to within ±0.1°C of the preset temperature. The relative humidity of the blended stream was measured with a dew-point hygrometer (EG&G, Model 911, Waltham, MA). Typically, an adsorption time of 1 to 3 hours was required for the activated carbon to reach equilibrium, while only about 0.5 to 1 hours was needed for complete desorption.

RESULTS AND DISCUSSION

The experimental results for equilibrium partitioning and adsorption/desorption kinetics are presented and discussed in this section along with the results and interpretation based on model predictions. The isotherm measurement results are first discussed. Then, experimental adsorption/desorption kinetic data are fitted by the diffusion model for a low water vapor concentration (RH ≤ 20%), employing only one adjustable parameter, D_e+D_s (the sum of the effective pore diffusivity and the surface diffusivity). The extracted parameter was then used to predict sorption kinetic data at higher water vapor concentrations (RH ≤ 36% and RH ≤ 60%). The very good conformance of the model predictions to the experimental data for these cases suggests that pore diffusion is much

more important than surface diffusion in this system at water vapor concentrations up to RH = 60%. As water vapor concentration increases (RH > 60%), we find that the model must account for both pore and surface diffusion to accurately describe the experimental kinetic data.

Sorption Isotherm. A type V isotherm, based on the IUPAC classification (Sing et al., 1985), was observed for the sorption of water vapor to activated carbon as shown in Figure 1. Similar isotherms have previously been observed for the adsorption of water vapor on different activated carbons (Tsunoda, 1990; Hassan et al., 1991; Rudisill et al., 1992). This isotherm shape indicates that the adsorbent-adsorbate interaction is weak; at high relative humidities, condensation occurs in the intraparticle pores (Gregg and Sing, 1982).

To model the sorption kinetics of water vapor to activated carbon, two desorption isotherms were measured: one was initiated with the AC at equilibrium with RH=86%; the second was started at RH=60%. Hysteresis was observed in the adsorption/desorption isotherms (Figure 1). The presence of hysteresis may result from capillary condensation in mesopore structures (Sing et al., 1985) and from filling of micropore structures (Dubinin, 1980). The lower closure points of both adsorption/desorption hysteresis loops occurred at RH $\approx$ 30%. Similar hysteresis behavior and lower closure points have previously been found for several activated carbons by Tsunoda (1990).

The lower portion of the isotherm, up to RH $\approx$ 20%, is well approximated by a linear equation, as shown in the small box within Figure 1. For RH > 20%, the isotherms were described by a combination of linear sections between adjacent points plotted in Figure 1.

Sorption Kinetics at 20% RH. With the sorption isotherm described by a linear equation, k_i' becomes unity and, if the surface diffusivity is constant throughout the range of interest, governing Equation (5) is reduced to a similar form as that of the pore diffusion model, Equation (10), with θ replaced by θ'. Although surface diffusivity is

known to increase as the amount adsorbed increases (Kapoor et al., 1989; Kapoor and Yang, 1991), a constant surface diffusivity is assumed here. The HIO model (Kapoor and Yang, 1991), based on a random walk of molecules from one sorption site to another, indicates that the surface diffusivity is strongly dependent on the fraction of surface sorption sites that are occupied, λ, according to

$$D_s = \frac{D_{so}}{1-\lambda} \tag{12}$$

where $\lambda=q/q_m$, q_m is the sorption capacity that corresponds to full occupancy of the surface sorption sites by water vapor molecules, and D_{so} is the value of the surface diffusivity at $\lambda=0$. Dubinin (1980) has suggested that all of the hydrophilic surface sites of activated carbon are occupied by water molecules at a relative humidity of about 60%, which corresponds to q = 0.130 g water per g activated carbon in our system. Accordingly, λ of water molecules on the activated carbon at RH = 20% is estimated to be about 0.08. It is reasonable, therefore, to treat D_s as a constant value, D_{so}, from 0 to 20% RH. The adsorption/desorption kinetic curves are obtained by solving first Equation (10) and then Equation (9).

Experimental adsorption (desorption) curves were plotted as relative mass gain (or mass loss), M_θ/M_∞ ($1-M_\theta/M_\infty$), versus square root of dimensionless time, i.e. $(\theta')^{0.5}=[(D_e+D_s)t/a^2]^{0.5}$. A scheme similar to the least-squares method was used to determine the best fit of the experimental data to the model (Chapter II). In this scheme, (D_e+D_s) was varied, and the difference in M_θ/M_∞ between experimental data points and the corresponding model predictions were squared and summed. The value of (D_e+D_s) was systematically varied until the minimum summation value was obtained. Figure 2 shows the water vapor sorption kinetic data for 20% RH and the best fit obtained from the model. Because the isotherm is linear, coincident adsorption and desorption curves are expected. The model conforms well to the experimental data for both adsorption and desorption kinetic curves with only the one adjustable parameter, (D_e+D_s). The best fit of (D_e+D_s)

was found to be 3.7×10^{-10} m^2 s^{-1}. Assuming negligible surface diffusion flux, this result implies that the pore diffusivity is $D_p = 1.2 \times 10^{-6}$ m^2 s^{-1}.

Sorption Kinetics at 36% and 60% RH. For RH > 20%, the isotherm becomes concave with respect to the adsorption capacity axis (Figure 1). Under this condition, Equation (10) no longer adequately represents transport within the grain unless the surface diffusion flux is much less than the pore diffusion flux. To test for significance of surface diffusion, we attempted to predict adsorption/desorption kinetics for $0 \leq$ RH $\leq$ 36% and $0 \leq$ RH $\leq$ 60% using the D_p value extracted from the kinetic experiment at 20% RH, and neglecting surface diffusion. Figure 3 presents a comparison between the adsorption/desorption kinetic data and the corresponding model predictions. The fit is reasonably good for both sets of the data, although a moderate deviation is revealed in the experiments at 60% RH. The fact that the model predictions conform well to the experimental data, even though the surface coverage is much larger than at 20% RH and the isotherm is no longer linear, suggests that surface diffusion flux is not substantial for RH $\leq$ 60% in our system.

A further test was conducted to discern whether surface diffusion is important at 60% RH in our system. Two adsorption kinetic experiments were conducted with a step increase of water vapor concentration from 57 to 61% RH. For this small change of concentration, the equilibrium isotherm can be well represented as linear and Equation (10) can be used to predict the kinetic behavior, assuming that transport due to surface diffusion is negligible. Figure 4 shows that the predictions, assuming $D_p = 1.2 \times 10^{-6}$ cm^2 s^{-1} and $D_s = 0$, again fit the data very well; this finding reinforces the inference that surface diffusion is not important relative to pore diffusion for RH $\leq$ 60% in our system.

We also carried out a numerical effort to estimate the contribution of surface diffusion to transport within the AC grains at RH = 60%. Equation (5) was solved in concert with Equations (7) and (8) (initial and boundary conditions).

Although surface diffusivity is known to be a function of adsorbed-phase concentration (Kapoor et al., 1989; Kapoor and Yang, 1991), for the sake of mathematical simplicity, a constant surface diffusivity was used. This assumption is justified on the following basis. Kapoor and Yang (1991) have suggested that, for adsorption of hexane on activated carbon, a model that ignores the concentration dependence of D_s yields surface diffusivity values that are too high by a factor of 2-3. However, in their example calculation, surface diffusion dominated overall intraparticle mass transfer. The adsorption of water molecules onto activated carbon probably involves hydrogen bonding between the chemisorbed oxygen molecules on the carbon surface and the water molecules (Gregg and Sing, 1982). Therefore, surface diffusivity is expected to be smaller for water on AC than for hexane. Assuming that D_s is constant, we infer that the contribution of surface diffusion to intraparticle transport is no greater than 30% of the total flux for RH $\leq$ 86%. With this small contribution to the total intragranular flux, it seems reasonable to approximate D_s as constant.

In the numerical approach, the ratio D_s/D_e was varied, while D_p was maintained at a value of 1.2×10^{-6} m^2 s^{-1}, as obtained for RH $\leq$ 20%. The ratio of D_s/D_e that yielded the best fit between predictions and measurements according to a least-squares criterion was determined. It was observed that accounting for surface diffusion did not have much impact on the early stages of adsorption ($M_\theta/M_\infty << 1$) or desorption ($[1-M_\theta/M_\infty] << 1$), as can be seen by comparing Figure 3b and Figure 5. However, adding surface diffusion did improve the overall fit to the data, especially for the latter part of the adsorption kinetic curve. The best model fit to the data is shown in Figure 5, for which D_s/D_e is approximately equal to 0.5. With this ratio of D_s/D_e, surface diffusion accounts for about 10% of the total intragranular flux.

Sorption Kinetics at 86% RH. The adsorption/desorption kinetic data for 0 $\leq$ RH $\leq$ 86% were again first compared to model predictions based on pore diffusion alone, as shown in Figure 6a. As shown in this figure, the pore diffusion model does not

accurately predict the adsorption/desorption kinetic curves. The disagreement between model and measurement results prevailed, even when the pore diffusivity was permitted to vary.

Since surface diffusion increases in relative importance as the amount of sorbed species increases, surface diffusion is expected to contribute more to the total flux in this case than in the previous case. Again using a numerical procedure to solve Equation (5) with $D_p = 1.2 \times 10^{-6}$ m^2 s^{-1}, the ratio D_s/D_e was varied to generate the best fit of the model predictions to the measured data. The resulting best-fit model predictions, based on $D_s/D_e = 0.6$, are presented in Figure 6b, and conform well to the experimental data. In this case, about 30% of the total intragranular flux of water is attributable to surface diffusion. As was observed for $0 \leq RH \leq 60\%$, surface diffusion did not significantly influence the kinetics during the initial stages of either the adsorption or desorption, but it did substantially hasten the final approach to equilibrium.

Summary of Sorption Kinetics. A summary of the best-fit model results used to fit and/or predict kinetic adsorption/desorption curves (Figures 2 through 6) is presented in Table 1. For the 20% RH case (Figure 2), the only adjustable parameter was D_p which was determined to be 1.2×10^{-6} m^2 s^{-1}. For all other cases, this value of D_p was maintained. Good agreement between model predictions and measurements was obtained assuming intragranular transport by pore diffusion alone for 36% RH and 60% RH (Figures 3a, 3b, and 4). To refine the model results for the 60% RH case, surface diffusion was added to the pore diffusion model with the best fit presented in Figure 5. The best-fit value of D_s revealed that surface diffusion accounts for about 10% of the total intraparticle flux. Since surface diffusion becomes more important as sorbate concentration increases, one would anticipate, as we observed, that a model based on pore diffusion alone would not accurately predict the adsorption/desorption kinetic curves for 86% RH (Figure 6a). So, a model that accounts for both pore and surface diffusion was fit to the experimental data as shown in Figure 6b. This model conforms well to the experimental

data; the corresponding surface flux contributes about 30% of the total intragranular flux in this case.

Thus, a relatively simple model can effectively describe sorption kinetics in granular activated carbon for a broad range of water vapor concentrations. One limitation of the model is that the pore structure is assumed to be static, independent of the amount of water adsorbed. At 86% RH, the equilibrium sorption capacity for water is sufficient to occupy about 50% of the intragranular pore space. That good agreement between model and measurement is obtained suggests that the micropores may be responsible for the high sorption capacity at high RH. In this interpretation, the mesopores would have to contribute the dominant resistance for intragranular transport; due to their relatively large dimensions, their structure would not be expected to change significantly even on exposure to 86% RH.

If the models presented in this chapter and its companion (Chapter V) represented completely accurate descriptions of intragranular transport and sorption in activated carbon, one would expect the extracted values of pore diffusivity, D_p, to be consistent across the three sorbates studied. In fact, the values agree in magnitude, but no better: inferred values of D_p are 1.2×10^{-6}, 1.8×10^{-6}, and 4.2×10^{-6} $m^2 s^{-1}$ for water vapor, benzene, and vinyl chloride, respectively. Water vapor, being the lightest and smallest of the three molecules, should exhibit the highest value of D_p, at about 2 × the corresponding values for benzene or vinyl chloride, based on the relative diffusivities of these species in air.

Nevertheless, our findings support the general idea that the degree of asymmetry between adsorption and desorption kinetics is largely dependent on the shape of the adsorption isotherm (Ruthven and Derrah, 1972; Garg and Ruthven, 1972; Gray and Do, 1989a, 1989b, 1990 and 1991; Desai et al., 1992; Chapter II of this dissertation). In most of the sorbate/sorbent systems previously studied, the adsorption isotherms were either linear or convex with respect to the sorption capacity axis. In those cases, the rate of adsorption rate is either equal to or faster than the desorption rates. In the present study of

water vapor sorption on GAC, it was observed that the adsorption/desorption kinetic curves were symmetric for $0 \leq RH \leq 20\%$, as expected because of the linear shape of the isotherm. For values of RH above this range, the isotherm was predominantly concave with respect to the sorption capacity axis, and the rates of adsorption were observed to be slower than the desorption rates (Figures 3, 5, 6).

SUMMARY

A Type V adsorption isotherm with adsorption-desorption hysteresis was found in this study, as is typical for water vapor on activated carbon. A piecewise-linear description of the isotherm, with more than 13 sections, was used to approximate equilibrium partitioning data. An intragranular transport model that couples pore and surface diffusion with the experimentally determined isotherm was used to interpret experimental data on the kinetics of adsorption and desorption. The model fits all of the experimental data very well with a minimal number of fitted parameters, and the asymmetry between adsorption and desorption rates was well resolved, even though the isotherm shape is complex and exhibited hysteresis. Considering pore diffusion only, the model describes the experimental results fairly well for $RH \leq 60\%$. For higher water vapor concentrations, transport due to surface diffusion becomes more important.

APPENDIX I. REFERENCES

Crank, J. (1975). *The Mathematics of Diffusion*, 2nd ed., Oxford University Press, London, England.

Crittenden, J.C., Cortright, R.D., Rick, B., Tang, S.-R., and Perram, D. (1988). "Using GAC to remove VOCs from air stripper off-gas." *J. AWWA, 80,* 73-84.

Desai, R., Hussain, M., and Ruthven, D.M. (1992). "Adsorption on activated alumina. II. Kinetic behaviour." *Can. J. Chem. Eng., 70,* 707-715.

Dubinin, M.M. (1980). "Water vapor adsorption and the microporous structures of carbonaceous adsorbents." *Carbon, 18,* 355-364.

Finlayson, B.A. (1980). *Nonlinear Analysis in Chemical Engineering.* McGraw-Hill, New York, N.Y.

Garg, D.R., and Ruthven, D.M. (1972). "The effect of the concentration dependence of diffusivity on zeolite sorption curves." *Chem. Eng. Sci., 27,* 417-423.

Gray, P.G., and Do, D.D. (1989a). "Adsorption and desorption of gaseous sorbates on a bidispersed particle with Freundlich isotherm: I. Theoretical analysis." *Gas Sep. Purif., 3,* 193-200.

Gray, P.G., and Do, D.D. (1989b). "Adsorption and desorption of gaseous sorbates on a bidispersed particle with Freundlich isotherm: II. Experimental study of sulphur dioxide sorption on activated carbon particles." *Gas Sep. Purif., 3,* 201-208.

Gray, P.G., and Do, D.D. (1990). "Adsorption and desorption dynamics of sulphur dioxide on a single large activated carbon particle." *Chem. Eng. Comm., 96,* 141-154.

Gray, P.G., and Do, D.D. (1991). "Dynamics of carbon dioxide sorption on activated-carbon particles" *AICHE J., 37,* 1027-1034.

Gregg, S.J., and Sing, K.S.W. (1982). *Adsorption, Surface Area and Porosity,* 2nd ed., Academic Press, London, England.

Hassan, N.M., Ghosh, T.K., Hines, A.L., and Loyalka, S.K. (1991). "Adsorption of water vapor on BPL activated carbon." *Carbon, 29*, 681-683.

Kapoor, A., and Yang, R.T. (1991). "Contribution of concentration-dependent surface diffusion to rate of adsorption." *Chem. Eng. Sci., 46,* 1995-2002.

Kapoor, A., Yang, R.T., and Wong, C. (1989). "Surface diffusion." *Catal. Rev.-Sci. Eng., 31*, 129-214.

Leigh, C.D., and Smith, D.M. (1993). "A piecewise-linear approximation to diffusion with nonlinear interactions: Nonlinear sorption." *Chem. Eng. Sci., 48*, 1153-1161.

Liu, R.-T. (1993). "Model simulation of the performance of activated carbon adsorbers for the control of indoor VOCs." *Proceedings of the 6th International Conference on Indoor Air Quality and Climate*, Vol. 6, Indoor Air '93, Helsinki, Finland, pp. 421-428.

Rudisill, E.N., Hacskaylo, J.J., and LeVan, M.D. (1992). "Coadsorption of hydrocarbons and water on BPL activated carbon." *Ind. Eng. Chem. Res., 31*, 1122-1130.

Ruthven, D.M., and Derrah, R.I. (1972). "Sorption in Davison 5A molecular sieves." *Can. J. Chem. Eng., 50*, 743-747.

Sing, K.S.W., Everett, D.H., Haul, R.A.W., Moscou, L., Pierotti, R.A., Rouquerol, J., and Siemieniewska, T. (1985). "Reporting physisorption data for gas/solid systems: With special reference to the determination of surface area and porosity." *Pure & Appl. Chem., 57*, 603-619.

Tsunoda, R. (1990). "Adsorption of water vapor on activated carbons: Estimation of pore width." *J. Colloid Interface Sci., 137*, 563-570.

Wakao, N. and Funazkri, T. (1978). "Effect of fluid dispersion coefficients on particle-to-fluid mass transfer coefficients in packed beds." *Chem. Eng. Sci., 33*, 1375-1384.

APPENDIX II. NOMENCLATURE

a	radius of carbon grain (m)
b_i	parameter in piecewise-linear isotherm (g sorbate per g sorbent)

B	Biot number [$= (k_f\, a)\, (\varepsilon_p\, D_p)^{-1}$] (dimensionless)
C	gas-phase sorbate concentration (g m^{-3})
C_o	imposed gas-phase sorbate concentration (g m^{-3})
C_s	gas-phase species concentration at external surface of carbon grain (g m^{-3})
D_e	effective gas phase diffusivity ($m^2\ s^{-1}$)
D_p	effective pore diffusivity in carbon grain ($m^2\ s^{-1}$)
D_s	effective surface diffusivity in carbon grain ($m^2\ s^{-1}$)
D_{so}	effective surface diffusivity in carbon grain at q=0 ($m^2\ s^{-1}$)
$f(C)$	isotherm function (g sorbate per g sorbent at equilibrium)
$f'(C)$	$= \partial f/\partial C$ [g sorbate per g sorbent)/(g sorbate m^{-3})]
k_i	isotherm slope for piecewise-linear segment i [(g sorbate per g sorbent) (g sorbate $m^{-3})^{-1}$]
k_i'	normalized isotherm slope for piecewise-linear segment i [$= k_i\, k_{io}^{-1}$] (dimensionless)
k_{io}	isotherm slope for piecewise-linear segment at C_o [(g sorbate per g sorbent) (g sorbate $m^{-3})^{-1}$]
k_f	gas-film mass-transfer coefficient (m s^{-1})
M_θ/M_∞	cumulative mass gain relative to that in equilibrium with C_o (dimensionless)
n	Freundlich isotherm parameter (dimensionless)
q	sorbed mass (g sorbate per g sorbent)
q_m	equilibrium sorption capacity for a sorbate monolayer (g sorbate per g sorbent)
q_o	equilibrium sorption capacity (g sorbate per g sorbent)
Q	normalized gas-phase sorbate concentration [$= C\, C_o^{-1}$] (dimensionless)
Q_s	normalized gas-phase sorbate conc. on grain surface [$= C_s\, C_o^{-1}$] (dimensionless)
r	radial coordinate in carbon grain (m)
t	time (s)
x	normalized radial coordinate in carbon grain [$= r\, a^{-1}$] (dimensionless)
ε_p	grain porosity (dimensionless)
λ	fraction of hydrophilic surface sites occupied by water molecules (dimensionless)
θ	normalized adsorption or desorption time [$= t\, D_e\, a^{-2}$] (dimensionless)
θ'	normalized adsorption or desorption time [$= t\, (D_e+D_s)\, a^{-2}$] (dimensionless)
ρ_p	solid density of carbon grain (g m^{-3})

Table 1. Summary of Model Results for Sorption Kinetics [a]

RH	Corresponding Figure	Corresponding Model	k_{io} [g/g]/[g/m^3]	D_e [m^2 s^{-1}]	D_s/D_e	Method of Obtaining D_e and D_s
20%	2	Pore	3.0×10^{-3}	3.7×10^{-10}	0	best fit of D_e
36%	3a	Pore	9.1×10^{-3}	1.2×10^{-10}	0	prediction [b]
60%	3b	Pore	56×10^{-3}	2.0×10^{-11}	0	prediction [b]
57-61%	4	Pore	56×10^{-3}	2.0×10^{-11}	0	prediction [b]
60%	5	Pore+Surface	56×10^{-3}	2.0×10^{-11}	0.50	best fit of D_s
86%	6a	Pore	42×10^{-3}	2.6×10^{-11}	0	prediction [b]
86%	6b	Pore+Surface	42×10^{-3}	2.6×10^{-11}	0.60	best fit of D_s

[a]Symbols defined in text and in Appendix II.

[b] Predictions are based on the measured piecewise linear isotherm plus the pore diffusivity inferred from the 20% RH kinetic experiment.

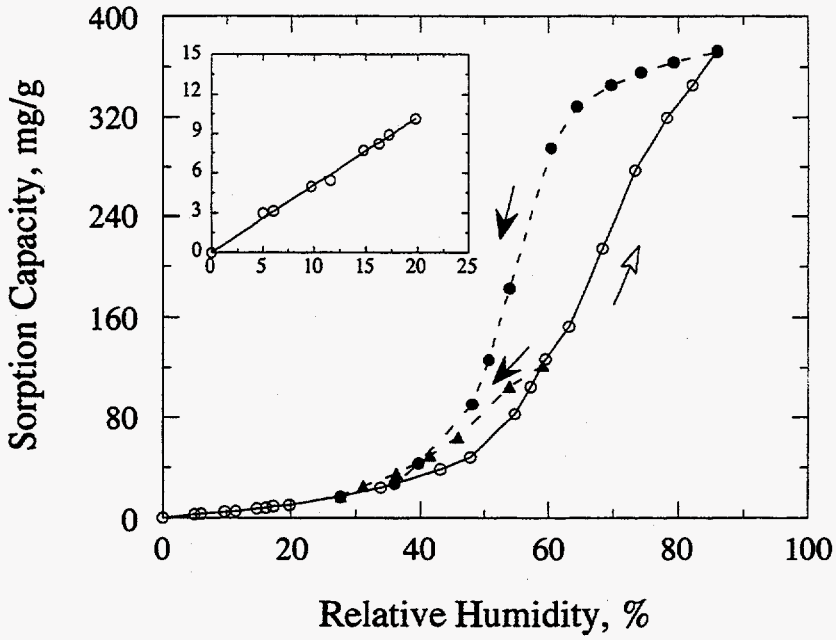

Figure 1. Sorption isotherms for water vapor on granular activated carbon, where open and filled symbols denote experimental adsorption and desorption data, respectively. The small box contains an expanded version of the sorption isotherm for 0 to 20% relative humidity.

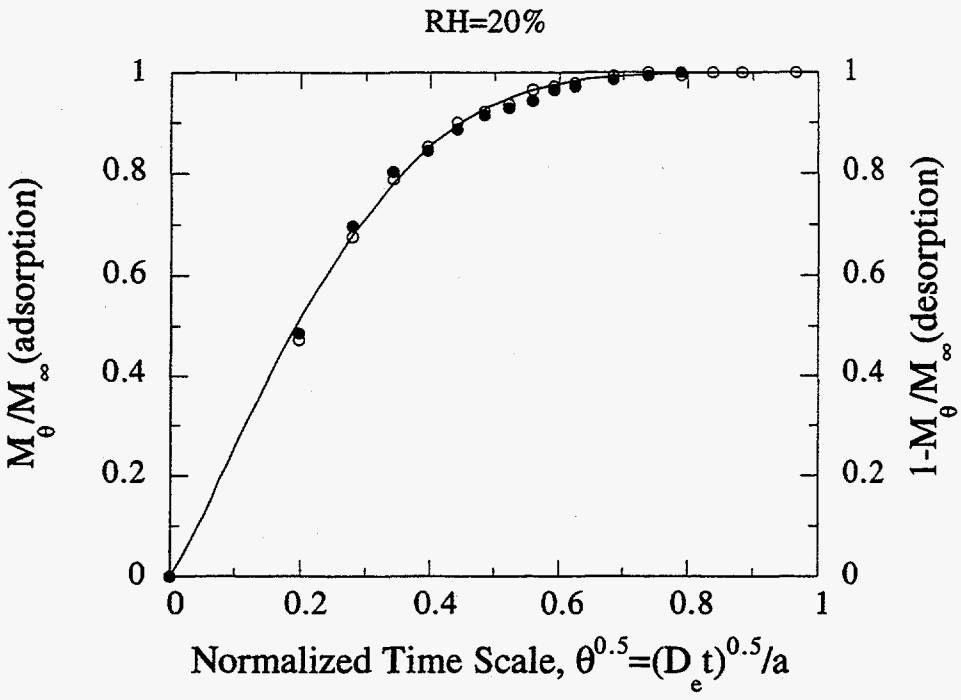

Figure 2. Adsorption/desorption kinetics for water vapor onto granular activated carbon in response to a step change between 0 and 20% RH. See Appendix II for definition of parameters. The open and filled symbols denote experimental adsorption and desorption data, respectively. The fitted model, shown as a solid line, applies for both adsorption and desorption.

(a)

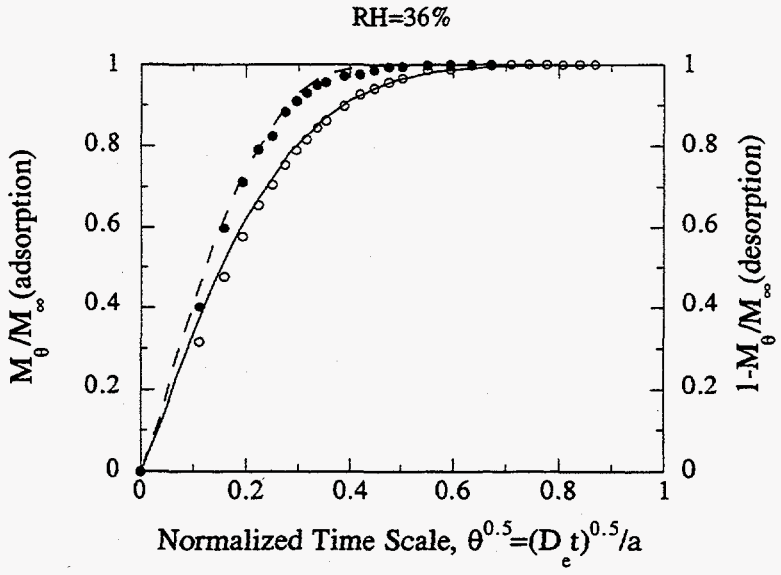

(b)

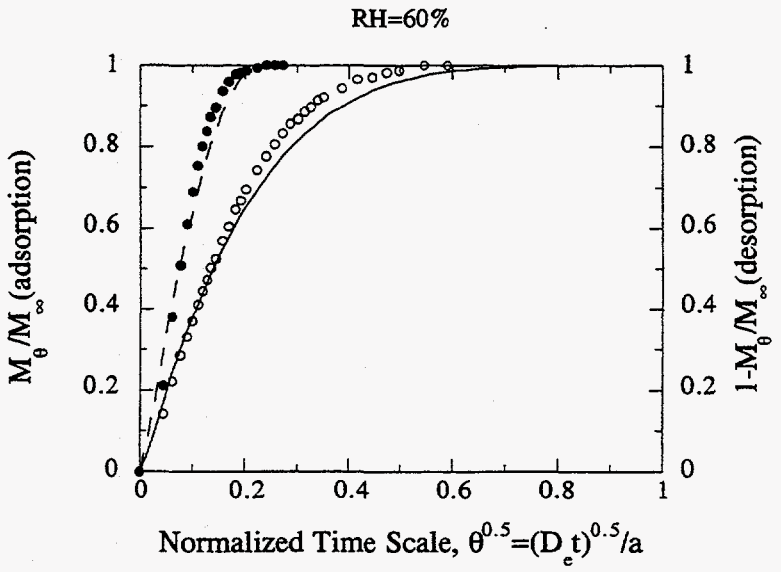

Figure 3. Adsorption/desorption kinetics for water vapor onto granular activated carbon where (a) represents response to a step change between 0 and 36% RH and (b) represents response to a step change between 0 and 60% RH. See Appendix II for definition of parameters. The open and filled symbols denote experimental adsorption and desorption data, respectively. The model prediction, which is based on transport by pore diffusion only, is shown as a solid line for adsorption and as a dashed line for desorption.

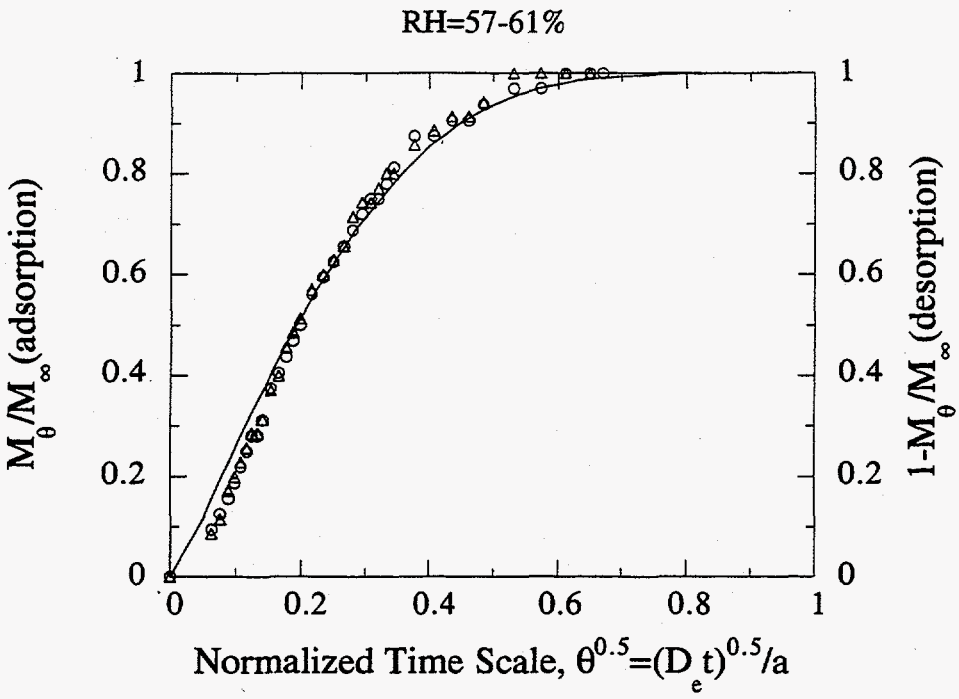

Figure 4. Adsorption kinetics of water vapor onto granular activated carbon in response to a step increase of water vapor concentration from 57 to 61% RH. See Appendix II for definition of parameters. The symbols denote two different sets of experimental adsorption data. The model prediction, shown by a solid line, accounts for transport by pore diffusion only.

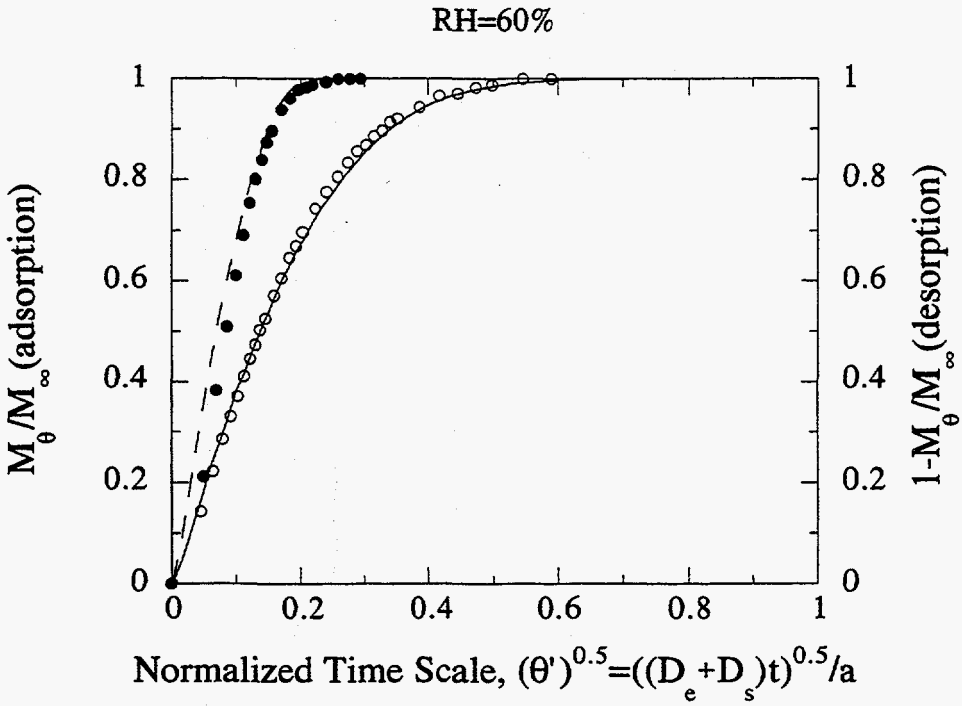

Figure 5. Adsorption/desorption kinetics for water vapor onto granular activated carbon in response to a step change between 0 and 60% RH. See Appendix II for parameter definitions. The open and filled symbols denote experimental adsorption and desorption data, respectively. The fitted model accounts for both pore and surface diffusion and is shown as a solid line for adsorption and as a dashed line for desorption.

Chapter VII

Conclusions

SUMMARY

The experimental and theoretical findings of this research indicate that intraparticle diffusion processes in combination with nonlinear sorption equilibrium are responsible for the slow and asymmetric sorption-desorption rates observed for volatile organic compounds (VOCs) and water vapor on dry soil mineral grains, peat grains, and activated carbon grains and fibers. Deterministic mathematical models were developed and applied to account for intragranular sorption and diffusion processes. These models incorporated independently measured parameters plus one or two fitted parameters in generating predictions. Overall, the models were found to describe well the experimental sorption-desorption rate data at the individual particle scale. In addition, the observed internal diffusion coefficients were found to be reasonable.

A scheme was developed from the relationships among intraparticle pore diffusion, isotherm nonlinearity and sorption rate asymmetry, to predict sorption isotherm and column BTCs based on parameters extracted from only one kinetic experiment. Tests of this scheme were successful for VOC sorption and transport in both soil mineral columns and granular activated carbon columns. This scheme holds promise as a useful tool to reduce the experimental effort required to determine input parameters for modeling VOC migration in porous sorbent systems, such as an adsorber. With appropriate modification, this scheme may be able to be used in more complex systems, such as those involving multicomponent sorption and transport or temperature change.

The results obtained from this research provide fundamental insight into the transport and sorption problems associated with several environmental systems. Although some of the conditions tested are idealized, for example the dry soil case, the mechanisms

(a)

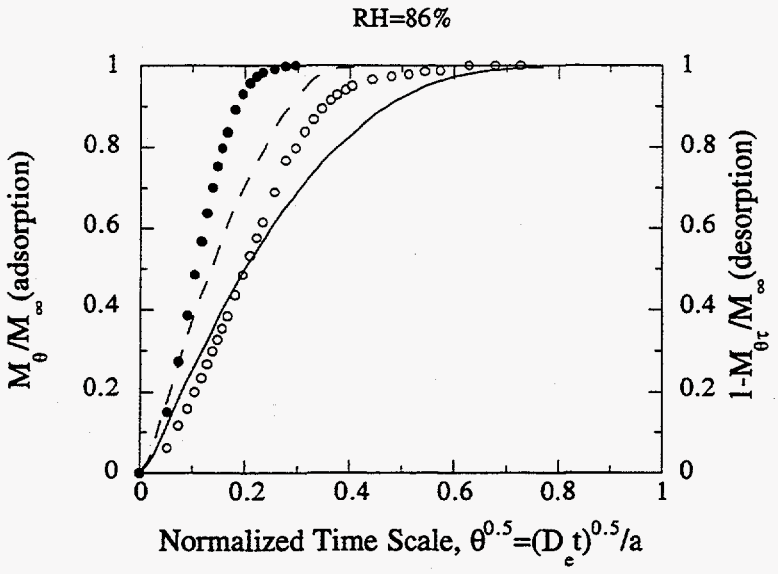

(b)

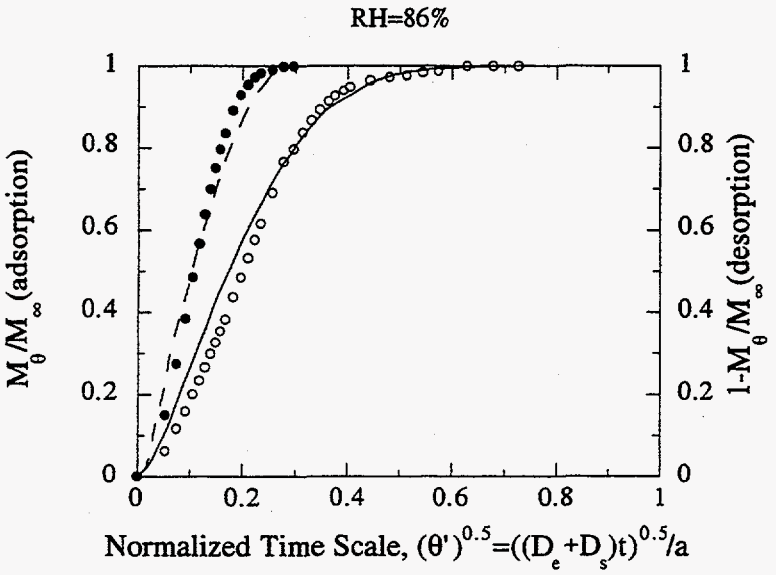

Figure 6. Adsorption/desorption kinetics for water vapor onto granular activated carbon in response to a step change between 0 and 86% RH. The open and filled symbols denote experimental adsorption and desorption data, respectively. Model predictions are shown as a solid line for adsorption and as a dashed line for desorption. The predictions in (a) account for transport only by pore diffusion whereas in (b) surface diffusion is included. See Appendix II for parameter definitions.

elucidated in this study should give a useful perspective when experiments are designed for more complex systems. The implications of this research are discussed in the next section together with future research directions; a chapter-level summary is presented in the following paragraphs:

Analysis of the experimental data obtained in this study demonstrates that the sorption capacity of dry soil grains is strongly related to the available mineral surface area. The vast majority of the accessible surface area is located inside the soil grains, even for a sand sample which has a grain porosity of only 1.4%. In addition, most of the internal surface area is associated with pores smaller than about 5 nm. A diffusional process governs the rate at which gas-phase species of benzene, trichloroethylene and water vapor reach the intragranular surfaces. However, the rate of diffusion into the grain is retarded by the strong and nonlinear local sorption equilibrium between the gas-phase in the pores and the internal grain surface.

A porous sphere model which couples intragrain diffusion with the experimentally measured nonlinear Freundlich isotherm provides good resolution of the asymmetry in the kinetics of adsorption and desorption. The model is used to infer a single effective diffusivity from the experimental data for both uptake and release. After allowing for Knudsen diffusion using a volume averaged representative pore size, the effective diffusivity was used to obtain a pore diffusion coefficient and hence a tortuosity factor. For the three test mineral soils (SSM, McAFB and sand), the tortuosities for the porous sphere model ranged from 10 to 33. These values agree well with previous experimental findings for low porosity nickel oxide pellets. The tortuosities for benzene, TCE and water vapor in SSM were reasonably close to one another, as expected theoretically.

A parallel pore model, which more completely accounts for the measured pore size distribution in the soil grains, was tested for one set of data. The model follows the experimental data somewhat better than the porous sphere model, especially at later times. However, the fact that the inferred tortuosity, 0.1, is significantly less than one suggests

that some key aspect of intragranular sorption is lacking in the model description. It is clear that the parallel pore model depends strongly on the assumptions made when inferring the pore size distribution from the mercury intrusion data. The model used to interpret the intrusion data may be a gross simplification of the actual internal pore structure. Also, it is assumed that the length of all the pores is equal to the grain radius, a fact that cannot be verified from the experimental measurements. If the average pore length is shorter than the grain radius, the calculated tortuosity will increase. Clearly, more accurate methods for characterizing the physical structure of soil grains will be of considerable value.

The structural similarity between the mineral soils and other porous sorbents, such as soil abundant in organic matter (e.g., peat) and activated carbon, leads to an interest in applying the porous sphere model to other media. The porous sphere model was either applied directly or modified to some extent to describe the transport and sorption behavior at individual sorbent grain/fiber scale for various sorbate/sorbent combinations, which include direct application for benzene on moist soil (Chapter IV) and VOCs on activated carbon (Chapter V). Coordinate modification was undertaken to model VOC sorption and transport in activated carbon fibers (ACF) (Chapter V). A refinement was introduced to account for surface diffusion for water vapor on activated carbon (Chapter VI). An enhancement was introduced to account for uptake in the soil organic matter (SOM) matrix for water vapor and benzene on peat (Chapter III). The models all coupled pore (gaseous) diffusion only or both pore and solid (surface) diffusion with the isotherm equation (measured or predicted) to describe the sorption kinetic data.

The pore diffusion model provides good fits to the experimental sorption kinetic data for VOCs to soil (Chapters II and IV), and VOC to granular activated carbon (GAC) and ACF (Chapter V). In these systems, the asymmetry between sorption and desorption rates are all well resolved by the model using two adjustable parameters, the effective diffusivity and the exponent in the Freundlich equation. It was found that the nonlinearity (or the shape) of the isotherm governs the degree of the asymmetry for sorption-desorption

rates. Consequently, the sorption isotherm can be predicted based on data obtained from a single kinetic experiment (Chapter IV and V). Excellent agreement (5% on average) was obtained for all the systems tested when comparing with the predictions with corresponding experimental measurements. This favorable result was obtained whether the kinetic experiment was conducted using an electrobalance (activated carbon) or a differential adsorption bed (DAB), with sorption capacities determined by column experiments. The achievement of good agreement even across measurement methods substantiates the model that underlies this predictive procedure, particularly when one considers the vast differences between measuring principles and sample mass among the approaches.

A dual diffusion model, which includes gas-phase pore diffusion within peat grains and solid-phase diffusion within microspheres of SOM, was used to interpret the asymmetric sorption rate data for water vapor and benzene to peat, a model SOM. Considering gas-phase pore diffusion only, the model resolved the asymmetry of sorption rates and described the experimental data very well for water vapor at three different concentrations. Although no satisfactory isotherm was obtained for benzene, a preliminary analysis was performed to fit the models to the kinetic sorption data for the benzene/peat system. The pore diffusion model failed to capture the dominant features of the experimental data. As a refinement, an alternative model prediction was developed assuming that solid-phase intra-SOM diffusion is the rate-limiting mechanism. The results of this model produced a better description of the highly asymmetric kinetic data. As a first-order estimate, the average solid-phase diffusivity for benzene within the matrix of SOM (peat) is inferred to be about 4.0×10^{-17} m^2 s^{-1}.

Predictions of VOC transport through sorbent columns are made possible by combining mass transfer equations for the mobile gas phase with the internal diffusion model developed for individual sorbent grains. The mass transfer model for the mobile phase used in this study is the advection-dispersion-sorption (ADS) equation (or dispersed plug flow model with sorption term). The model suggests that only one kinetic experiment

is needed to generate all the parameters for BTC prediction. The model predictions show good agreement with the experimental BTCs using the parameters determined from the kinetic experiment for both soil and activated carbon systems (Chapter IV and V). For engineering purposes, a simplified model, based on the constant pattern approach, was also used to describe the movement of vinyl chloride through activated carbon columns (Chapter V). Similar results were obtained from this model as from the full model, even though the required mathematical effort is much less. The findings strongly suggest that, relative to the current practice, these models could be employed to reduce the number of experiments required for designing an adsorber or estimating movement of VOCs in a similar system.

Several simplified versions of the transport model for columns are also introduced for the VOC/moist soil system. Since the isotherm for moist soil is linear, analytical solutions are found to be applicable. Experimental findings and model results suggest that the transport model assuming equilibrium between mobile and immobile phases is appropriate for slow flow conditions (Pe<10). However, the BTCs for advection-dominated cases can only be predicted by a model that explicitly accounts for internal diffusion.

The model considering pore diffusion only combined with the experimentally determined piecewise-linear isotherm captures the dominant features of the kinetic data for water vapor sorption on activated carbon up to RH=60% (Chapter VI). As the water vapor concentration becomes higher, surface diffusion on the pore wall needs to be included in the model. In most sorption systems of interest, adsorption rates are faster than desorption rates. However, for the water vapor/activated carbon system, adsorption rates are slower than desorption rates in many instances because of the concave shape of isotherms (as viewed from the sorption capacity axis). These experimental findings support the general idea that the asymmetry between sorption and desorption rates is largely determined by the shape of the isotherm.

IMPLICATIONS AND FUTURE RESEARCH DIRECTIONS

From the theoretical and experimental findings of this dissertation, several research directions and implications directly related to transport and sorption of VOCs in porous media are recommended as follows:

A first area of research is to investigate the transport of VOCs in a regular soil system (with higher SOM content). The soil systems utilized in studying gas-phase VOC transport are often simplified by neglecting the organic matter and using the mineral portion only. In fact, SOM is a very important sorptive medium and often plays a dominant role in the sorption processes in soil systems. However, the physical structure of SOM as well as the sorption and transport mechanisms of contaminants within SOM are still not very clear. A more comprehensive understanding of the physical structure of SOM as well as the transport and sorption behavior of VOCs within the SOM matrix, including diffusion coefficients, would improve our ability to characterize the migration of VOCs within regular soil systems.

A second area of interest is to characterize appropriate sorbents for indoor VOC control. Considering the large time people spend indoors and the elevated indoor concentrations of many VOCs relative to outdoor concentrations, the dominant contribution to the total exposure for many species results from inhalation of indoor air. Although several investigators have begun to explore the use of sorbents such as activated carbon and silica gel to remove various pollutants from indoor air (Parmar and Grosjean, 1991; Weschler et al., 1993; Shaughnessy et al., 1994), to our knowledge, no studies have been conducted to systematically investigate VOC sorption by a broad range of sorbents in conditions appropriate to the indoor environment. Indoor concentrations of total VOCs are normally at the ppm level (Shah and Singh, 1988; Daisey et al., 1994). At such a low concentration, the time required to characterize sorption properties, including isotherms and effective diffusivities, is relatively long because of the isotherm nonlinearity. The scheme developed in this thesis to characterize both isotherm and breakthrough curves (BTCs)

using a single kinetic experiment has the potential to predict both sorption capacities as well as effective diffusivities for lower concentrations than measured. Significant time may be saved in characterizing sorbent properties using this scheme.

The transport of multicomponent VOCs (including the effects of water vapor) in porous sorbents in the presence of variable temperatures is also a worthwhile area to investigate. In typical environmental systems, such as soil gas at gasoline-contaminated sites and polluted indoor air, more than one component is present. It may be possible to modify the scheme developed in Chapter IV for predicting sorption isotherms and column BTCs from a single kinetic experiment so that the behavior of multicomponent systems can be predicted. The models for single components, if coupled with appropriate thermodynamic models for multicomponent sorption equilibrium, such as ideal adsorbed solution theory (IAST) (Myers and Prausnitz, 1969), may be able to predict both the multicomponent sorption isotherm and the BTCs based on just a few kinetic experiments (i.e., one for each component in the system). When accounting for the effect of temperature on sorption equilibrium constants, it may be possible to adapt the model to predict both sorption isotherms and BTCs at different temperatures.

A fourth area to investigate is contaminant transport and sorption processes in the subsurface systems accompanied by other important mechanisms, such as biological transformations by microorganisms. For example, recent field work has shown that the migration of gasoline vapor in the soil gas near a building is hindered by the combined effects of a low permeability soil layer and biodegradation (Fischer et al., 1995). To predict the migration of gasoline vapor into the building in this case, both biological and sorptive processes must be accounted for in a subsurface, soil-gas transport model. Another example involving participation of microorganisms in subsurface transport can be found in using in-situ biological remediation of groundwater (Alvarez-Cohen et al., 1993). Again, both biotransformation and sorption processes need to be considered in modeling the effectiveness of treatment techniques.

One of the most potentially fruitful, but perhaps most difficult areas to study is VOC transport in the natural subsurface environments. Although many studies have been conducted for elucidating subsurface VOC transport, very few have been conducted in the field. The idealized laboratory environment does provide an excellent tool for exploring certain phenomena under well-controlled conditions. However, field tests are normally needed to validate the outcomes of laboratory studies. The investigation of field sites, which may be difficult to arrange and typically are more complex to conduct, due to larger scale and greater heterogeneity, sometimes yield unexpected findings. Such findings can stimulate the design of more effective laboratory and modeling investigations that focus on improving our understanding of key environmental processes.

CLOSING REMARK

This study provides some fundamental information on the transport and sorption of VOCs and water vapor in soil and activated carbon systems. Intraparticle diffusion processes along with sorbent properties and sorption equilibria are shown to have a strong impact on sorbate transport at grain/fiber scale and, under certain conditions, in laboratory columns. Although the systems studied were designed to be simple, the findings from this research provide a partial basis for conducting theoretical and experimental investigations of more complex environmental systems. Many problems remain to be solved in the area of contaminant transport in porous sorbent systems, especially in subsurface environments. More investigations in this area are necessary to improve our ability to understand and effectively control complicated environmental transport problems.

APPENDIX I. REFERENCES

Alvarez-Cohen, L., McCarty, P.L., and Roberts, P.V. (1993). "Sorption of trichloroethylene onto a zeolite accompanied by methanotrophic biotransformation." *Environ. Sci. Technol., 27*, 2141-2148.

Daisey, J.M., Hodgson, A.T., Fisk, W.J., Mendell, M.J., and Ten Brinke, J. (1994). "Volatile organic compounds in twelve California office buildings: Classes, concentrations and sources." *Atmospheric Environment, 28*, 3557-3562.

Fischer, M.L. (1995) Unpublished Field Data, Indoor Environment Program, Lawrence Berkeley Laboratory.

Myers, A.L., and Prausnitz, J.M. (1969). "Thermodynamics of mixed-gas adsorption." *AIChE Journal, 11*, 121-127.

Parmar, S.S., and Grosjean, D. (1991). "Sorbent removal of air pollutants from museum display cases." *Environmental International, 17*, 39-50.

Shah, J.J., and Singh, H.B. (1988). "Distribution of volatile organic chemicals in outdoor and indoor air." *Environ. Sci. Technol., 22*, 1381-1388.

Shaughnessy, R.J., Levetin, E., Blocker, J., and Sublette, K.L. (1994). "Effectiveness of portable air cleaners: Sensory testing results." *Indoor Air, 4*, 179-188.

Weschler, C.J., Shields, H.C., and Naik, D.V. (1993). "An evaluation of activated carbon filters for control of ozone, sulfur dioxide, and selected volatile organic compounds." *Proceedings of IAQ 92: Environments for people,* American Society of Heating, Refrigeration and Air-Conditioning Engineers, Atlanta, Georgia, pp. 233-239.